OPTIMIZATION OF DYNAMIC TRANSMISSION NETWORK EXPANSION PLANNING USING IMPROVED BINARY PARTICLE SWARM OPTIMIZATION ALGORITHM

FAITH ESERI INYANGA

MASTER OF SCIENCE IN
ELECTRICAL ENGINEERING

JOMO KENYATTA UNIVERSITY
OF
AGRICULTURE AND TECHNOLOGY

2026

Optimization of Dynamic Transmission Network Expansion Planning Using Improved Binary Particle Swarm Optimization Algorithm

Faith Eseri Inyanga

A Thesis Submitted in Partial Fulfillment of the Requirements for the Degree of Master of Science in Electrical Engineering of the Jomo Kenyatta University of Agriculture and Technology

2025

DECLARATION

This thesis is my original work and has not been presented for a degree in any other University

Signature…….……..…..…..…..…..Date: ……..…..…..…..

Faith Eseri Inyanga

This thesis has been submitted for examination with our approval as the University Supervisors

Signature…….……..…..…..…..…..Date……..…..…..…..

Dr. Keren K. Kaberere, PhD

JKUAT, Kenya

Signature…….……..…..…..…..…..Date……..…..…..…..

Dr. Irene N. Muisyo, PhD

JKUAT, Kenya

DEDICATION

To my mother, Violet.

ACKNOWLEDGEMENT

I wish to sincerely thank my supervisors, Dr. Keren Kaberere and Dr. Irene Muisyo for their valuable and continual guidance, patience and useful critiques throughout my research. You have been a source of great inspiration to me in the duration of my research. It was an utmost honor to work under your supervision.

I am grateful to my mom, for indulging my ambition and holding my hand through this process. For the tireless struggle to support me financially and the patience for me to see this through. You remain my rock.

My special gratitude goes to my family for their continuous emotional support throughout my life without which I would not be where I am now.

I am also grateful to my colleagues, who were always willing to engage with me in useful research discussions and with whom we shared our experiences in undertaking this academic journey.

Finally, I am most grateful for my husband. Despite the untimeliness that hit us, which brought us our greatest joy, and the intermittent struggle to beat research deadlines, we got to the best part anyway. I am humbled.

TABLE OF CONTENTS

LIST OF TABLES

LIST OF FIGURES

LIST OF APPENDICES

ACRONYMS AND ABBREVIATIONS

AC	Alternating Current
ACO	Ant Colony Optimization
AFC	All Feasible Candidates
AGC	All Good Candidates
APC	All Possible Candidates
BPSO	Binary Particle Swarm Optimization
CHA	Constructive Heuristic Algorithm
DC	Direct Current
DP	Dynamic Programming
DPSO	Discrete Particle Swarm Optimization
DTNEP	Dynamic Transmission Network Expansion Planning
EMF	Electromotive force
FACTS	Flexible Alternating Current Transmission System
FY	Financial Year
GA	Genetic Algorithm
GDP	Gross Domestic Product
GEP	Generation Expansion Planning
GRASP	Greedy Randomized Adaptive Search Procedure

GS	Generating Station
IBPSO	Improved Binary Particle Swarm Optimization
IEEE	Institute of Electrical and Electronics Engineers
KCL	Kirchhoff's Current Law
KETRACO	Kenya Transmission Construction Company Limited
KVL	Kirchhoff's Voltage Law
IP	Integer Programming
LSHADE	Linear population-size reduction Success History Adaptation Differential Evolution
LP	Linear Programming
MATLAB	MATrix LABoratory
NLP	Non-Linear Problem
OF	Objective Function
PSO	Particle Swarm Optimization
Pu	Per Unit
SA	Simulated Annealing
SPACMA	Semi-parameter Adaptation hybrid Covariance Matrix Adaptation
SQP	Successive Quadratic Programming
SSSC	Static Synchronous Series Compensator
STATCOM	Static Synchronous Compensator

STNEP	Static Transmission Network Expansion Planning
SVCs	Static VAR Compensators
SVS	Static VAr System
TCPST	Thyristor Controlled Phase Shifting Transformer
TCSC	Thyristor Controlled Series Capacitors
TNEP	Transmission Network Expansion Planning
TS	Tabu Search
UPFC	Unified Power Flow Controller

ABSTRACT

A transmission system is one of the most important components of a power system for relaying electric power to load centers. Increasing capacities of existing generating units and construction of new generating plants to supply the additional electric power demand has resulted in congestion of transmission networks. Congestion is as a result of reaching or exceeding the voltage, transmission lines' loading or steady-state stability limits. Persistent congestion is alleviated by construction of additional transmission lines. The Transmission Network Expansion Planning (TNEP) task is needed to determine the best set of transmission lines that can be added to a power system at minimum expansion cost without violating the network constraints during a defined planning period. In this research, voltage limit violations are penalized in a constrained Dynamic Transmission Network Expansion Planning (DTNEP) optimization problem. The number of transmission lines and their optimal location required to minimize the costs of line construction and transmission losses associated with the transmission network operations are determined. Improved Binary Particle Swarm Optimization (IBPSO) algorithm is applied to optimize the DTNEP results. IBPSO algorithm allows discrete TNEP problems to be solved by Particle Swarm Optimization (PSO) algorithm. IBPSO algorithm addresses the limitation of the BPSO algorithm by jumping out of the local optimal position to explore the search space area. The developed model is tested on Garver's 6-bus and IEEE 30-bus systems using MATLAB. The obtained DTNEP results minimize the costs of constructing new transmission lines when compared to using Linear Programming and Linear population-size reduction Success History Adaptation Differential Evolution Semi-Parameter Adaptation hybrid Covariance Matrix Adaptation (LSHADE-SPACMA). Congestion in the network was alleviated by ensuring the transmission lines' thermal loading were maintained at 80 % of their capacities and bus voltage limits (± 5 % of nominal voltage) were obeyed. Alleviating congestion in the network improved the adequacy of the transmission network system allowing for increased active power transfer. The developed methodology may be applied to a large power system for further studies. IBPSO algorithm may be applied with other metaheuristic methods to improve speed of convergence for DTNEP problems.

CHAPTER ONE

INTRODUCTION

1.1 Background

Accessibility of electricity has a direct impact on the pace of development of any country. Electricity is easy and efficient to transport from the production centers to the point of use because electrical power can be converted to any desired form, such as mechanical, thermal, light, or chemical. A properly designed and operated power system must meet the continually changing load demand for active and reactive power. The power system should supply energy at a minimum cost and with minimum ecological impact (Kundur, 1994). An electrical power system comprises many components connected to form a large, complex system capable of generating, transmitting, and distributing electrical energy over large areas (Saadat, 2002; Seifi & Sepasian, 2011).

Electricity is generated in bulk at the generating stations by converting mechanical, thermal, chemical or solar PV energy into electrical energy, then transmitted over long distances to the load points. Electric power is usually generated at lower voltages between 11 kV and 33 kV, and then fed into the transmission system using a step-up transformer. The transmission system interconnects all the generating stations and major load centers of a power system. Since the power loss in a transmission line is proportional to the square of the line current, the transmission lines operate at high voltage levels to minimize these transmission losses. Transmission lines also interconnect the utilities neighboring each other to allow economic power dispatch across the regions in normal conditions and emergencies. Transmission voltage is stepped down and fed to the distribution system for power transfer to the end-users (Seifi & Sepasian, 2011).

The global energy system has transformed since the Industrial Revolution. Demand and consumption of energy across many countries are notably growing as the gross national product and population increase (Ritchie et al., 2023). According to Kenya

Electricity Transmission Company Limited (KETRACO) transmission master plan 2023-2042, installed generation capacity in Kenya has grown from 2,351 MW in June 2018 to 3,322 MW in January 2023. The growth equates to a 41.3 % increase over five years, inclusive of off-grid capacity. Electricity demand grew from a peak of 1,802 MW in the financial year 2017/2018 to 2,149 MW in January 2023. This is an estimated 19.26 % increase over four years (Kenya Transmission Construction Company Limited, 2023).

The cumulative energy purchased stood at 12,653 GWh, and the energy sales at 9,813 GWh in the year 2021/2022. Estimated annual power and energy losses were 101.8 MW and 495.8 GWh, translating to 4.74 % and 3.44 %, respectively, when compared to 2,149 MW peak demand and 13,484 GWh projection for energy purchased in 2023. The losses are attributed to inefficient power evacuation from generation sources to load centers (Kenya Transmission Construction Company Limited, 2023).

Kenyan current power system suffers from constraints that present stability challenges during system operations. The constraints include under voltages, over voltages, over frequency, under frequency and overloading of transmission lines and power transformers. To address these system violations and improve the power system reliability, KETRACO is currently developing additional transmission projects consisting of power evacuation projects, grid strengthening and region interconnectors. The additional transmission line under implementation is 2,199 km circuit length, and the substation total capacity to be added by 2027 is 6,418 MVA. The total completed and operational circuit length is 9,011 km with a substation capacity of 5,928 km (Kenya Transmission Construction Company Limited, 2023).

As demand for electricity increases, the power system network is expanded to accommodate the increased power supply. Upgrade of the existing power system network and construction of new networks become necessary for effective power evacuation from generating stations to load centers. For a forecasted load increase, the generation capacity is expanded to cater for the future increase in demand. Transmission network system expansion alleviates network congestion and reduces network losses for reliable and quality power transfer (Seifi & Sepasian, 2011).

Planning of network systems is initiated by load forecasts for a predefined period, long-term energy forecasts, restrictions on systems operation, and feasibility concerning technical, financial, and time aspects (Seifi & Sepasian, 2011). Detailed power system planning requires a systematic approach that account for the time and financial restrictions from the network investigations while satisfying all the economic and technical requirements of a power system (Freitas et al., 2019). Efforts applied to reduce the power system expansion cost leads to significant savings on capital.

For large power systems, DC mathematical models are most adopted in expansion planning problems due to their simplified approach (F. Zhang et al., 2013). DC models are, however, not a correct representation of a typical power system because the focus is only on the active power requirements of a network system. Formulations based on AC models are used to improve the reliability of power system planning results. A full AC model incorporating all network constraints requires high computation effort making the planning process exhaustive. The planner expertly selects the desired network requirements to be met to reduce computation time (Abdelaziz, 2000; M. Mahdavi, Macedo, et al., 2018).

The solution techniques used for expansion planning are classified into mathematical, heuristics and metaheuristics methods. Metaheuristics methods have been used in recent years because of their capacity to find good or suboptimal solutions in large systems. Metaheuristics methods include (Alvarez et al., 2018; Asadzadeh et al., 2011; S. G. Binato et al., 2001; Inyanga et al., 2025; Kennedy & Eberhart, 1997; Khandelwal et al., 2019; Kwang & Zita, 2020; Romero et al., 1996; E. L. Silva et al., 2001; Sum-Im et al., 2009); Genetic Algorithm (GA) (Abdelaziz, 2000; Asadzadeh et al., 2011; Inyanga et al., 2025; Khandelwal et al., 2019; Kwang & Zita, 2020), Greedy Randomized Adaptive Search Procedure GRASP) (S. G. Binato et al., 2001; Kwang & Zita, 2020), Simulated annealing (SA) (Khandelwal et al., 2019; Kwang & Zita, 2020; Romero et al., 1996), Ant Colony Optimization (ACO) (Alvarez et al., 2018; Khandelwal et al., 2019; Kwang & Zita, 2020), Differential Evolution (DE) (Sum-Im et al., 2009),Tabu Search (TS) (Khandelwal et al., 2019; Kwang & Zita, 2020; E. L. Silva et al., 2001) and Binary Particle Swarm Optimization (BPSO) (Kennedy & Eberhart, 1997; Khandelwal et al., 2019).

Transmission network expansion is achieved through optimal Transmission Network Expansion Planning (TNEP) (Inyanga et al., 2025; Khandelwal et al., 2019). TNEP facilitates alternative paths for power transfer from generation plants to the load centers while ensuring the adequacy of the transmission lines for a defined planning horizon is met. Traditionally, transmission network planning is solved in two ways; static and dynamic planning. Static planning determines the number of transmission lines added to each transmission system corridor in a single planning horizon (Bizon et al., 2013; Kwang & Zita, 2020; Shayeghi H. & Mahdavi, 2013). Static planning determines the investment cost at the beginning of the planning period. In contrast, dynamic planning defines where, how many and when transmission lines should be added to the network in multiple stages in the duration of the planning. Dynamic planning calculates the investment cost at the start of every planning stage (Bizon et al., 2013; Kwang & Zita, 2020; Seifi & Sepasian, 2011; Shivaie et al., 2019).

TNEP aims to minimize the cost of construction of additional transmission lines and to reduce the costs of transmission network operation resulting from transmission system losses and system congestion. TNEP is usually performed using a constrained optimization model that minimizes the total network expansion costs while meeting defined economic, technical and reliability constraints (Jenkins et al., 2012; Kishore & Singal, 2014).

1.2 Problem Statement

Due to power system load growth requiring subsequent increases in generation capacity to meet the load demand, the transmission network has become inadequate to evacuate the generated power to load centers. This has resulted in congestion in a power system transmission network characterized by under-voltages and overloading of transmission lines. Congestion causes power system instability and reduces effectiveness in power system operation. As the load demand continues to increase the existing transmission lines become increasingly loaded. Reactive power compensation for voltage magnitude control can be used to relieve the congestion until the system can no longer operate adequately creating the need for construction of new transmission lines. Transmission network expansion is an expensive undertaking, and

its planning is time-consuming. A planner strives to meet all network constraints for a successful novel TNEP resulting in long and complex computational problems. Enforcing the voltage magnitude and transmission line loading constraints in a fitness function ensures reliable TNEP results. A heuristic algorithm is applied to the TNEP problem to optimize the results.

1.4 Justification

TNEP seeks to address the inadequacy of a power system to evacuate power from generation stations to load centers. Power system researchers have come up with scaled computation where the planner selects the network constraints to be focused on for a given problem solution and scenario. The approach reduces the network expansion costs and the computational time involved, allowing for the saving of a significant amount of capital. In this research work, reactive power compensation is used for voltage magnitude control to relieve congestion in a demand-increasing system until system operation becomes inadequate, requiring network expansion. In a transmission network expansion problem, violations in system voltage magnitude are penalized for a multi-objective problem solution, and an improved binary PSO (IBPSO) algorithm is applied for optimal selection and location of transmission lines to be added to the network. The penalty factor ensures results obtained fit the planner's objective, while the IBPSO algorithm optimizes these results to minimize total investment costs. Application of the IBPSO algorithm has better precision and suitability for discrete variables operation in TNEP problems compared to the BPSO algorithm. Penalizing voltage magnitude violation favors operation near nominal value to improve the transmission line loading adequacy and active power transferred. Improving system adequacy and increasing the active power transferable reduces the transmission losses. Significant savings of costs associated with transmission losses are achieved and therefore, minimizing the investment cost for network expansion.

1.5 Objectives

1.5.1 Main Objectives

The main objective of this research is to optimize Dynamic Transmission Network Expansion Planning (DTNEP) using Improved Binary Particle Swarm Optimization (IBPSO) algorithm.

1.5.2 Specific Objectives

i. To model the Garver's 6-bus and IEEE 30-bus test systems, increase demand and generation, and use reactive power compensation to mitigate power system congestion.
ii. To formulate the DTNEP problem for minimizing capital costs of additional transmission lines and active power losses for a 10-year planning horizon.
iii. To develop and apply an improved BPSO algorithm for optimizing DTNEP results of the test systems.
iv. To test the system performance on the DTNEP using BPSO and IBPSO algorithms and validate the results with previous similar works (Garver, 1970; Refaat et al., 2021).

1.6 Assumptions

i. It is not effective to plan for transmission network expansion without considering Generation Expansion Planning (GEP). For an increasing demand, generation has to be planned to meet the increasing power requirement. In this research model, it is assumed that GEP was conducted before the DTNEP and that generation capacity information is known to the planner (Khandelwal et al., 2019; Kundur, 1994).
ii. TNEP was realised by assuming the planner can select the expansion plan parallel to all existing and pre-planned transmission branches without any restriction of right-of-way (Khandelwal et al., 2019).

iii. While running AC load flow for reactive power compensation, load demand is assumed to grow by 10 % at constant power factor on existing load buses over a 10-year planning horizon.

iv. Load forecasting assumes that new load centers can be created in the system. The summation of the load increase in a single year is taken as load demand for a new load center.

1.7 Scope

In this work, Garver's 6-bus and IEEE 30-bus test systems are analyzed using the AC load flow model instead of the commonly adopted DC load flow for large TNEP problems. During reactive power compensation, only static compensators are used because they are economical and have a small physical equipment footprint. Static compensators are reactive power devices used to either supply or absorb reactive power. The total costs are a sum of the capital costs of new transmission lines and power losses. The transmission line losses considered in the total cost formulation are limited to active power losses due to line resistance. The dielectric heating, radiation, coupling and corona losses in transmission lines are ignored. The study does not take into account long transmission lines. Instead, it focuses on short and medium lengths transmission lines to facilitate an examination of the thermal rating and to assess the impact of voltage regulation on their transfer capability (Kundur, 1994; Zhang & Pal, 2006). Transmission voltage magnitude limits are enforced by penalizing deviations from ($\pm$ 5 % of nominal voltage). The transmission line thermal loading limit must not be violated during the optimization process.

1.8 Thesis Organization

The content of this thesis is arranged as follows; Chapter One covers an introduction to power systems, research objectives, problem statement and justification; Chapter Two outlines the structure of a typical power system, discusses the transmission transfer capability, addresses the reactive power compensation devices, discusses the planning of power system, the transmission network expansion optimization methods and models, the research-related studies and the research gap; Chapter Three documents the Garver's 6-bus and IEEE 30-bus case studies, the research methodology

for DTNEP problem and development of IBPSO algorithm; Chapter Four provides the results of research simulation, results analysis and their interpretation; Chapter Five provides conclusions and recommendations.

CHAPTER TWO

LITERATURE REVIEW

This chapter outlines the structure of a typical power system and the characteristics of reactive power compensating devices and presents power system planning leading to TNEP. It also reviews the fundamental concepts, algorithms, and models for TNEP. TNEP problem and the studies relating to the optimization of the DTNEP problem are discussed and finally, the research gap is presented.

2.1 Structure of a Power System

Electric power systems differ in size and is made up of various elements as shown in Figure 2.1 (Kwang & Zita, 2020; Saadat, 2002).

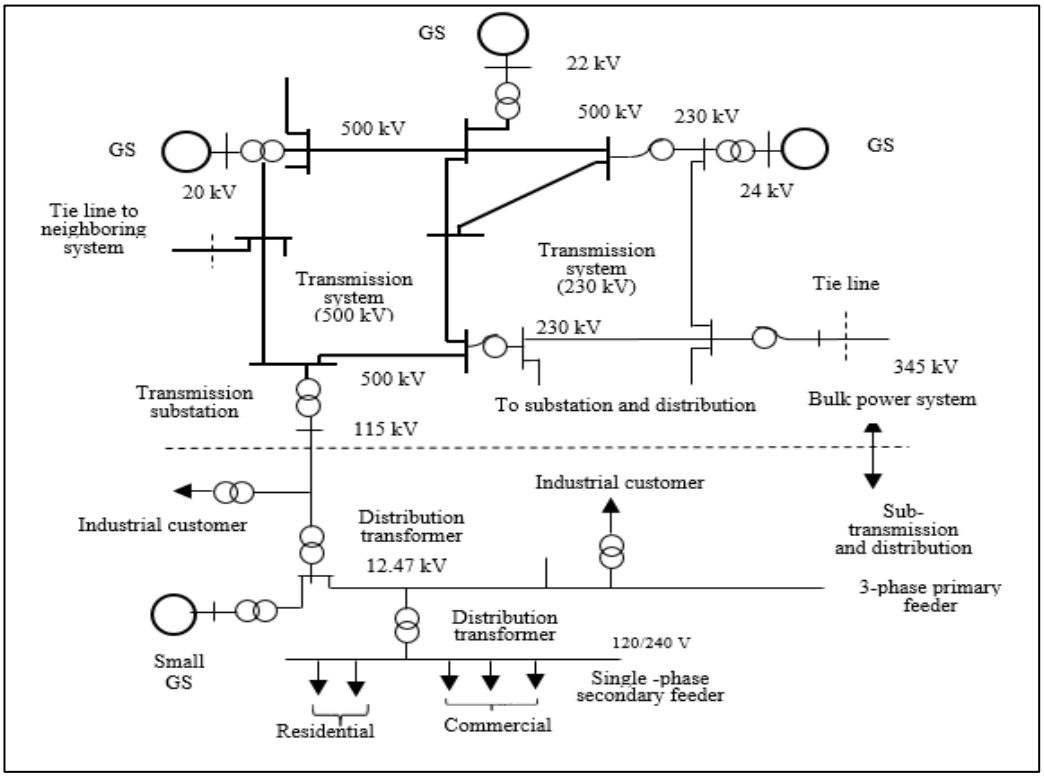

Figure 2.1: Basic Elements of a Power System

Figure 2.1 comprises Generating stations (GS), transmission systems, sub-transmission and distribution systems (Andersen & Nilsson, 2020; Bizon et al., 2013;

Kwang & Zita, 2020). The bulk power system is made of generating stations and transmission systems (Momoh & Lamine, 2010), whereas the sub-transmission and distribution form the distribution system (J. Das, 2015). Bulk generation facilities are normally situated far away from the load centers. Small generation stations are situated close to the loads and are usually connected directly to the sub-transmission or distribution system. Generation of electric power is at 20 kV, 22 kV, and 24 kV. The electric power is then stepped up to 239 kV, 345 kV and 500 kV depending on the transmission distance to reduce the transmission power losses that occur during transmission (Kaekhoungning et al., 2022). The large power systems located remotely are interconnected by a tie line acting as a synchronous AC, an asynchronous HVDC link or a hybrid synchronous link. Transmission substations have transformers that step the voltages appropriately for distribution to various customer categories. The customers are industrial, commercial or residential. The multiple generating resources and several layers of transmission networks provide a high degree of structural redundancy that enables the system to withstand unusual contingencies without service disruption to customers. The voltages may be for example, in Kenya, 11 kV to 33 kV for generation, 230 kV and above for transmission, 63 kV and 132 kV for sub-transmission and 33 kV, 11 kV, 400 V for distribution.

Figure 2.2 illustrates the layout of a typical substation (Seifi & Sepasian, 2011).

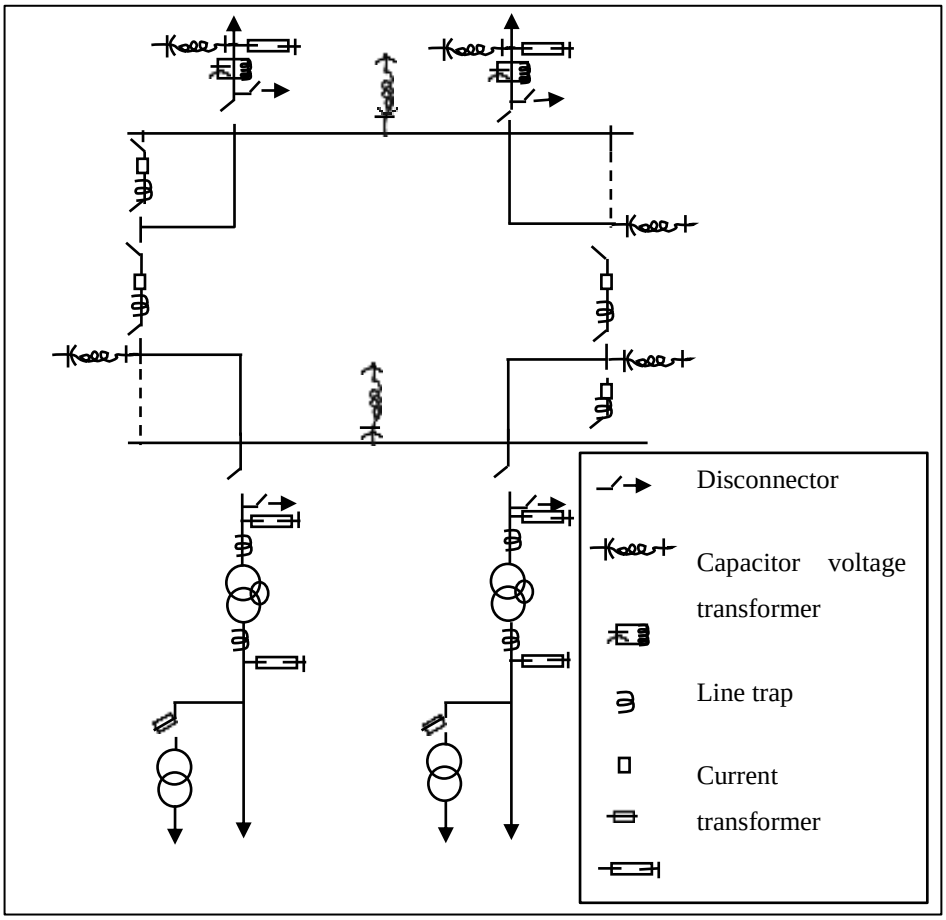

Figure 2.2: Typical Layout of a Substation

In Figure 2.2, transformers are located throughout the grid at substations to facilitate changes in voltage levels in an interconnected power system. The substation is equipped with protective switching devices. These include disconnectors, circuit breakers, fuses, isolators, and lightning arrestors.

2.2 Power Transmission Transfer Capability

The restrictions and limitations on the power transmission transfer capability define a network's capability to transfer power reliably. The development of multiple parallel paths in a transmission network is restricted by the desire for a high system security level despite the availability of capital and financing. In this instance, transmission networks are designed with large capacity margins and conservative loading to prevent blackouts and prolonged power outages. Where capital and financing are unavailable and the addition of transmission capacity is prevented by environmental restrictions,

reliability standards applied are less stringent such that a power outage involving a major transmission element initiates load curtailment. The transfer capability limits guidelines are agreed upon among the power utilities of a region (Andersen & Nilsson, 2020; Zaker et al., 2017). The quantity of power that can be transferred between the systems or buses at any given time depends on the generation capacity, load demands and the availability patterns of the circuits within the power system (Kwang & Zita, 2020; Lai, 2001).

2.2.1 Transmission Line Loading and Limits

The capability of a transmission line to absorb and dissipate the heat created by the current flowing through it sets the line's thermal limit (Lai, 2001). This limit is expressed as the allowable maximum temperature rise above the specified ambient conditions. The thermal limit is given by the current-carrying capacity of the transmission line specified in the manufacturer's data. The specification prevents extreme temperatures on the lines which causes equipment damage and sagging of the lines (Kundur, 1994). The limit on thermal loading in kVA is given by,

$$S_{thermal} = \sqrt{3}\, V_{Lrated} I_{thermal} \tag{2.1}$$

where;

$I_{thermal}$ -current-carrying capacity in A

V_{Lrated} -rated line voltage in kV.

For a short line, the thermal limit dictates the maximum power that can be transferred. The end-users are supplied with power at stipulated voltage levels. This voltage should be maintained within some defined limits e.g. ± 5 %. Thus, it is important to keep the transmission line voltage regulation within acceptable range. For medium length lines, the transfer capability is limited by voltage regulation. Real power transfer over a lossless line is given by Equation (2.2).

$$P_{3\varphi} = \frac{|V_{S(L-L)}||V_{R(L-L)}|}{X'} \sin\delta \tag{2.2}$$

Where;

$V_{S(L-L)}, V_{R(L-L)}$ -sending and receiving end line-to-line voltage magnitudes respectively

δ -power or load angle

X' -line reactance.

The power transfer for a single-system voltage is proportional to the sine of the power angle. For a lossless line, the theoretical steady-state limit is 90^0. However, a transmission system and its connected synchronous machines should withstand sudden changes in generation, demand and system faults without losing stability. Thus, the practical operating load angle is limited to the range of 35^0-45^0. Figure 2.3 shows the general loadability curve for overhead transmission lines (Kundur, 1994).

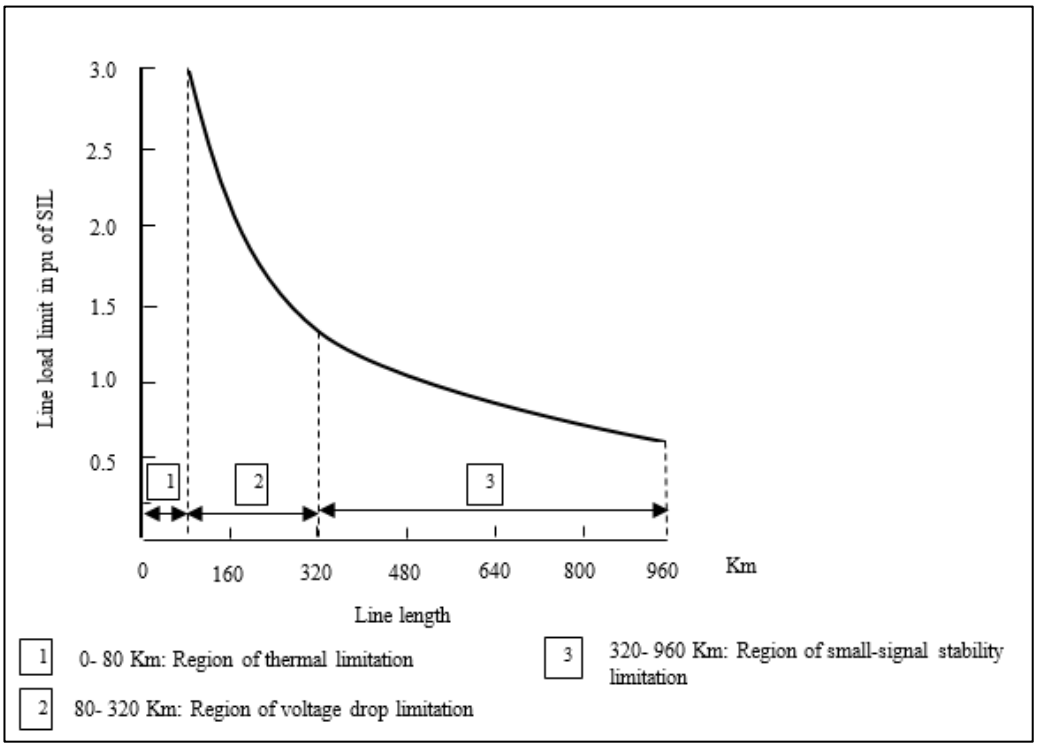

Figure 2.3: Typical Loadability Curve for a Transmission Line

Figure 2.3 gives the limiting values of power transmitted as a function of line length, as influenced by the thermal, voltage drop and steady-state stability limits ("IEEE

Guide for Planning DC Links Terminating at AC Locations Having Low Short-Circuit Capacities," 1997; Transmission Code 2007- Network and System Rules of the German Transmission System Operators, 2007). As the line length enters the region of steady-state stability, the loadability becomes less than the Surge Impedance Loading (SIL). In determining the loadability curve, the maximum voltage drop is 5 % and the minimum steady-state stability margin is 30 % defined as Equation (2.3) (Kundur, 1994).

$$percent\ stability\ margin = \frac{P_{max} - P_{limit}}{P_{max}} \times 100 \quad (2.3)$$

where P_{max} and P_{limit} are the transmission line transfer capacity and limit respectively.

The transfer capability limit for a long transmission line is set by the loadability curve in Figure 2.3. Loading a transmission line at its surge impedance loading eliminates the net reactive power flow. When a long transmission line is heavily loaded beyond SIL, a large voltage drop is experienced due to the increased reactive power losses due to the line reactance. When the loading is light (below SIL), the voltage rises on the receiving end due to excess charging reactive power injected by the line capacitance. The loadability of a transmission line can be increased by reactive power compensation (Saadat, 2002).

2.2.2 Power System Limitations

The interplay of the system and economic limitations gives rise to voltage-VAR-related conditions and stability considerations. Large high-voltage and consumer equipment are limited to excursions of ($\pm$5 %) of their rated voltage. The voltage magnitude bandwidth tolerance on the system is affected by the ability of various voltage-correcting devices to restore voltages to a bandwidth acceptable to the apparatus (Kundur, 1994; Saadat, 2002).

2.3 Reactive Power Compensation Devices

Compensating devices regulate the system voltage levels by varying the production, absorption and flow of reactive power in a power system (Kwang & Zita, 2020; Zaker

et al., 2017). The main reactive power compensation devices include the shunt reactors, shunt capacitors, synchronous condensers, Flexible AC Transmission System (FACTS) devices and the series capacitors (Saadat, 2002; Seifi & Sepasian, 2011; Zhang & Pal, 2006).

2.3.1 Shunt Reactors

Shunt reactors absorb reactive power to limit the voltage rise on open circuits or light loading conditions. Shunt reactors are only used on long transmission lines but apply to short transmission lines if the supply is from a weak system. A sufficiently sized shunt reactor is connected to the short transmission line permanently to limit the temporary fundamental-frequency overvoltage and the switching transients. Shunt reactors may be single or three-phase with a single winding on an iron core with air gaps and immersed in oil. Figure 2.4 shows a tapped shunt reactor (Kundur, 1994).

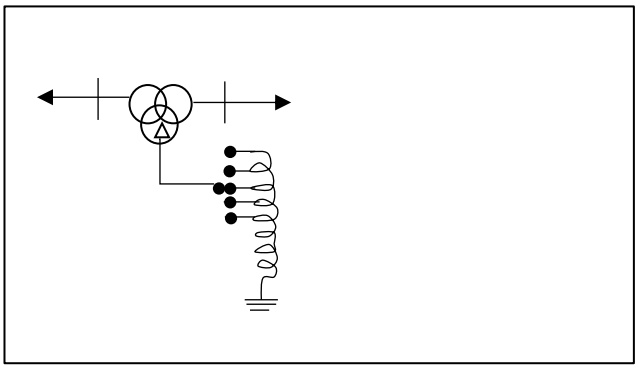

Figure 2.4: Three-Phased Tapped Shunt Reactor

The tapped shunt reactor in Figure 2.4 has on-voltage tap-change control facilities to allow for variation in the value of reactance.

2.3.2 Shunt Capacitors

Shunt capacitors boost local voltages by supplying reactive power. The reactive power injected Q_C is given by Equation (2.4).

$$Q_C = \frac{V_R^2}{X_C} MVAr \tag{2.4}$$

Where;

V_R -line voltage in kV

X_C -per phase capacitive reactance of the bank in ohms (Pablo et al., 2014).

Shunt capacitors are used in distribution systems to control feeder voltage and for power factor correction. Switched shunt capacitors are installed along the length of the feeder to ensure voltages at all points are maintained at the desired range as the loads vary. The objective of power factor correction is to provide reactive power close to the load. Power is transmitted at a non-unity power factor for the loads with lagging power factor. Lagging power factor increases active power losses and reduces thermal capability for transmission. The power factor is improved by injecting reactive power at the load. Shunt capacitors are connected to either the transformer tertiary winding or to a bus bar and arranged along the route to reduce the losses and voltage drops during heavy loading conditions (Grimble & Johnson, 2015; Zhang & Pal, 2006). The capacitor bank connections are shown in Figure 2.5 (Kundur, 1994).

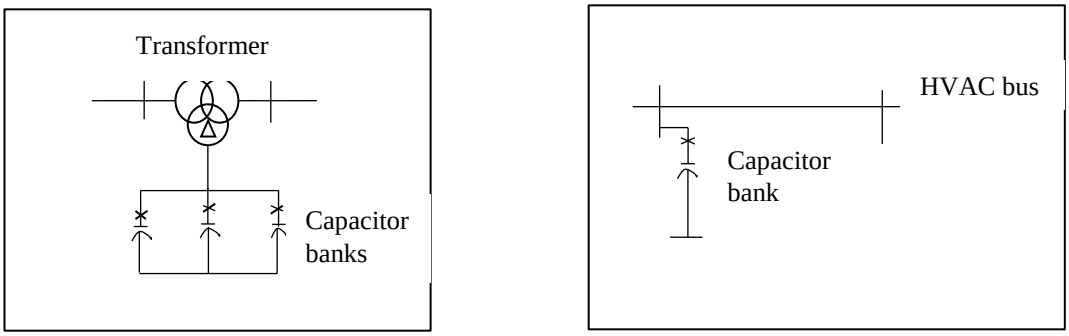

(a) Tertiary connected capacitor banks (b) HV capacitor bank

Figure 2.5: Shunt Capacitor Bank Connections

Figure 2.5(a) shows the capacitor banks connected to the tertiary winding of the main transformer and Figure 2.5(b) shows the capacitor bank connected directly to the high-voltage bus (Andersen & Nilsson, 2020). The capacitor banks can be switched manually using a breaker or automatically using a voltage relay.

Shunt capacitors are the most economical means of providing reactive power and voltage support (Andersen & Nilsson, 2020). The main limitation of shunt capacitors is that, at the connection location, reactive power output is proportional to the square of the bus voltage, as seen in 2.3. When the bus voltage is low, the shunt capacitor reactive power output is also low, reducing their effectiveness (Kundur, 1994).

2.3.3 Synchronous Condensers

Synchronous condensers are unloaded synchronous machines whose active power output is given in Equation (2.5).

$$P_G = \mathrm{R}_e V_a I_a^* \approx \frac{E_a V_a}{X_s} \sin \delta_m \tag{2.5}$$

Where;

E_a -generator's internal electromotive force (Emf)

V_a -terminal voltage

I_a^* -terminal current

X_s -synchronous reactance

δ_m -power angle between E_a and V_a.

From Equation (2.5), if

$\delta_m > 0$ $P_G > 0$ (Generator)

$\delta_m < 0$ $P_G < 0$ (Motor)

$\delta_m = 0 P_G = 0$ (Unloaded)

Neglecting the machine resistance, the reactive power supplied/absorbed is given by Equation (2.6).

$$Q_G = \frac{(V_a(E_a \cos \delta_m - V_a))}{X_s} \tag{2.6}$$

For $\delta_m = 0$, reactive power supplied/absorbed is given by Equation (2.7).

$$Q_G = \frac{(V_a(E_a - V_a))}{X_s} \tag{2.7}$$

Synchronous condensers supply reactive power when run in over-excited mode and absorb reactive power when run in under-excited mode. Synchronous condensers are flexible to operate for all load conditions due to their internal voltage source. The reactive power production is thus unaffected by the system voltage. Synchronous condensers are, however, expensive and difficult to install, operate and maintain. It is also difficult to increase their capacity (Kundur, 1994; Kwang & Zita, 2020).

2.3.4 Flexible AC Transmission System Devices

Static VAR Compensators (SVCs) is a Flexible AC Transmission System (FACTS) devices (Kwang & Zita, 2020) that can both supply and absorb reactive power, operating without any moving parts (Bizon et al., 2013; Kwang & Zita, 2020; Zaker et al., 2017). SVCs consist of shunt reactors, shunt capacitors and thyristor switches. Dynamic response of SVCs is very fast and the variation for compensation of reactive power is smooth and step-less. As the system voltage drops, SVCs degrade in their reactive power capability. SVCs also require harmonic filters in their operation to reduce the number of harmonics injected into the power system (Kundur, 1994; Saadat, 2002). Figure 2.6 shows a SVC (Kundur, 1994).

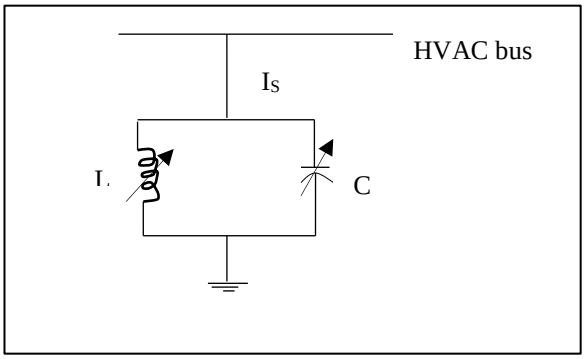

Figure 2.6: Static VAr Compensator

The SVC in Figure 2.6 has both the adjustable shunt capacitor (C) and shunt inductor (L) for voltage and reactive power control at either its terminals or at a nearby prescribed bus. (I_S) is the reactive current flowing through the SVC. SVC holds

constant voltage, provides instantaneous response and unlimitedly generates or absorbs VAr without power losses.

Other FACTS devices include (Bizon et al., 2013; Kwang & Zita, 2020; Zhang & Pal, 2006); the static synchronous compensator (STATCOM) utilized for managing reactive power flow and voltage regulation (Kwang & Zita, 2020), the Thyristor-controlled series capacitors (TCSC) and thyristor-controlled phase shifting transformer (TCPST) primarily used to enhance transient stability and for oscillation suppression (Kwang & Zita, 2020; X. R. C. , Zhang & Pal, 2006), and the Static synchronous series compensator (SSSC) and unified power flow controller (UPFC) (Kwang & Zita, 2020) combine reactive power flow and regulation of voltage with active power control, transient stability and oscillation inhibition (Jiankun & Zhen, 2017).

2.3.5 Series Capacitors

Reactive power supplied by series capacitors is independent of the bus voltages. Series capacitors are, therefore, self-regulating and is presented in Figure 2.7 (Kundur, 1994).

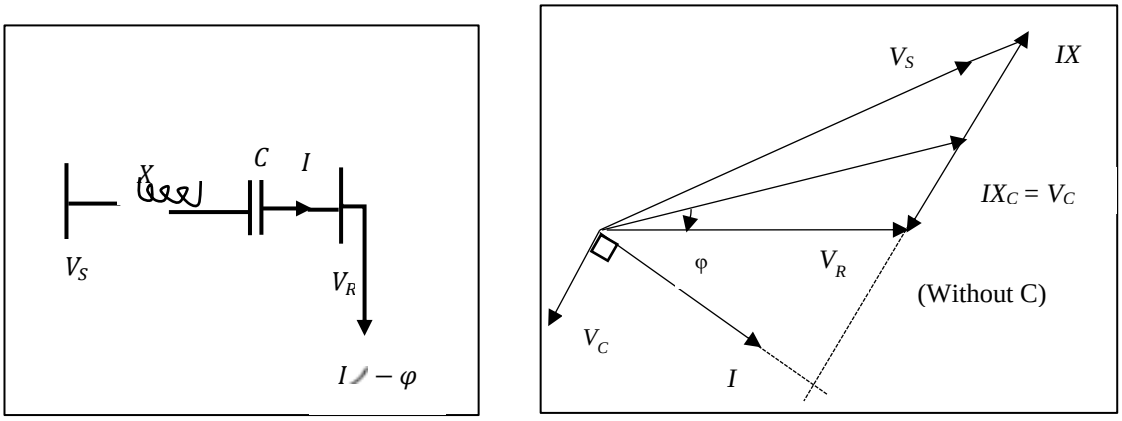

(a) (b)

Figure 2.7: A Series Capacitor

In Figure 2.7 (a), capacitor (C) is connected in series with line conductors to reduce the inductive reactance between supply and load. Reduced inductive reactance, in turn, reduces the transfer reactance between the buses and the I^2R losses, thus increasing

the maximum power transmitted. Voltage regulation is also improved. Equations (2.8) and (2.9) give the power transfer before (P_1) and after (P_2) compensation, respectively, as shown in Figure 2.7 (b) and (2.10) the ratio of (P_2) to (P_1) (Kundur, 1994; Saadat, 2002).

$$P_1 = \frac{V_S V_R}{X_L} \sin \varphi \tag{2.8}$$

$$P_2 = \frac{V_S V_R}{X_L - X_C} \sin \varphi \tag{2.9}$$

$$\frac{P_2}{P_1} = \frac{X_L}{X_L - X_C} = \frac{1}{1 - \frac{X_C}{X_L}} = \frac{1}{1-k} \tag{2.10}$$

where;

V_S, V_R -sending-end, receiving-end voltages respectively

X_L -line inductive reactance

X_C -capacitive reactance of series compensator

φ -phase angle between sending and receiving-end phase voltages

k -compensation factor.

Typical values of compensation factor k range between 0.4-0.7 (Kundur, 1994; Kwang & Zita, 2020). The reactive power produced increases with increased power transfer. However, voltage rise on one side of the capacitor may be excessive during high-line reactive-current flow resulting from heavy power transfers.

Series capacitors are used to shorten long lines effectively and can be located at the midpoint of the line, at line terminals, ⅓ or ¼ point of the line (Kwang & Zita, 2020). The location of series capacitors is chosen considering the costs, accessibility, fault

level, protective relaying considerations and the effectiveness to improve power transfer capability (Kundur, 1994; Kwang & Zita, 2020).

Special protective devices are required to protect the capacitors from the high current produced when a short circuit occurs. A resonance circuit oscillating at a frequency below the normal synchronous frequency upon a disturbance is created by the series capacitor inclusion. If the difference between the synchronous and the electrical resonance frequency nears the frequency of the turbine-generator natural torsional modes, the turbine-generator may be damaged (Kundur, 1994).

2.4 Power System Planning

Power system planning determines the new power system infrastructure required and the upgrade of existing ones to adequately satisfy the load demand for a defined planning horizon. Planning involves simultaneous economic and reliability evaluation of alternatives. Generation, transmission, and distribution planning make up power system planning (Khandelwal et al., 2019; Kwang & Zita, 2020). Bulk power system planning involves both generation and transmission planning. Efforts at planning one without considering the other results in less desirable plans in terms of plans in terms of reliability and economic viability. The decisions to be made are on location, when to install, and what to select in terms of specifications for the power system component to be added in the expansion plan (Wood et al., 2014).

2.4.1 Classification of Power System Planning

I. Static Versus Dynamic Planning

Static Planning

Static planning focuses on a single-stage planning horizon. Planning is made for the final projected future year. Static planning answers only what power system components must be added to the system and where they must be added (Jalilzadeh et al., 2009). Due to the discrete nature of power system planning variables, each partial solution in static planning can be 0 or integer multiples of 1(Huanca et al., 2022). The number of circuits each branch is upgraded with is an integer. Static planning can be

extended to a multi-year context because it is simpler than dynamic planning and allows solutions for large-sized systems in a shorter period (Seifi & Sepasian, 2011).

In static planning, the decision maker is only interested in finding the optimal network configuration for the projected future year. The cost of expansion is determined at the start of the planning year (Inyanga et al., 2025; Romero et al., 2003). Equation (2.11) gives the optimal solution for static planning (Seifi & Sepasian, 2011).

$$S^k = [\, s_1^k \quad s_2^k \quad \dots \quad s_n^k] \tag{2.11}$$

An optimal configuration (S^k) from the candidate pool (k) is formed by a set of candidate lines (n). Equation (2.11) solves the optimal set of transmission lines (s) from a candidate plan (k) to upgrade transmission corridors in a single planning stage.

Dynamic Planning

Dynamic planning focuses on a multi-stage planning horizon. TNEP is typically a dynamic problem. In dynamic planning, several stages that may be varied are considered. The period may either be year-by-year, or a horizon-year with extrapolation to fill the intermediate years. Going from the initial year through the horizon makes dynamic planning very complex and large. Dynamic planning is a realistic representation of TNEP despite the computational effort required to obtain an optimal solution (Refaat et al., 2021).

Besides the where and what of transmission facilities to be added to the network, when the grid reinforcements should be implemented is also defined in the solution given by Equation (2.12) (Seifi & Sepasian, 2011).

$$\begin{aligned} S_t^k \quad = \quad [\quad & s_{11}^k \quad s_{12}^k \quad \dots \, s_{1n}^k \\ & s_{21}^k \quad s_{22}^k \quad \dots \, s_{2n}^k \\ & \qquad\qquad s_{y1}^k \quad s_{y2}^k \quad \dots \quad s_{yn}^k \,] \end{aligned} \tag{2.12}$$

An optimal configuration (S_t^k), from candidate plan (k), for planning horizon (t) is formed by a set of candidate lines (n) in a series of semi-static problems (S_{yn}^k). The candidate lines (n) are selected during each planning stage (y). The planning horizon

equals the total number of planning stages. To attain a reasonable computational time, the dynamic problem is simplified by solving a series of static sub-problems called semi-static or quasi-static problems. Figure 2.8 shows the Static and Dynamic TNEP periods (Seifi & Sepasian, 2011).

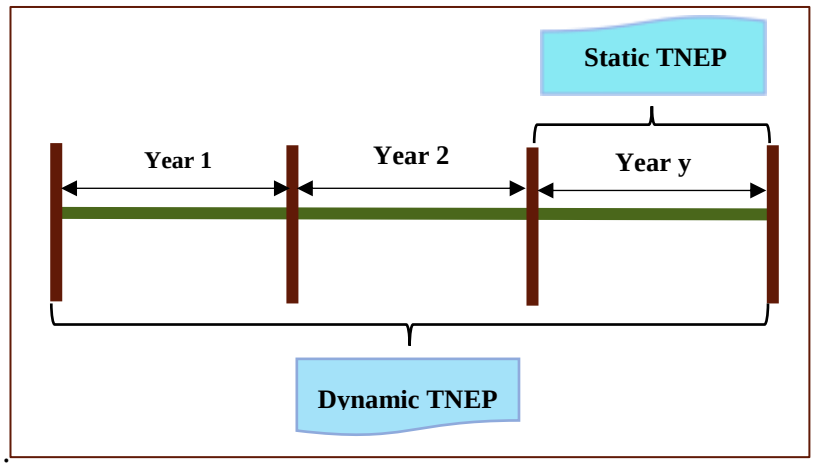

Figure 2.8: Static and Dynamic Transmission Expansion Planning Periods

In Figure 2.8, static TNEP plans for a single stage (Year y), while dynamic TNEP plans for multiple stages from (Year 1) through to the final planning year (Year y).

In a dynamic TNEP problem, economic and financial considerations are applied to the results of each stage to cater for uncertainties associated with capital costs and advanced to the following year over the entire planning period (Inyanga et al., 2025; Romero et al., 2003).

II. Long-term versus short-term planning

A period of less than one year falls into short-term planning, useful for power systems operation planning. Operation planning includes unit commitment, economic dispatch, load power flow and load management, scheduling system maintenance and planning fuel procurement. Long-term planning ranges from a year to decades. Long-term planning is employed to determine the expansion plans for system generation and transmission, regulate tariff and facilitate energy trading (Kwang & Zita, 2020; Seifi & Sepasian, 2011).

III. Bulk power system planning versus Distribution planning

Bulk power system planning includes both generation and transmission planning because of their inherent interdependencies (Conejo et al., 2016; Seifi & Sepasian, 2011). To address forecasted load demand, generation capacity is expanded. In tandem, the transmission network is enhanced to transfer the supplied power to the load centers (Conejo et al., 2016; Kaekhoungning et al., 2022; Kwang & Zita, 2020). Often bulk power system planning includes the acquiring of new land, whether for the construction of power plants or for establishing transmission right-of-way (Monteiro & Zambroni De Souza, 2021; Seifi & Sepasian, 2011).

Distribution planning focuses on distribution lines and often makes use of available roadside utility right-of-way. Figure 2.9 shows a typical distribution network (Seifi & Sepasian, 2011).

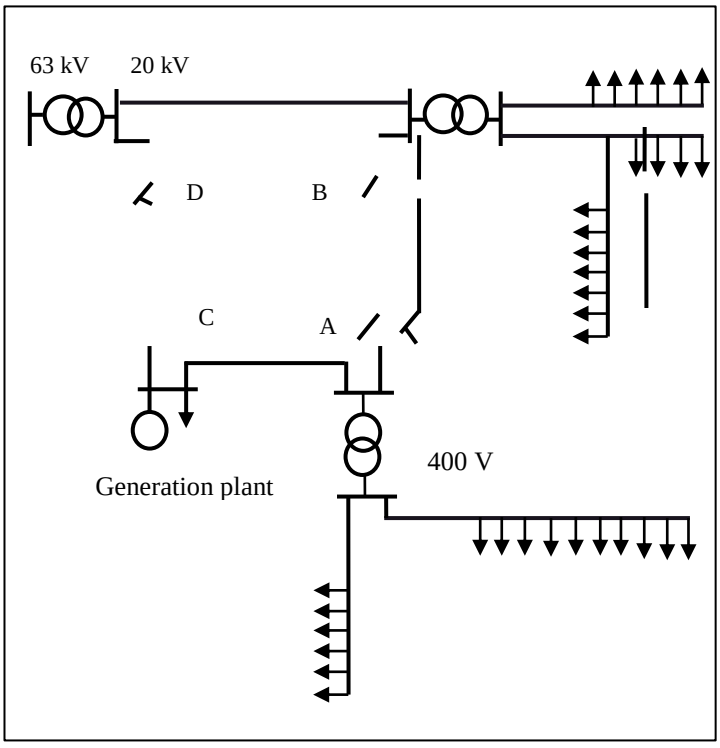

Figure 2.9: A typical Radial Distribution Network

In Figure 2.9, the distribution network voltage profile starts from a 63 kV: 20 kV substation with loads via the 20 kV and 400 V feeders (Seifi & Sepasian, 2011; Shivaie

et al., 2019; Zhang & Pal, 2006). A, B, C and D are switches. Switches A and B are the normally open while C and D are the normally closed switches (Kwang & Zita, 2020; Seifi & Sepasian, 2011; Zhang & Pal, 2006). In current industrial practices, a small generation plant is connected to the network in line with DGs. Both transmission and distribution networks comprise lines, substations and generators. A distribution network being planned or operated radially is a characteristic that separates it from transmission planning.

2.4.2 Power System Planning Components

Power system planning incorporates load forecasting, generation resources and transmission networks to come up with a feasible expansion plan. The generation capacity needs to expand for a forecasted load demand, prompting transmission network expansion to evacuate the additional power for supply to the load centers (Seifi & Sepasian, 2011).

I. Load forecasting

Load forecasting predicts the peak load demand which is critical in identifying the total load for which to plan. From the forecasted load, the annual load factor can be calculated by Equation (2.13) (Seifi & Sepasian, 2011).

$$L.F_{Annual} = \frac{\text{total annual energy demand (MWh)}}{\text{peak load (MW)}\times 8760} \tag{2.13}$$

The annual load factor $L.F_{Annual}$ is the ratio of annual total energy demand (MWh) to the peak load (MW). The load factor measures the utilization rate of the energy. A high load factor indicates that the total plant capacity is utilized for the maximum period, thus lowering the cost of generating electricity (Seifi & Sepasian, 2011).

The parameters affecting load forecasting can be classified as time, economic and weather factors. Short-term time factors are characterized by sudden changes in weather such that a sunny day increases solar isolation, leading to increased use of cooling appliances. Medium-term time factors are characterized by seasonal climate change. During the winter season, people stay indoors and switch on heating

appliances to keep warm, increasing the consumption of electricity. In the summer, there is an increased usage of cooling appliances when the temperature rises. Long-term time factors are characterized by changes in the gross national product implying economic growth and a growing population, which increases power demand. The daily load pattern based on daily activities of people such as working, leisure and sleeping hours also varies the daily load demand (Seifi & Sepasian, 2011).

In economic factors, a high population growth rate, industry development in a particular area, and Gross Domestic Product (GDP) increases power consumption. When the price of electricity is affordable, the electricity consumption also increases (Azeem et al., 2021).

Weather condition factors such as temperature rise and fall increase the use of cooling and heating appliances respectively, thus increasing load consumption. Increased wind speed increases the use of heating appliances for body warmth, thus increasing load consumption. When there is no cloud cover during the day, solar insolation is reduced lowering the use of cooling appliances (Azeem et al., 2021; Deshpande, 2009).

II. Generation requirement

Generation capacity must satisfy load demand. The amount of new generation capacity required is determined by the forecasted load demand and economic considerations. Generation Expansion Planning (GEP) is done after load forecast studies and must be sufficient for consumption and additional reserves for reliable power system operation. The installed generation capacity is greater than the expected peak demand to cater for any surge in load growth, to reduce power constraints under operating conditions such as sudden peak power demands and to allow for scheduled maintenance involving unit outages. The generation capacity margin is taken as 20 % for adequate generation security (Seifi & Sepasian, 2011; Wood et al., 2014).

The acquisition of new land for power plant construction, the availability and type of fuel needed for power generation, and the anticipated plant value are the key economic factors that influence generation requirement (Conejo et al., 2016). Additionally, the

power plant site should be easily accessible to the transmission network to facilitate evacuation of the generated power (Conejo et al., 2016; Wood et al., 2014).

III. Transmission Network Expansion

Transmission network expansion involves expanding the network to meet the forecasted load under normal and contingency conditions. In network expansion planning, the amount of new generation capacity and the forecasted load demand have to be made available to the planner for an efficient network expansion plan. GEP is interdependent with TNEP and is initiated by an increase in demand from the load forecasts along a planning horizon. TNEP is necessary to meet power system requirements for the future demand and generation configuration without violating any operational constraints (Niharika & Mukherjee, 2016).

2.5 Transmission Network Expansion Planning

An optimal TNEP solution provides reliable service to all customers, minimizes investment costs, reduces power losses, meets environmental regulations, alleviates network congestion, maximizes social welfare, and/or minimizes generation re-dispatching expenses (Inyanga et al., 2025; Kwang & Zita, 2020; Seifi & Sepasian, 2011). Both certain and uncertain data are required to solve a TNEP problem. Certain data are known at the time of planning while uncertain data are not. Uncertain data can be caused by environmental regulation, inflation and interest rates, economic growth, demand growth, and available technologies. Non-random uncertainties cannot be repeated or statistically represented from past experiments, unlike random uncertainties. Random uncertainties are related to the availability of power system facilities, loads, and the generators' outputs. Transmission network expansion costs and shutting down of generators are grouped as non-random uncertainties. From the perspective of uncertainties in the power system, TNEP is divided into two categories, deterministic and non-deterministic TNEP (Saadat, 2002; Seifi & Sepasian, 2011);

i. Deterministic TNEP

Deterministic TNEP is formulated based on a single system operating profile, or the worst-case scenario, without taking into account the likelihood that the system condition will occur. The scenario can be the worst peak load demand level, loss of a generation unit, or N-1 contingency. Deterministic TNEP uses a fixed load forecast value for a defined planning horizon. This approach neglects the experience and future expectations of system input variables so that the expansion solution for the future condition is optimal only if it occurs as predicted. Power system inputs and conditions surrounding the operation and planning of power systems exhibit some degree of randomness but ignore the uncertainties of power systems. The transmission network is planned in a preventive mode to ensure the network is robust against all contingencies (Choi & Mount, 2006; Seifi & Sepasian, 2011).

ii. Non- deterministic / Probabilistic TNEP

TNEP, based on a non-deterministic approach, considers the historical or past observations of the input random variables and assigns a probability to which each of them will occur. Several possible scenarios are analyzed and evaluated using security and performance analysis criteria. The approaches used in TNEP include the probabilistic load flow, scenario techniques, decision analysis and probabilistic reliability criteria. Consideration of uncertainties helps to identify a robust plan that is satisfactory under a range of possible outcomes. In the non-deterministic approach, the TNEP problem is solved either by stochastic optimization-based formulation, where the expected value is used to formulate the objective function, or by using a decision-making framework. Non-deterministic TNEP is challenging because of the uncertainty and the variations in the size of loads at substations to be modelled (Abdelaziz, 2000; Choi & Mount, 2006).

2.6 Optimization of Transmission Network Expansion Plan

An optimization problem is modelled depending on available tools and algorithms for problem-solving and simplification possibilities while observing the required

accuracy. For any optimization problem, the decision variables, the constraint and the objective functions are decided upon (Seifi & Sepasian, 2011);

i. Decision/ Optimization variables

Decision variables are independent variables. The optimum values of the independent decision variables are determined and then used to determine other dependent variables. In an optimal TNEP problem, the total costs for the construction of transmission lines is the decision variable**,** and the dependent variables is either transmission system losses (Shayeghi et al., 2010), line maintenance costs (Alhamrouni et al., 2014) or both.

Figure 2.10 illustrates a two-dimensional solution space for two decision variables (Seifi & Sepasian, 2011).

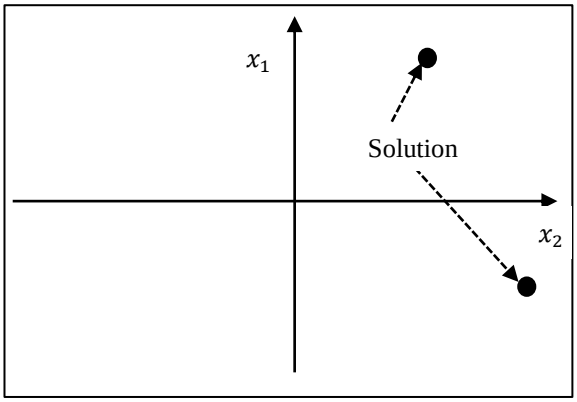

Figure 2.10: A Two-Dimensional Space

In Figure 2.10, (x_1) and (x_2) are the independent decision variables used to determine a solution. The solution falls at any point within the two-dimensional space.

ii. Constraint functions

Constraint functions determine if the defined decision variables lead to a feasible solution. Figure 2.11 shows feasible and non-feasible regions (Seifi & Sepasian, 2011).

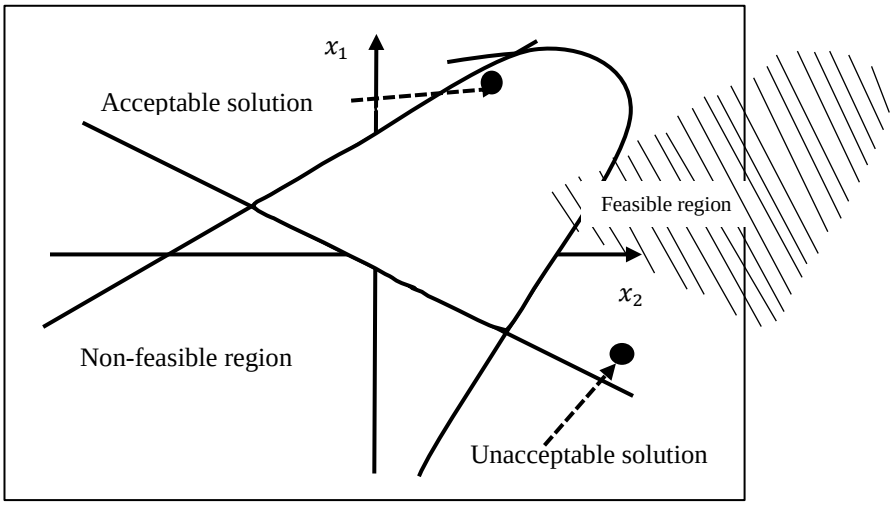

Figure 2.11: Feasible and Non-Feasible Regions Due To Constraints

Figure 2.11 shows x_1 and x_2 decision variables with the acceptable solution within the feasible region.

iii. Objective functions

An objective function is a function that is intended to be optimized with respect to the decision variables defined to give the desirable solution (Kwang & Zita, 2020; Seifi & Sepasian, 2011). A single problem is optimized in a single-objective function problem while multiple problems are optimized in a multi-objective function. Figure 2.12 shows optimum points in a two-dimensional solution space (Migliavacca, 2016; Seifi & Sepasian, 2011).

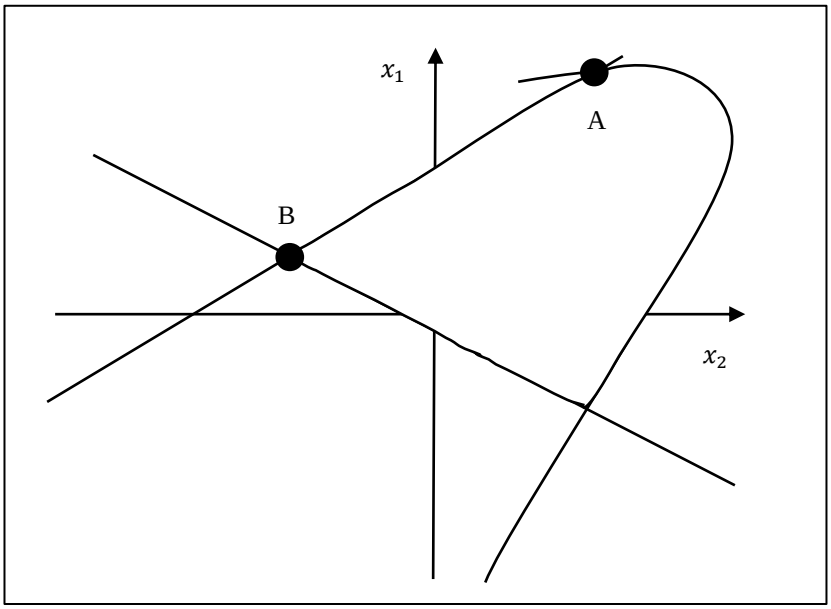

Figure 2.12: Two-Dimensional Space Optimum Points

In Figure 2.12, the objective function is optimizing a function of variable x_1. The maximization and minimization of this objective function are represented by solution point (A) for maximization and solution point (B) for minimization. Both points (A) and (B) fall in the feasible region of the solution space.

Figure 2.13 illustrates the local and global optimum points for a minimization problem (Seifi & Sepasian, 2011).

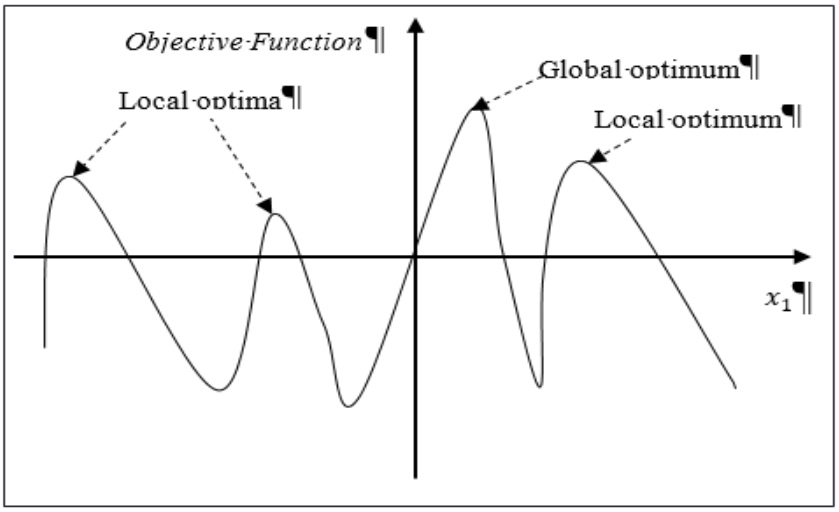

Figure 2.13: Local and Global Optimum Points for a Minimization Problem

In Figure 2.13, there are various local optima points and one global optimum point (Seifi & Sepasian, 2011).

2.6.1 Methods of Optimizing TNEP

The applied methods for solving TNEP are divided into three categories (Choi & Lee, 2022; Niharika & Mukherjee, 2016; Seifi & Sepasian, 2011);

I. Mathematical optimization models

Methods of mathematical optimization are categorized based on the features of the programming issues they are capable of addressing the optimal expansion plan derived from mathematically formulating the problem (Bizon et al., 2013; Seifi & Sepasian, 2011). Computation effort is reduced and the expansion plan simplified when selected aspects of the TNEP problem are focused on. The primary mathematical optimization methods for solving TNEP problem are discussed (M. Mahdavi, Sabillon Antunez, et al., 2018; Seifi & Sepasian, 2011).

i. Calculus methods

Calculus methods were used traditionally to seek optimum points. Continuous and differentiable functions of the objective and constraint terms use differential calculus, such as Lagrange multipliers, to locate the optimum points. Inequality constraints can only be applied when additional conditions of Kuhn-Tucker are observed, making the solution complex (Seifi & Sepasian, 2011).

ii. Linear Programming Method

Linear programming (LP) problems have linear objective functions, linear constraints, and continuous decision variables (Garver, 1970). Since maximizing (C_x) is equivalent to minimizing (-C_x) where (C_x) is the objective function of variable x , a LP problem can be stated as a minimization problem (Momoh & Lamine, 2010; Seifi & Sepasian, 2011). All constraints are equality type because any inequality constraint of the form given by Equations (2.14) and (2.15) can be transformed into an equality constraint as given by Equation (2.16) and Equation (2.17) respectively.

$$a_1' x_1 + a_2' x_2 + \cdots + a_n' x_n < b' \quad (2.14)$$

$$a_1'' x_1 + a_2'' x_2 + \cdots + a_n'' x_n > b'' \quad (2.15)$$

$$a_1' x_1 + a_2' x_2 + \cdots + a_n' x_n + x_{n+1}' = b' \quad (2.16)$$

$$a_1'' x_1 + a_2'' x_2 + \cdots + a_n'' x_n + x_{n+1}'' = b'' \quad (2.17)$$

, where x_{n+1}' and x_{n+1}'' are the surplus non-negative variables (Seifi & Sepasian, 2011). All decision variables are considered non-negative since any variable (x_j) unrestricted in sign can be written as in Equation (2.18) (Seifi & Sepasian, 2011).

$$x_j = x_j' - x_j'' \quad (2.18)$$

, where ($x_j' \geq 0$), ($x_j'' \leq 0$).

iii. Nonlinear programming

Nonlinear programming (NLP) is applied when the objective function and/or constraints are nonlinear functions of decision variables. The NLP methods include successive quadratic programming (SQP) and Newton's method. For an NLP constrained optimization, the constraints may be handled explicitly or converted into a sequence of unconstrained problems (Seifi & Sepasian, 2011).

NLP computations are based on derivatives. An iterative approach that uses gradient search necessitates the assessment of the first and possibly higher-order derivatives of the objective function (Kwang & Zita, 2020; Seifi & Sepasian, 2011). Second-order methods solves the second-order partial derivatives of the power-flow equations and other constraints (the Hessian) (Seifi & Sepasian, 2011; Sun et al., 2022).

iv. Dynamic Programming Method

Dynamic Programming (DP) method is used for multi-stage decision problems. In a multi-stage decision problem, optimal decisions are made over stages of different times. The result of one stage serves as the input to the subsequent stage while optimizing the overall objective function over all the stages (Seifi & Sepasian, 2011). A multi-stage decision problem is simplified and solved successively as single-stage problems (Rebennack et al., 2010). The optimal solution of the original problem is obtained from the single-stage problems' optimal solution during decomposition (Romero et al., 1996).

v. Integer Programming Method

Integer Programming (IP) restricts decision variables to integer values (Kwang' & El-Sharkawi, 2008; Seifi & Sepasian, 2011). Nevertheless, depending on problem's characteristics, mixed-integer programming for both linear and nonlinear IP methods has been developed.

Advantages of mathematical methods

i. Mathematical methods are effective in solving simple and linear optimization problems with a small search space
ii. A suitable convergence is obtained (Hemmatu et al., 2013).

Disadvantages of mathematical methods

i. Most mathematical-based algorithms guarantee to reach an optimal solution but do not always guarantee to reach a global optimum due to problem simplifications (Saadat, 2002).
ii. Managing power system equations in an optimization programming model is difficult (Niharika & Mukherjee, 2016).
iii. Only static studies can be carried out. Dynamic studies such as stability analysis cannot be performed (Hemmatu et al., 2013; Niharika & Mukherjee, 2016).

II. Heuristic Algorithms

Heuristic methods were adopted as the solution to the computation limitations of mathematical methods. Heuristic methods stepwise generate, evaluate and then select good expansion options based on search criteria defined by a planner in a heuristic function. The planner relates actual cost estimates from a given state to decide what nodes are next for exploration. The search is performed and terminated with the most feasible plan when it is unlikely to find a better plan. Heuristic algorithms were used to solve the TNEP problem by employing sensitivity analysis in the selection of a new transmission line added to a network (Garver, 1970).

Sensitivity analysis was performed using a sensitive indicator responsible for assessing the system performance and the expansion cost with respect to addition of transmission line. The sensitive indicator identifies the most attractive paths to which transmission lines can be added. This is achieved through checking the feasibility of the transmission network expansion plan for a given planning horizon to meet the demand without congestion or load shedding. If unfeasibility is detected, addition of a

transmission line is promoted based on the sensitivity indicator. The system is updated upon addition of the new transmission line and power flow performed to check for congestion. Normal system operation converges the process to a solution (Gomes & Saraiva, 2016a).

Advantages of Heuristic methods

i. Heuristic methods have faster convergence time and less computational effort compared to mathematical methods.
ii. Implementing heuristic methods is easy and dynamic studies can be performed (Hemmatu et al., 2013).

Disadvantages of heuristic methods

i. The resulting solution may not reach the global optimal solution
ii. More computation effort is required when applied to large-scale TNEP problems than for small-scale TNEP problems (Hemmatu et al., 2013).

III. Metaheuristics approach

The metaheuristic approach solves TNEP problems by combining features of mathematical optimization and heuristic methods, and applying the heuristic techniques iteratively to find good solutions using smart criteria (Kwang & Zita, 2020). The main metaheuristic approaches are (Kaekhoungning et al., 2022; Seifi & Sepasian, 2011):- Genetic Algorithm (GA) (Abdelaziz, 2000; Kwang & Zita, 2020; Kwang' & El-Sharkawi, 2008; Seifi & Sepasian, 2011), Simulated Annealing (SA) (Kwang & Zita, 2020; Romero et al., 1996; Seifi & Sepasian, 2011), Ant Colony Optimization (ACO) algorithm (Alvarez et al., 2018; Kwang & Zita, 2020; Seifi & Sepasian, 2011), Tabu Search (TS) (Kwang & Zita, 2020; Seifi & Sepasian, 2011; E. L. Silva et al., 2001) and Particle Swarm Optimization (PSO) algorithm (Abuishaiba et al., 2019; Kwang & Zita, 2020; Nezamabadi-pour et al., 2008; Refaat et al., 2021; Seifi & Sepasian, 2011) as discussed.

i. Genetic Algorithm

Genetic Algorithm (GA) is based on genetics and evolution. The decision variables in this context can be binary, continuous or represented as integer-coded called the problem chromosome (Seifi & Sepasian, 2011). These chromosomes are drawn from an evolving population. The fitness of each problem chromosome is evaluated using an objective function, which then informs the subsequent population (Seifi & Sepasian, 2011).

GA drives evolution through a sequential and iterative process that involves selection, crossover, and mutation operators. Initial chromosomes serve parents while regenerated chromosomes yield offspring (Kwang & Zita, 2020; Kwang' & El-Sharkawi, 2008; Seifi & Sepasian, 2011). The regeneration process aims to produce chromosomes with enhanced fitness values, ideally leading to a state where no further improvements can be made. Each gene within the chromosome is encoded as an integer representing the transmission line affected and the type of modification to be made on the line. The gene of the chromosome can store 0, indicating the absence of modification in the corresponding line, or a different value integer from 0, indicating the modification on the line or the number of transmission lines added to that particular transmission corridor to improve the fitness values. GA searches and gets to the global optimum vicinity but does not always convergence onto the global optimum point (Abdelaziz, 2000).

ii. Simulated Annealing Optimization

Simulated Annealing (SA) is based on thermodynamics principles. Metal atoms at a high temperature are unstable and during cooling, search for an energy state which is lower than their present state. SA algorithm is adaptable for handling combined optimization challenges and can be applied deal with combined optimization problems that may involve discontinuous, non-differentiable and non-convex functions. The optimization goal is to bring a system from the present state to a state with minimum possible energy. At each step, SA considers a neighboring state and then probabilistically decides between moving the system to that state and staying in the

old state until a state of equilibrium is reached (Kwang' & El-Sharkawi, 2008; Seifi & Sepasian, 2011).

The SA algorithm for the TNEP problem starts with identifying initial temperature, definitions of the initial number of iterations and the total number of candidate lines as the control parameters (Kwang & Zita, 2020). The iteration is increased until a termination criterion is satisfied. If the loss of load for the current configuration is smaller than tolerance, the removal, swap or addition of the selected candidate line is simulated. If the stopping criterion is satisfied, a local search is performed for the last temperature level, providing solutions in thermal equilibrium to obtain the optimal solution. SA algorithm is capable of finding the global optimum with a high probability due to its extensive global search. The main drawback of SA is the large number of function evaluations, which increases computation time and system requirements (Romero et al., 1996).

iii. Particle Swarm Optimization

The Particle Swarm Optimization (PSO) algorithm imitates the behavior of biological swarms, such as fish swarms and birds flock (Seifi & Sepasian, 2011). In PSO algorithm, particles in a swarm, move around in a search space to obtain the best solution to an optimization problem. PSO algorithm adjusts trajectories of a population of particles through the problem space based on the information about each particle's and the particle's neighbors best previous performances (Refaat et al., 2021; Seifi & Sepasian, 2011).

A potential problem solution is represented in D-dimensional space as a particle with coordinates (x_d) and a rate of velocity change (v_d). The *i* particle is represented by ($X_i = (x_{i1}, x_{i2} \ldots x_{id})$). Each particle tracks its coordinates in the dimensional space relating to the fitness function solution attained so far. The fitness value is stored as ($P_{i=} p_{i1}, p_{i2} \ldots p_{id}$) to represent personal best value (p_{best}) and global best value (g_{best}). The particle *i* changes position based on its velocity ($V_i = (v_{i1}, v_{i2} \ldots v_{id})$). The velocity and position updating equations for the particle *i* are given by Equations (2.19) and (2.20) respectively (Abuishaiba et al., 2019; Nezamabadi-pour et al., 2008).

$$v_{id}(\mathrm{t}+1) = w \times\ v(t) + c_1 r_1(p_{id} - x_{id}(\mathrm{t})) + c_2 r_2(p_{gd} - x_{id}(\mathrm{t})) \quad (2.19)$$

$$x_{id}(\mathrm{t}+1) = x_{id}(\mathrm{t}) + v_{id}(\mathrm{t}+1) \quad (2.20)$$

, where;

p_{id}, p_{gd} -historical and the global best solutions of the particle i respectively.

v_{id}, x_{id} -velocity and position for particle i respectively

c_1, c_2 - position constants

r_1, r_2 - constant random values generated between [0, 1]

t -the current iteration number

w -inertia weight.

In Equation (2.19), the terms $c_1 r_1(p_{id} - x_{id}(\mathrm{t}))$ and $c_2 r_2(p_{gd} - x_{id}(\mathrm{t}))$ represent the cognitive movement and the social behavior for finding the global best solution. Inertia weight is updated with each iteration as shown by Equation (2.21).

$$w_i = w_{imax} - \frac{w_{imax} - w_{imin}}{t_{imax}}\ t_i \quad (2.21)$$

, where;

w_i -inertia weight

w_{imax} -maximum inertia weight

w_{imin} -minimum inertia weight

t_{imax} -maximum iteration number.

PSO algorithm procedure is repeated until the maximum iteration or the minimum error is reached as the stopping criteria. PSO employs a simple methodology and

outperforms gradient-based optimization techniques that necessitate the differentiability of the optimization problem (Kwang' & El-Sharkawi, 2008). Additionally, PSO can effectively tackle problems addressed by GA without the challenges related to convergence speed and achieving the global optima solution (Kwang & Zita, 2020; Nezamabadi-pour et al., 2008).

vi. Binary Particle Swarm Optimization

Binary Particle Swarm Optimization **(**BPSO) (Kwang & Zita, 2020; Seifi & Sepasian, 2011) is a variant of PSO that allows the computation of discrete variable-type problems, like TNEP. The moving velocity for the particles in the search space is the probability that a bit will be in one state or the other in a space constrained between 0 and 1 values on each dimension (Kwang & Zita, 2020). The cognitive and the social behavior terms in Equation (2.19) can take values -1, 1, or 0 with the velocity constrained to the interval [0.0. 1.0] by the definition of a logistic function transformation (S (v_{id})) as given in Equation (2.22) (Meisam M. & Amir, 2018; Nezamabadi-pour et al., 2008).

$$S\,(v_{id}) = Sigmoid(v_{id}) = \frac{1}{1+e^{-v_{id}}} \tag{2.22}$$

Position update is performed by comparison of a randomly generated number with the update velocity given as in Equation (2.23).

$$if\ rand(\,) < S\big(v_{id}(t+1)\big)\ then, \quad x_{id}(t+1) = 1$$
$$else \quad x_{id}(t+1) = 0 \tag{2.23}$$

BPSO algorithm has a higher convergence speed compared to continuous-valued PSO and applies to discrete-valued problems such as TNEP problems. The drawbacks of BPSO are the tendency to get stuck in local optima and that the particle position update is not realized by the position and velocity information as in the case of continuous PSO. Big values of velocity show improper particle position with a big distance to reach the optimum position, while small velocity values imply near optimum solution for which velocity becomes zero (Nezamabadi-pour et al., 2008).

iv. Tabu Search

Tabu refers to things that cannot be touched because they are sacred. Tabu Search (TS) algorithm employs a neighborhood search procedure to iteratively move from one potential solution to another while seeking improvements on the best solution encountered (Bizon et al., 2013). The implementation of TS uses memory structures that describe the visited solutions. A solution previously visited within a certain short-time period, or that violated a rule is marked as tabu so that TS does not consider that possibility repeatedly (Seifi & Sepasian, 2011).

In application to transmission network expansion, the network is not fully connected because of new generation or load centers. Non-tabu candidate lines with minimum costs are added to connect the network. The fundamental principles in the application of the TS algorithm application include, initially the neighborhood search movement that derives the present solution as a collection of all feasible solutions by either removing or adding a candidate line; next, the Tabu list and aspiration criterion that help to avoid cycles and limit the inclusion of a large number of parallel circuits unless the addition leads to improvement; third is intensification where a candidate circuit previously built is swapped for another for solutions with smaller investment costs, then to more expensive solutions to bypass optimal local solutions within the feasible region and finally, diversification which aggressively searches the unexplored regions of the search space using the long-term memory of TS algorithm (Kwang & Zita, 2020). The search makes the most frequented candidate line a tabu for the next expansion plan. The drawback of TS is that optimality cannot be assured (E. L. Silva et al., 2001).

v. Ant Colony Optimization

Ant Colony Optimization (ACO) algorithm is inspired by the ability of ants to navigate the shortest path from their colonies to food sources, regardless of obstacles on their way. As they move, each ant leaves behind a trail of pheromone chemical (Kwang & Zita, 2020; Seifi & Sepasian, 2011; Ude et al., 2019). All ants initially search for food in a random manner. For constant speed, the ant that finds food faster returns to the nest sooner depositing more pheromone along its path. The path richer in pheromone

is recognized as a promising path by the remaining ants (Kwang & Zita, 2020; Seifi & Sepasian, 2011).

The path to be chosen represents the eligible branches to receive reinforcement in an expansion plan. The rules applied in ACO are the state transition rule characterized by the addition of a transmission line to the network presented by the artificial ant as the lowest in cost for a specific year within the planning horizon, and the pheromone updating rule presenting the numerical values associated with pheromones deposits on the branches, which indicate the search intensity in the direction of previously established solutions (Alvarez et al., 2018).

Advantages of the Metaheuristic Approach

i. Metaheuristic methods yield better results with less computation burden for large-scale TNEP problems compared to heuristic algorithms (Choi & Lee, 2022; Seifi & Sepasian, 2011).
ii. Metaheuristic methods have the capacity to find good or suboptimal solutions when used for large power system planning.

Disadvantage of the Metaheuristic approach

i. With the metaheuristic approach, the larger the number of function evaluations, the more the computation time and system requirements (Choi & Lee, 2022).

2.6.2 Candidate Line Selection

In real systems, the primary cost of a line comes from the cost of acquisition for the right-of-way also referred to as corridor, which includes where the transmission line traverses (Seifi & Sepasian, 2011). Various alternatives arise for accommodating various capacities or different types of transmission lines within the acquired right-of-way (Kwang' & El-Sharkawi, 2008; Seifi & Sepasian, 2011). The approach yielding the optimal solution starts by identifying the least cost corridors, then choosing from the corridors the types and capacities of the required transmission lines (Seifi & Sepasian, 2011). The transmission lines may be of single-circuit with one set of three conductors designed to carry a specific capacity A, double-circuit with two

independent sets of three conductors having the same capacity A or two single-circuit type with two separate circuits operating at different capacities A and B. For a given power system transmission network, taking existing transmission lines as N, planned candidate transmission lines as M and the number of candidate lines feasible in each transmission branch, K, Equations (2.24) - (2.26) are formed (Jenkins et al., 2012).

$$(K+1)^M \tag{2.24}$$

$$\frac{K\times M}{K+1}+N \tag{2.25}$$

$$\left[1+N+\frac{K\times M}{K+1}\right] \tag{2.26}$$

Equations (2.24) -(2.26) give all the possible layouts of the transmission network system for the planned candidate transmission lines, the average number of contingencies and the load flow solutions for each network layout. A large candidate pool for transmission line selection is thus created. Consider Figure 2.14 of Garver's 6-bus test system (Inyanga et al., 2025; Kavitha & Swarup, 2010).

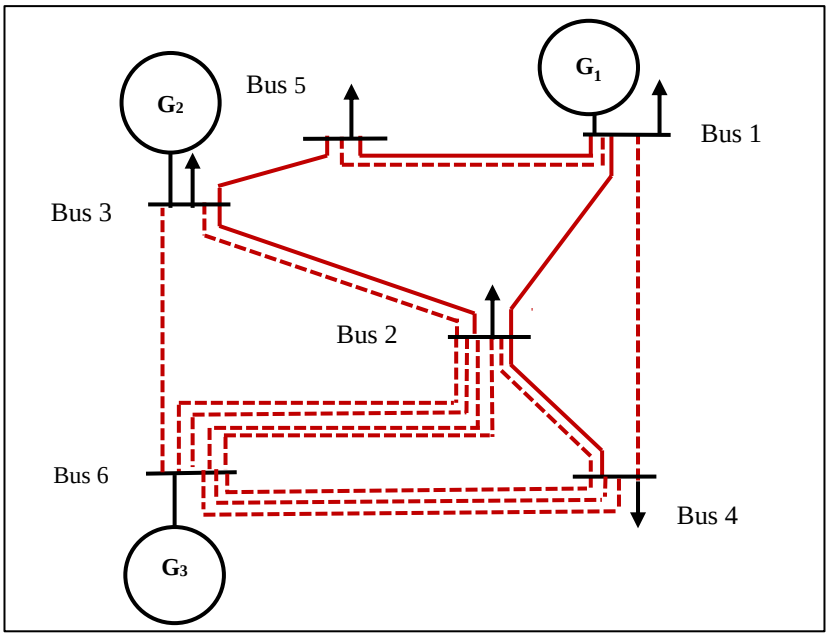

Figure 2.14: Garver's 6-Bus Test System

The Garver's 6-bus test system has 6 existing transmission lines, and 11 planned candidate transmission lines marked by dashed lines. Employing Equations (2.24) - (2.26), there are (5.0 x 10^{11}) possible network layouts, each layout having 9 possible

contingencies and 16 load flow solutions. The higher the number of candidate lines, the higher the solution time. The candidate lines are, however, not all feasible candidates as there may be violations in either their normal or N-1 reliability conditions. The strategies used to narrow down the candidate pool for the best transmission line selection and minimize solution time include first, generation of potential candidates between any two substations, second, removal of the non-feasible candidate lines violating the environmental limitations and defined constraints during the normal operating conditions, and finally, selection of most attractive candidate lines with the least investment costs. The selection is dependent on the planner's expertise in transmission lines and network expansion (Jenkins et al., 2012; Kwang' & El-Sharkawi, 2008; Seifi & Sepasian, 2011).

2.7 Transmission Network Expansion Models

Planning for a transmission network is a major issue in the electricity supply industry. Adequate models are employed to ensure the efficient operation of the power system. The transmission lines loading capacity is derived from the physical properties of the lines which comprises the type and the size of conductors, and the number of bundles (Seifi & Sepasian, 2011).

Integer decision variables are used to transform the TNEP problem into a mixed-integer optimization problem to capture the discrete and bundled nature of the transmission network. A binary decision variable can be employed by assigning it the value 1 if a transmission line is built, and 0 if no transmission line is built. Transmission expansion models are applied along with optimization methods to solve a TNEP problem. The transmission expansion models allow for load flow analysis to be performed to check the fitness for each candidate transmission line before addition to the transmission network. Transmission network models are limited in the handling of a disconnected system in the initial transmission planning stages when generators and loads have not been electrically connected to the network. It is also difficult to develop an efficient optimization technique and to work with large nonlinear problems arising from the objective function. After a transmission line is selected for addition, the system must obey all the load flow laws for the selected model. The transmission

network expansion models are the AC, DC, transport and hybrid models (Gomes & Saraiva, 2016a; H. Zhang et al., 2012).

2.7.1 AC Model

AC models have no simplification and are considered more accurate than other models. AC models allow for consideration of real and reactive power flow in the modeling. Both voltage and transient stability analysis are possible with AC models. The AC model objective function to minimize expansion costs of the transmission network $minimize\ C$ is given by Equation (2.27) (Wood et al., 2014).

$$minimize\ C = \sum_{i=1}^{NB} \sum_{j=1}^{NB} C_{ij} n_{ij} \tag{2.27}$$

Where;

NB -number of buses

C_{ij} -cost vector of the transmission circuit added to the transmission network

n_{ij} -number of added transmission lines from bus i to bus j.

The conventional equations of the AC power flow model taking the number of transmission lines n as variables are as given in Equations (2.28) and (2.29).

$$P(V, \theta, n) - P_G + P_D = 0 \tag{2.28}$$

$$Q(V, \theta, n) - Q_G + Q_D = 0 \tag{2.29}$$

Where;

P_G -power generation vector for real power

Q_G -generation vector for reactive power

P_D -real power demand

Q_D -reactive power demand

V -voltage magnitude vector

θ -phase angle (Kwang & Zita, 2020; Kwang' & El-Sharkawi, 2008).

The generator real and reactive power constraints are given in Equations (2.30) and (2.31) respectively (Rider et al., 2007).

$$P_{Gi}^{min} \leq P_{Gi} \leq P_{Gi}^{max} \tag{2.30}$$

$$Q_{Gi}^{min} \leq Q_{Gi} \leq Q_{Gi}^{max} \tag{2.31}$$

There is an allowable range for voltage magnitude at the bus i and the limit on maximum apparent power flowing through a transmission line n in the network system as given by Equations (2.32) and (2.33), respectively.

$$V^{min} \leq V_i \leq V^{max} \tag{2.32}$$

$$(n_i + n_i^0)S_i \leq (n_i + n_i^0)S_i^{max} \tag{2.33}$$

The constraints in Equations (2.33) and (2.34) solves the total number of transmission lines that can be added along a transmission corridor and the apparent power transmitted through the transmission line i (Kwang & Zita, 2020).

$$0 \leq n_i \leq n_i^{max} \tag{2.34}$$

$$S_i = P_i + jQ_i \qquad (i = 1, \dots, NB) \tag{2.35}$$

The capacity of a corridor to accommodate additional parallel lines at least cost determines the maximum number of lines n_i^{max} along that corridor (Conejo et al., 2016).

The constraints applicable when using AC power flow models are as given in Equations (2.28)-(2.35) (Inyanga et al., 2025). The vector elements for the AC power flow model (P (v, θ, n)), (Q (v, θ, n)) are calculated using Equations (2.36) and (2.37) (Kwang & Zita, 2020).

$$P_i(V, \theta, n) = V_i \sum_{j=1}^{NB} V_j \left[G_{ij}(n) cos\, \theta_{ij} + B_{ij}(n) sin\, \theta_{ij} \right] \tag{2.36}$$

$$Q_i(V, \theta, n) = V_i \sum_{j=1}^{NB} V_j \left[G_{ij}(n) \sin \theta_{ij} - B_{ij}(n) \cos \theta_{ij} \right] \tag{2.37}$$

Where;

ij -transmission line between buses i and j

$(\theta_{ij} = \theta_i - \theta_j)$ - buses i and j phase difference

n -number of transmission lines

G_{ij} -transmission line ij conductance

B_{ij} -transmission line ij susceptance.

The use of AC models in TNEP requires large computation effort despite being considered more accurate than other models (Rider et al., 2007; Wood et al., 2014).

2.7.2 DC Model

DC power flow models are used to reduce the computation effort experienced with the AC models in solving TNEP problems. DC models are linearized versions of the AC model with simplification assumptions. The DC models assume that the difference in phase angle between two ends of a transmission line is relatively small, the voltage magnitude at each bus is equal to 1.0 per unit and that transmission networks as lossless. DC model must, therefore, apply AC power flow at their final stage to ensure that all operational criteria and network constraints are respected (Seifi & Sepasian, 2011).

By applying all the assumptions, the mathematical formulation of the DC model is presented by Equation (2.27) reproduced here for ease of reference;

$$minimize\ C = \sum_{i=1}^{NB}\sum_{J=1}^{NB} C_{ij} n_{ij}$$

Equation (2.38) and Equation (2.39) are formed from the nonlinear equations corresponding to Kirchhoff's Current Law (KVL) given by Equation (2.28) and Equation (2.29) in the AC model.

$$P_{ij} = \frac{\left(\theta_i - \theta_j\right)}{X_i}$$

$$\left((i,j) = 1, \dots N\right)\left(i = 1, \dots n_j\right) \qquad (2.38)$$

$$Q_{IJ} = 0 \qquad (2.39)$$

When using DC models, Equations (2.31), (2.32) and (2.35) in the AC model are not considered since the reactive power flow in the transmission network system is neglected (Jenkins et al., 2012).

Like AC models, DC models are also subject to the constraint for real power in the generators given by Equation (2.30), the limit on maximum apparent power flowing through a transmission line i in Equation (2.33) and Equation (2.34) defining the

maximum number of transmission lines that can be constructed across a transmission corridor. The DC model active power balance at each node is enforced by the KCL Equation (2.28) from the AC model, and the KVL is represented by Equation (2.40).

$$P_l - B_l(n_l - n_l^0)\left(\theta_i - \theta_j\right) = 0 \qquad \left((i,j) = 1, \dots, n_j\right)(l = 1, \dots, n_l) \tag{2.40}$$

where;

n_l -transmission line l

B_l -transmission line l susceptance

$(\theta_i - \theta_j)$ -phase difference of the transmission line from buses i to j.

The simplifications applied to DC models make them suitable for solving long-term TNEP problems due to the reduced computation effort. The simplifications, however, make DC models less accurate than the AC models for TNEP problems (Choi & Lee, 2022).

2.7.3 Transport Model

The transport model is as a result of the relaxation of the Kirchhoff voltage law in Equation (2.40) applied in the DC model represented here for ease of reference.

$$P_l - B_l(n_l - n_l^0)\left(\theta_i - \theta_j\right) = 0 \qquad \left((i,j) = 1, \dots, n_j\right)(l = 1, \dots, n_l)$$

The relaxation eliminates nonlinearity in the transport model, transforming the TNEP problem into a mixed-integer linear programming problem that uses less computation effort while retaining the characteristics of the original DC model (Romero et al., 2002; Ude et al., 2019). The TNEP problem is transformed to a linear programming problem if the integrality of transmission line addition is relaxed by allowing for fractional capacities (Ude et al., 2019). However, this is not the case in practice as transmission capacities are usually available as discrete values. The expansion plans proposed using this model need to be further validated using a DC or an AC model to ensure that all the constraints are adhered to. Transport models are suitable when estimating the power exchange between areas and proposing possible transmission corridors (Gomes & Saraiva, 2016a; Jenkins et al., 2012; Wood et al., 2014).

2.7.4 Hybrid Model

Hybrid model combines features of DC and transport models. KCL is enforced on all buses, while KVL is only enforced on the existing circuits, leaving the candidate lines unrestricted. The model is easier to solve than the DC model although it is less accurate than the DC model (Gomes & Saraiva, 2016a; Jenkins et al., 2012; Seifi & Sepasian, 2011).

2.8 Related Studies

Garver introduced the earliest approach to solving the TNEP in 1970 where, the problem was represented as a power flow model and the most direct routes for transmission lines were identified by the LP algorithm (Bizon et al., 2013; Garver, 1970). Since that time, there has been significant research on TNEP with a variety of algorithms applied to tackle TNEP problems. The problem solution methods are; Genetic Algorithm (Abdelaziz, 2000), Greedy Randomized Adaptive Search Procedure (S. G. Binato et al., 2001), Simulated Annealing (Romero et al., 1996), Ant Colony Optimization (Alvarez et al., 2018), Differential Evolution (Sum-Im et al., 2009), Tabu Search (E. L. Silva et al., 2001), discrete PSO algorithm (Kennedy & Eberhart, 1997), Benders Decomposition algorithm (S. Binato et al., 2001), Artificial Intelligence (Al-Saba & El-Amin, 2002), and Minimum Cut theory (Chanda & Bhattacharjee, 1995). Other researchers considered parameters including power losses (Jalilzadeh et al., 2009; Shayeghi et al., 2010) transmission loading (Shayeghi et al., 2010) uncertainties in demand (Silva et al., 2005), N-1 reliability criteria (Fuerte Ledezma & Gutiérrez Alcaraz, 2020), and system reliability (Choi & Mount, 2006; I. D. J. Silva et al., 2005). BPSO has been used successfully for TNEP problems due to its ability to solve large-scale non-linear problems of discrete variables.

Meisam M. and B. Amir (Meisam M. & Amir, 2018) considered the transmission line adequacy for load demand support in studying the loading of transmission lines using BPSO algorithm. Ignoring the transmission network losses, a formulation to minimize the cost of additional line using DC power flow while considering the maximum transmission line loading of a network system was proposed. The methodology validation was tested on the Garver's 6-bus test system. It was concluded that adding

new transmission lines while considering the transmission lines thermal capacity produced a robust system. An expansion cost index on adequacy rate was defined in this approach to obtain best designs according to the cost of expansion and the network adequacy. Using expansion cost index on adequacy rate produced an optimized plan with low expansion cost for a specified adequacy.

Ledezma and Alcaraz (Fuerte Ledezma & Gutiérrez Alcaraz, 2020) solved the multistage expansion problem using hybridized BPSO algorithm. The BPSO algorithm was used for solution to the problem of investment cost while Quadratic programming was for the operational cost problem. In the problem formulation, the objective function included N-1 security and transmission losses parameters. To lower the computational effort associated with multistage TNEP, the line outage distribution factors were also added in the formulation of power flow considering the equality constraint of power balance, the generation capacity limit, the active power flow limit for transmission lines and the maximum number of transmission lines that can be added in a transmission right-of-way. Using Matlab 2014b and the IBM ILOG CPLEX Optimization Studio 12.5 for validation on the Garver's 6-bus test system, the results demonstrated that seven additional transmission lines were required and, that the transmission expansion capital cost and the time for convergence ware reduce for multi-stage TNEP.

Das et al. studied a multi-year AC transmission network expansion planning with security constraints to minimize the computational effort required for the solution of a dynamic security constrained AC-TNEP problem (S. Das et al., 2020). The solution methodology employed a decomposed approach that came up with solution strategies from simpler solutions of TNEP for the duration of the multi-stage solution process. Computation complexity is reduced by suitable truncation of the network variables sets into investment and operational variable parts and their successive solution. The model validation on Garver's 6-bus test system reduced the overall computation burden of solving the AC-TNEP problem by 98.7 %, even when generation and load uncertainties are considered.

Gomes and Saraiva (Gomes & Saraiva, 2016b) adopted a hybrid discrete evolutionary PSO (DEPSO) algorithm while to optimize DTNEP results while considering the total construction and the operation cost of transmission network. Using AC optimal power flow model, the generator capacity and the branch flow limits were imposed by the Constructive Heuristic Algorithm (CHA) to reduce the list of candidate lines, and the DEPSO algorithm for the TNEP. Illustrative tests on the IEEE 24-bus reliability test system using Matlab showed reduced search space and computation effort. The developed methodology produced better solutions of the multiyear TNEP problem with fewer particles and iterations compared to when DEPSO was used as a stand-alone.

2.9 Research Gap

Studies have been done on optimizing TNEP problems using different algorithms and models. Research that are based on DC power models are inadequate because they neglect the reactive power flow and bus voltage limits. AC models have also been used in relaxed mode to model the uncertainties and randomness of power systems. In most of these TNEP studies, the direct result of obeying voltage limit constraint on the formulation of DTNEP objective function has not been illustrated. The system condition resulting in congestion of power system and the application of reactive power compensation to mitigate the congestion has also not been illustrated. In this research work, a congested system is created from growing the system load demand in tandem with the generation requirement. For the congestion management, reactive power compensation is applied to the system until it can no longer operate adequately, justifying network expansion. The DTNEP problem considers voltage limits as a constraint in the cost formulation and the expansion results are optimized using IBPSO.

CHAPTER THREE

METHODOLOGY

This chapter gives an overview of how the research work was carried out. Presentation of the Garver's 6-bus and IEEE 30-bus test systems used in the research is done and the associated system data defined. Next, a discussion on the profile for load demand and the use of reactive power compensation to mitigate congestion is presented. Finally the mathematical formulation for DTNEP problem and the optimization algorithm applied to the DTNEP problem based on BPSO are presented as well as validation of the IBPSO algorithm.

3.1 Case Studies

The developed methodology which applies IBPSO algorithm to optimize DTNEP has been implemented on Garver's 6-bus and IEEE 30-bus test systems for illustrative tests (Inyanga et al., 2025).

3.1.1 Garver's 6-bus Test System

The single-line diagram of Garver's 6-bus test system used in TNEP is shown in Figure 3.1 (Garver, 1970; Inyanga et al., 2025).

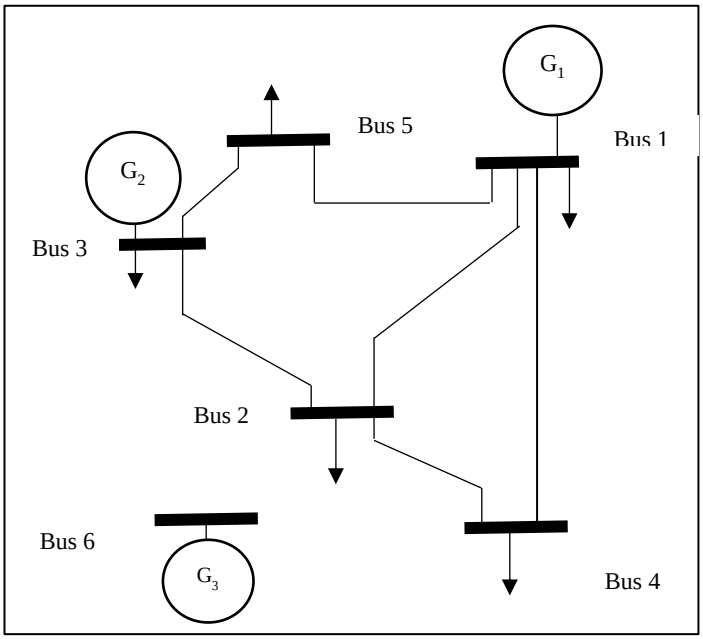

Figure 3.1: Single-Line Diagram of Garver's 6-Bus Test System

The Garver's 6-bus test system is made of six transmission lines and five buses. The Garver's 6-bus test system includes two generator buses, viz, Bus 1, which is the slack bus and has three 30 MW units and one 60 MW unit. Generator Bus 3 has two 60 MW units. There are also five load buses in the system. Bus 6 is taken as a pre-planned generator bus. The total active and reactive power demand is 190 MW and 38 MVAR, respectively. All the existing and pre-planned transmission right-of-way were feasible candidate transmission lines (Inyanga et al., 2025; Zhang & Pal, 2006). The data for Garver's 6-bus test system is presented in Appendix I.

3.1.2 IEEE 30-Bus Test System

The single-line diagram of IEEE 30-bus test system as documented in Matpower and used by researchers and students to perform power system studies is shown in Figure 3.2 (Mathworks, 2018; Tietze et al., 2008).

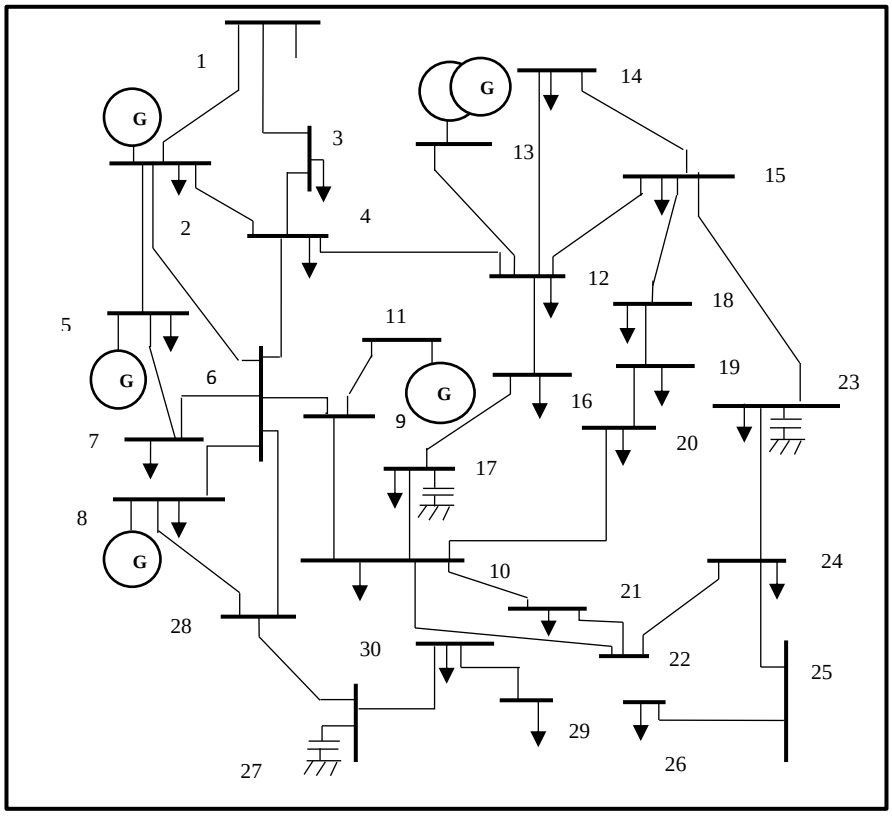

Figure 3.2: Single-Line Diagram for IEEE 30-Bus Test System.

The IEEE 30-bus system has 30 buses and 41 existing transmission lines. There are 5 generator buses; 26 to 30, and slack bus 25, with a total generation capacity of 335.0 MW. The load buses are 21 with a total system active and reactive power demand of 342.9 MW and 152.7 MVAR, respectively (Inyanga et al., 2025; Mathworks, 2018). All existing and pre-planned transmission corridors were considered feasible for candidate transmission lines. The IEEE 30-bus test system data is presented in Appendix 2.

3.2 Reactive Power Compensation

Simulations were performed on both the Garver's 6-bus (Garver, 1970) and IEEE 30-bus systems (Mathworks, 2018; Tietze et al., 2008) for a predicted load growth. The AC load flow was conducted on the test bus systems using the MATLAB Matpower toolbox. The system load demand was increased by 10 % at constant power factor on every load bus and the summation of the load increase in a single year taken as load demand for a new load center introduced in year 8 of the planning horizon. The new

load center is determined based on bus sensitivity performance during power flow simulations. As the load demand increased, so did the generation system requirement to cater for the power equality constraint. The interdependence between generation and transmission planning, therefore, assumes a uniform load growth rate. Every time the load demand increased, transmission thermal line loading and voltage magnitude performance in the power system were monitored. Reactive power was injected at buses with voltage magnitudes below 0.95 per unit in increments of 10 MVAr using shunt capacitors (Kundur, 1994; Seifi & Sepasian, 2011).

Congestion results when thermal line loading for the transmission lines is exceeded and/or bus voltage magnitude limits violate the defined deviation (5 % of the nominal voltage). The exceeded thermal loading limits of transmission lines and violated bus voltage magnitudes limits indicate power system congestion. Seven scenarios were simulated for the Garver's 6-bus test system as given in Table 3.1.

Table 3.1: Garver's 6-Bus Study Scenarios.

Parameters	**Base case**	**Case I**	**Case II**	**Case III**	**Case IV**	**Case V**	**Case VI**
Load growth	0 %	0 %	10 %	20 %	30 %	30 %	40 %
Load demand (MW)	190.0	190.00	209	230	252.58	252.58	277.95
Generating capacity added	3 x 30 MW at Bus 1, 2 x 60 MW at Bus 3		3 x 30 MW at Bus 1, 2 x 60 MW at Bus 3, 1 x 60 MW at Bus 1				3 x 30 MW at Bus 1, 2 x 60 MW at Bus 3, 1 x 60 MW at Bus 1, 1 x 120 MW at Bus 3
Reactive power injection (MVAr)	0	10	10	10	10	20	20

More generating units were brought online as the load demand was increased; one 60 MW unit at Bus 1 after 10 % load increase and two 60 MW at Bus 3 after 40 % load increase respectively. Reactive power compensation was also performed in Cases I and V to manage congestion resulting from bus voltage magnitude lower limit violation. The voltage magnitudes values were below the 0.95 pu lower limit. In Case I and Case V, reactive power of 10 MVAr each was applied at the buses to improve their voltages.

IEEE 30-bus test system simulation resulted in four scenarios as given in Table 3.2.

Table 3.2: IEEE 30-Bus Study Scenarios

Parameters	**Base case**	**Case I**	**Case II**	**Case III**
Load growth	0 %	10 %	10 %	20 %
Load demand (MW)	283.4	311.74	311.74	342.81
Generating units added	362.8 MW at Bus 1	362.8 MW at Bus 1	362.8 MW at Bus 1	362.8 MW at Bus 1
Reactive power compensation (MVAr)	0	0	10	0

From Table 3.2, after increasing the load demand by 10 % in Case I, reactive power was injected in Case II to manage congestion resulting from bus voltage magnitude lower limit violation. At 20 % load growth, the system congestion could not be managed by reactive power compensation thus necessitating DTNEP to alleviate the transmission network congestion

Figure 3.3 gives the research summary flowchart.

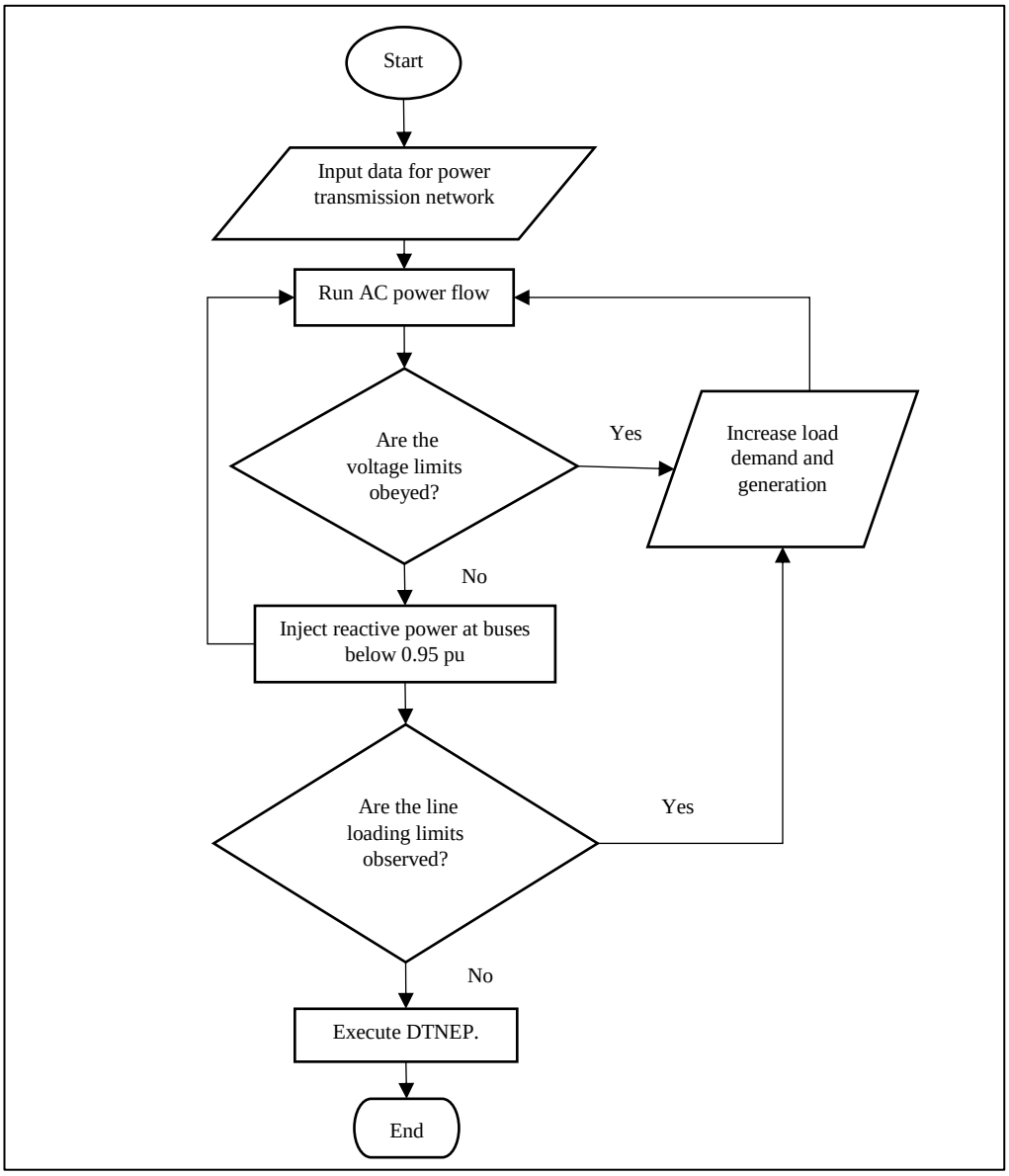

Figure 3.3: Research Summary Flowchart

In Figure 3.3, AC power flow was performed on the transmission network data and the voltage and transmission line loading were monitored for violations. If the system operation was found to be adequate, the load demand was grown in tandem with system generation requirements while still monitoring the bus voltages and transmission line loading limits. The system operation adequacy is assured when there is no congestion in the network system by checking for voltage limits alongside transmission line loading violations. For an adequate system operation, the load demand is increased**.** Suppose a bus voltage was under 0.95 pu, reactive power was

injected at that bus in increments of 10 MVAr to mitigate the congestion by restoring the voltage to within the defined range. The process was repeated and when system operation becomes inadequate, DTNEP is implemented.

3.3 DTNEP Problem Formulation

The objective function finds the solution to DTNEP problem to minimize the total cost of constructing additional transmission lines and the cost of transmission line losses. The voltage magnitude and the transmission line loading constraints are enforced in a fitness function.

3.3.1 Objective Function

The objective function for the DTNEP problem C , in this research work is represented by Equation (3.1) (Seifi & Sepasian, 2011).

$$minimize\ C = \sum_{t=1}^{N} \left[(1+k)^{t-1} \sum_{i=1}^{L_c} \left(CF_{t,i} + CL_{t,i} \right) \right] \qquad (3.1)$$

Where;

L_c -number of candidate lines for expansion

$CF_{t,i}$ -construction cost in US dollars for i candidate line in t expansion year

N -sum of planning stages in years

k -discounted inflation rate

$CL_{t,i}$ candidate line i cost of active power losses in US dollars for planning year t (Inyanga et al., 2025).

The economic and financial considerations are applied to DTNEP cost in Equation (3.1) to account for the uncertainties resulting from capital costs of expansion (Sohtaoglu, 1998). The inflation-adjusted discount rate is the disparity between the nominal discount and inflation rates, forming the relationship between the discount rate d and the inflation rate r . The inflation-adjusted discount rate is moved from one year to another over the planning period. Equation (3.2) gives inflation-adjusted discount rate k (Cassidy & Schirra, 1997; Delson, 1992).

$$1 + k = \frac{1 + d}{1 + r}$$

$$k = \frac{1 + d}{1 + r} - 1 \tag{3.2}$$

Equation (3.3) gives the formulation for the total annual cost of transmission losses.

$$CL_{t,i} = 8760 \times C_{MWh} \times K_{loss} \times Loss \tag{3.3}$$

Where;

C_{MWh} -cost per MWh of energy in US dollars

K_{loss} -loss coefficient

$Loss$ -total network loss in MW at the end of a planning year.

Loss coefficient caters for the changes in load voltages by coordinating transmission power losses of various loads. Typical value for K_{loss} is 0.5 (E. Mahdavi & Mahdavi, 2011). The annual load growth varies the transmission line loss and is time-dependent. The transmission line loss is given by Equation (3.4).

$$Loss = (LGC)^{t-1} \times P_{loss\,i,t} \tag{3.4}$$

, where LGC is the load growth coefficient. Variable LGC is included in the active power loss formulation for rapid return on investment through correct computation of the total expansion and operation costs (E. Mahdavi & Mahdavi, 2011; Shayeghi et al., 2009). The transmission line loss for year t, ($P_{loss\,i,\,t}$) is given by Equation (3.5).

$$P_{loss\,i,\,t} = I_i^2 \times R_i \tag{3.5}$$

Where I_i and R_i are the transmission line i current and the resistance of line i, respectively (Inyanga et al., 2025; Zhang & Pal, 2006).

The values for the objective function parameters are presented in Table 3.3 (Cassidy & Schirra, 1997; Delson, 1992; E. Mahdavi & Mahdavi, 2011; Sohtaoglu, 1998).

Table 3.3: Value of parameters for the objective function.

Parameter	Value
C_{MWh}	36.1
LGC	1.1
K_{loss}	0.5
k	4 %
d	15 %
r	10 %

Parameters C_{MWh}, LGC and K_{loss} give the unit of energy cost, the load growth coefficient and the loss coefficient simulating the changes in load (Inyanga et al., 2025). The economic and financial accounting in the total investment cost formulation are given by parameters k, d and r.

3.3.2 Constraints

The DTNEP objective function is subject to voltage constraint given in Equation (3.6),

$$\mathrm{V}_{imin} \leq \mathrm{V}_i \leq \mathrm{V}_{imax} \tag{3.6}$$

, and transmission line loading capacity in Equation (3.7).

$$|S_{ij}| \leq S_{ijmax} \tag{"3.7)"}$$

where minimum (V_{imin}) and maximum (V_{imax}) voltage magnitudes at the bus i are taken as 0.95 pu and 1.05 pu, respectively, in this work (Seifi & Sepasian, 2011) and S_{ij} is the apparent power flow through a transmission line connected between the bus i and j. Constraints in Equations (3.6) and (3.7) are the nonlinearities in the DTNEP problem formulation which are constrained by a fitness function in Equation (3.8) to realize the best solution.

$$FF = C + P_1 + P_2 \tag{3.8}$$

where;

FF -fitness function

C -total investment cost of network expansion

P_1, P_2 -equality and inequality constraint penalty functions respectively.

The system power supply meets the load demand in the equality constraint P_1. The value for P_1 is therefore taken as 0. The inequality constraint penalty function P_2 is summed as in Equation (3.9).

$$P_2 = \beta(\sum_{i=1}^{NB} f(V_i) + \sum_{i=1}^{n} f(S_{ij})) \tag{3.9}$$

, where;

NB -number of buses

n -number of candidate transmission lines.

The penalty constant (β) is taken as 10,000,000 US dollars per unit deviation from the defined limits (Charles et al., 2020; Seifi & Sepasian, 2011). V_i and S_{ij} are sub-fractions that represent the distance to the feasible regions such that;

$$f(x) = \begin{cases} 0 & if\ x_{min} \le x \le x_{max} \\ x - x_{max} & if\ x > x_{max} \\ x_{min} - x & if\ x < x_{min} \end{cases}$$

x, represents the variable that is to be optimized.

3.4 Improved BPSO Algorithm for Optimizing DTNEP Results

BPSO algorithm used to solve discrete variable-type TNEP problems is derived from PSO algorithm. IBPSO algorithm is employed in this research work to overcome the shortcoming of BPSO algorithm being stuck in the local optima when optimizing DTNEP. The velocity update equation for the BPSO algorithm is as given in Equation (3.10).

$$v_{id}(\mathrm{t}+1) = v_{id}(t) + c_1 r_1(p_{id} - x_{id}(\mathrm{t})) + c_2 r_2(p_{gd} - x_{id}(\mathrm{t})) \tag{3.10}$$

, subject to

$$p_{id} - x_{id}(\mathrm{t}) = 1\,; \quad \text{if } p_{id} = 1, x_{id} = 0 \tag{3.11}$$

$$p_{id} - x_{id}(\mathrm{t}) = 0\,; \quad \text{if } p_{id}\,, x_{id} = 0 \; or \; p_{id}\,, x_{id} = 1 \tag{3.12}$$

$$p_{id} - x_{id}(\mathrm{t}) = -1\,; \quad \text{if } p_{id} = 0, x_{id} = 1 \tag{3.13}$$

$$p_{gd} - x_{id}(\mathrm{t}) = 1\,; \quad \text{if } p_{gd} = 1, x_{id} = 0 \tag{3.14}$$

$$p_{gd} - x_{id}(\mathrm{t}) = 0\,; \quad \text{if } p_{gd}\,, x_{id} = 0 \; or \; p_{gd}\,, x_{id} = 1 \tag{3.15}$$

$$p_{gd} - x_{id}(\mathrm{t}) = -1; \quad \text{if } p_{gd} = 0, x_{id} = 1 \tag{3.16}$$

where, t is the number of algorithm iterations and the velocity $v_{id}(\mathrm{t}+1)$ is a real number in the range [-V_{max}, V_{max}] (Bizon et al., 2013; Inyanga et al., 2025). To enable the addition of $v_{id}(\mathrm{t}+1)$ to $x_{id}(\mathrm{t})$; real and binary values respectively in Equation (3.11), the velocity transfer function defined must constrain the velocity to between 0 and 1 (Inyanga et al., 2025).

The probability function in IBPSO algorithm removes the drawback of big positive or negative values that produce a bigger probability for the particle position. The probability function is given in Equation (3.17) (Nezamabadi-pour et al., 2008).

$$S'(v_{id}) = 2 \times |sigmoid(v_{id}) - 0.5| \tag{3.17}$$

The IBPSO performance is also enhanced by the adoption of previous information of position in position update (Nezamabadi-pour et al., 2008) as given in Equations (3.18) and (3.19).

If $rand() < S'(v_{id}(t+1))$, *then*

$$x_{id}(t+1) = exchange\; x_{id}(t) \tag{3.18}$$

, else

$$x_{id}(t+1) = x_{id}(t) \tag{3.19}$$

A constant random number $rand$ between 0 and 1 is created and the value compared to $S(v_{id}(t+1))$ for particle i position update.

Figure 3.4 shows a flowchart summary of the IBPSO algorithm applied to DTNEP.

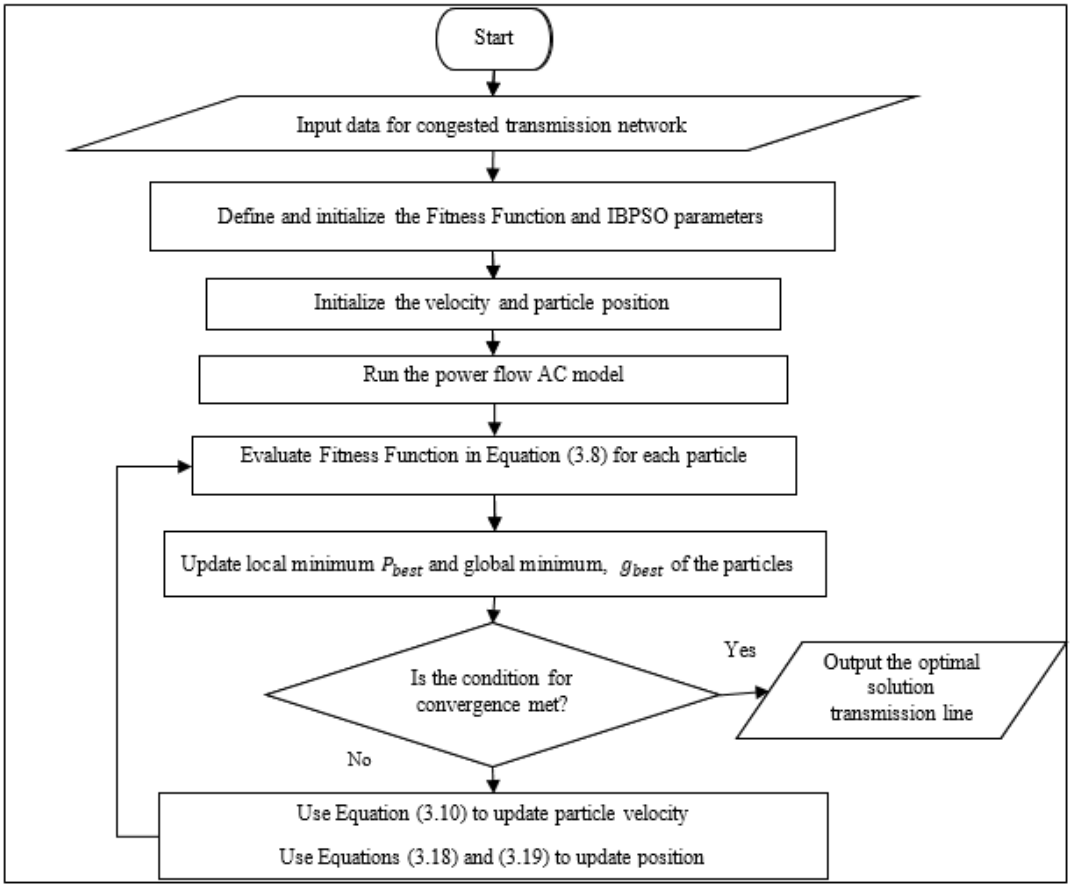

Figure 3.4: Flowchart of DTNEP Using IBPSO Algorithm

In Figure 3.4, the input was the data for the created congested system. The parameter values for the fitness function and IBPSO algorithm were subsequently defined. The particle position and velocity were set and how each candidate line performed examined using AC power flow. The initial P_{best} and g_{best} was determined for each particle and the value compared with the particle's fitness value, to renew P_{best} and g_{best} with the best fitness value. The Equation (3.10) to update velocity uses the probability function that allows particle to jump out of the local optima positions and Equations (3.18) and (3.19) uses historical data for position update. The output transmission line was selected once the convergence condition was met. Failing to meet the convergence condition, the particle velocity and position were updated, and the fitness function for each particle re-evaluated. The stopping condition for

convergence was attained when the maximum number of iterations or minimum error requirement was attained.

3.4 Effectiveness and Validation of IBPSO Algorithm

The effectiveness of the IBPSO algorithm developed was demonstrated by the IBPSO algorithm application on the Garver's 6-bus test system alongside the original BPSO algorithm. The convergence curves for IBPSO and BPSO algorithms were analyzed, and the total cost of expansion and the number of selected transmission lines compared to previous DTNEP research works for validation (Garver, 1970; Refaat et al., 2021). IBPSO algorithm was applied in the developed methodology neglecting and considering voltage limits for Garver's 6-bus and IEEE 30-bus test systems, and the voltage magnitudes, transmission line loading and the transmission lines active power losses monitored and analyzed for the two scenarios (Inyanga et al., 2025).

CHAPTER FOUR

RESULTS, DISCUSSION AND ANALYSIS

In this chapter, the Base load flow results for Garver's 6-bus and IEEE 30-bus test systems are first given followed by a presentation of the results from load demand growth and reactive power compensation. The IBPSO and BPSO algorithms as applied to DTNEP results for Garver's 6-bus system are then discussed. The output of IBPSO algorithm applied to optimize DTNEP results are for both Garver's 6-bus and IEEE 30-bus test systems are also presented and finally, the effectiveness and validation of the research methodology is given.

4.1 Base Cases Load Flow Results

The simulations of AC load flow were carried out on the Base cases of Garver's 6-bus and IEEE 30-bus test systems.

4.1.1 Garver's 6-bus System

The Garver's 6-bus Base case load flow results are presented in Table 4.1.

Table 4.1: Garver's 6-Bus System Load Flow Results

System Summary				
System components	**No. of components**	**Component parameter value**	**P (MW)**	**Q (MVAR)**
Generators	2	Online capacity	530.0	-20.0 to 149.0
Committed generators	2	Generation (actual)	191.9	47.7
Loads	5	Load (Fixed)	190.0	38.8
Shunt capacitors	1	Shunt	-0.0	9.4
Branches	6	Losses (I^2 *z)	1.91	19.11

From Table 4.1, Garver's 6-bus system had 5 buses and 2 generation centers with a total generation capacity of 530 MW. The active and reactive power demand was 190.0 MW and 38.8 MVAR respectively. The system's active transmission loss for the Base case load flow is 1.91 MW and the bus voltage results presented in Table 4.2.

Table 4.2: Garver's 6-Bus System Base Case Voltage Results

Bus Number	Voltage magnitude (pu)	Angle (radians)
1	1.0000	0.0000
2	0.9611	-3.5049
3	1.0000	3.8635
4	0.9404	-7.9513
5	0.9792	-1.5127

Table 4.2 shows the voltage at bus 4 was 0.9404, a violation of the 0.95 voltage lower limit.

4.1.2 IEEE 30-Bus System

The IEEE 30-bus system load flow results are given in Table 4.3.

Table 4.3: IEEE 30-Bus System Load Flow Results

System Summary				
System components	**No. of components**	**Component parameter value**	**P (MW)**	**Q (MVAR)**
Generators	6	Online capacity	900.2	-102.0 to 188.0
Committed generators	6	Generation (actual)	362.8	154.1
Loads (Fixed)	21	Load	283.4	126.2
Shunt capacitors	3	Shunt	-0.0	22.4
Branches	44	Losses (I^2 *Z)	1.048	8.85

From Table 4.3, the IEEE 30-bus had 30 buses and 6 generation centers having a total generation capacity of 900.2 MW. The active and reactive power demand for the simulation were 283.4 MW and 126.2 MVAR respectively. The system's active transmission loss was 1.048 MW and the bus voltage results presented in Table 4.4.

Table 4.4: IEEE 30-Bus Base Case Voltage Results

Bus No.	Voltage magnitude (pu)	Angle (radians)	Bus No.	Voltage magnitude (pu)	Angle (radians)	Bus No.	Voltage magnitude (pu)	Angle (radians)
1	1.0000	0.0000	15	0.9799	-17.9853	29	0.9661	-19.1246
2	1.0000	-6.3353	16	0.9875	-17.5622	30	0.9541	-20.0778
3	0.9783	-8.6944	17	0.9853	-17.9653	31	1.0000	0.0000
4	0.9740	-10.7001	18	0.9712	-18.6990	32	1.0000	-6.3353
5	1.0000	-16.2549	19	0.9694	-18.9087	33	0.9783	-8.6944
6	0.9829	-12.7845	20	0.9742	-18.6970	34	0.9740	-10.7002
7	0.9819	-14.7568	21	0.9792	-18.2935	35	1.0000	-16.2549
8	1.0000	-13.8616	22	0.9799	-18.2768	36	0.9829	-12.7845
9	0.9967	-16.0538	23	0.9716	-18.4504	37	0.9819	-14.7568
10	0.9919	-17.8050	24	0.9695	-18.6835	38	1.0000	-13.8616
11	1.0000	-16.0538	25	0.9746	-18.3169	39	0.9967	-16.0538
12	0.9984	-16.8501	26	0.9561	-18.7750	40	0.9919	-17.8051
13	1.0000	-16.8502	27	0.9867	-17.7998	41	1.0000	-16.0538
14	0.9837	-17.8540	28	0.9819	-13.5041			

There was no violation of the voltage limits for the IEEE 30-bus system Base case load flow. All the bus voltage magnitudes were maintained in the range of 0.95-1.05 pu.

4.2 Load Demand Growth and Reactive Power Compensation

The Load demand was raised by 10 % in every load bus at a constant power factor and the shunt capacitors used to inject reactive power at buses below 0.95 pu voltage magnitude.

4.2.1 Garver's 6-Bus System

At 10 % load growth, a 60 MW unit at Bus 3 was added. The 60 MW unit at Bus 3 was also brought online at 40 % load growth. The reactive power was injected at buses with voltages below 0.95 per unit using shunt capacitors in increments of 10 MVAr.

During the load growth and reactive power compensation for congestion mitigation, the bus voltage magnitudes, transmission lines loading, and active power losses were monitored.

Bus voltage magnitudes

The bus voltage magnitudes for the seven scenarios outlined in Chapter 3 are presented in Figure 4.1.

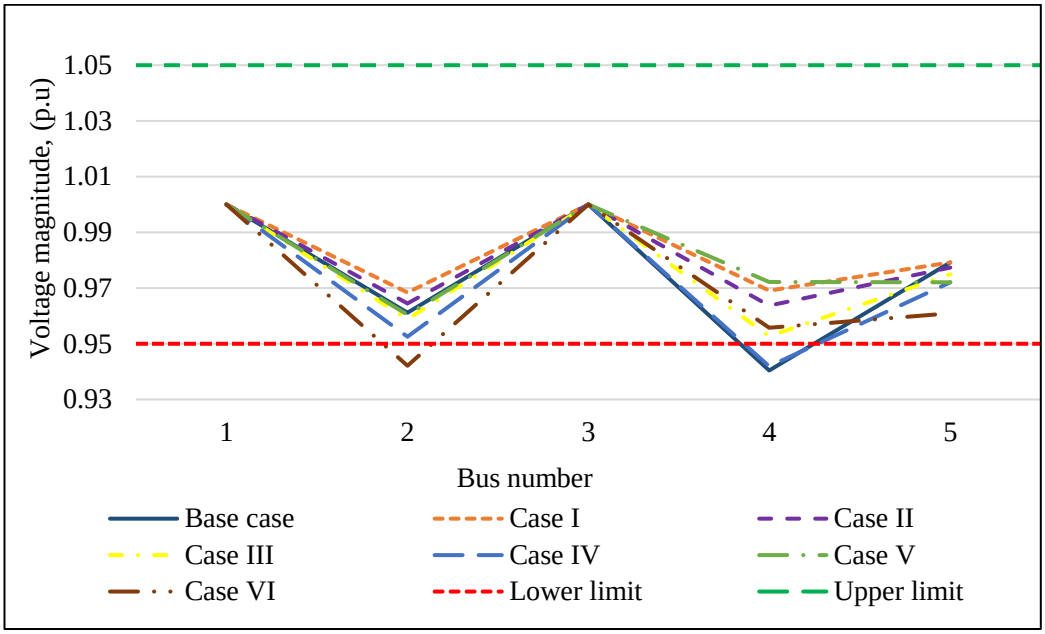

Figure 4.1: Garver's 6-Bus Voltage Magnitudes

Figure 4.1 shows the Base case voltage magnitude at bus 4 was 0.9404, which is lower than the 0.95 pu lower limit. The 10 MVAr injection at bus 4 in Case I enhanced the voltage magnitudes at buses 2 and 4. The voltages for Case II and Case III were constrained within the 0.95-1.05 pu range. The voltage magnitude at bus 4 in Case IV was 0.9419 pu which is lower than the 0.95 pu lower limit. Hence, an extra 10 MVAr was injected at bus 4, enhancing the bus voltages for Case V. Case VI showed that the voltage magnitude at bus 2 was 0.9421 pu. The transmission line loading limits were also exceeded in Case VI, resulting in network congestion, thus terminating reactive power injection. Voltages at buses 1 and 3 remain unchanged because they are the generator buses. Voltage magnitudes at buses 4 and 2 were lower than the 0.95 pu limit because, as the load demand continued to grow, the active and reactive power demand of the system increased. This led to an increase in voltage drop resulting to poor voltage control. Consumer loads are manufactured with specific voltages of operation. Some devices are however unable to meet their manufacture's rated limits thus operating at voltage values which are different from the system voltage.

Transmission line loading

The transmission line loading for the studied scenarios are presented in Figure 4.2.

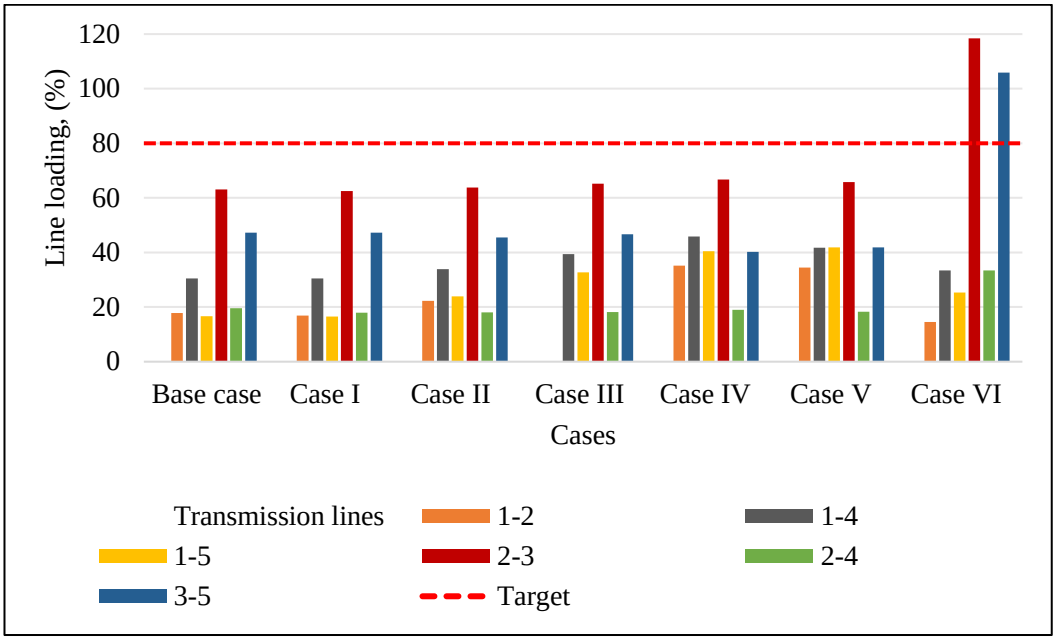

Figure 4.2: Garver's 6-Bus Transmission Line's Loading

All the transmission lines in Base case through to Case V are below the 80 % thermal loading limit. Case VI, however, exceeded their thermal loading capacities at 118.45 % and 105.91 %, in transmission lines (2-3) and (3-5) respectively. The voltage violations in Base case and Case IV were rectified by the reactive power injected in the buses 2 and 4, respectively. By rectifying the voltage violations, the transmission lines' transfer capability were increased. The thermal limit of the transmission lines (2-3) and (3-5) had been exceeded in Case VI necessitating DTNEP.

Active Power Losses

Figure 4.3 presents the system's active power losses for the scenarios studied.

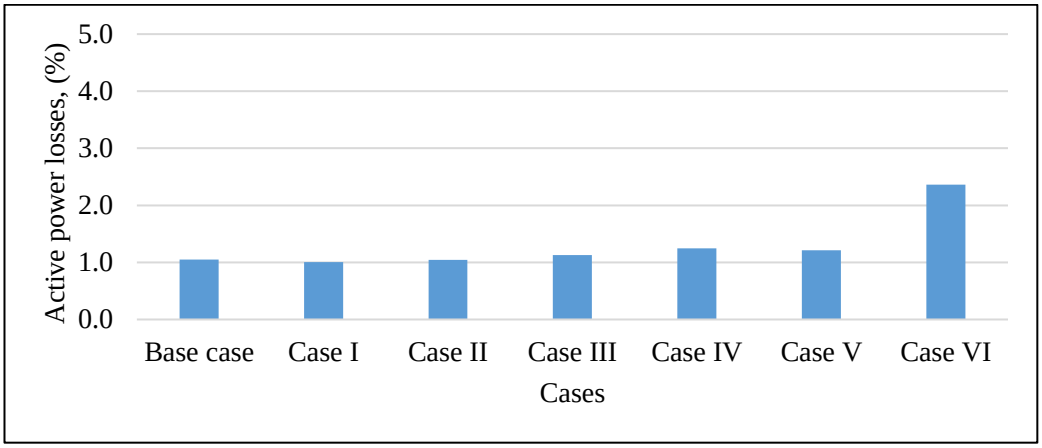

Figure 4.3: Garver's 6-Bus Active Power Losses

Figure 4.3 active power loss were lowered from 1.048 % in the Base case to 1.005 % in Case I following reactive power injection. The active power losses were raised from 1.005 % in the Case I to 1.046 % in Case II following a 10 % load growth. The growing load demand increased current flowing through the transmission lines thus raising the power loss. A 20 % load growth increased the active power losses from 1.046 % in Case II to 1.128 % in Case III whereas a 30 % load growth increased the active power losses from 1.128 % in Case III to 1.248 % in Case IV. After the injection of 10 MVAr reactive power, the active power loss fell from 1.248 % in Case V to 1.212 % in Case V. When reactive power is injected to a bus, the current flowing in the transmission lines is reduced which reduces the power loss. With the reduced loss, the transmission system adequacy is improved for active power transmission. The active power losses increased from 1.212 % in Case V to 2.362 % in Case VI when load demand increased by 40 % at which point the system was congested and reactive power compensation or load demand growth was terminated.

4.2.2 IEEE 30-Bus System

In IEEE 30-bus, reactive power was injected on the buses with voltages below 0.95 pu while growing load demand which resulted in the four scenarios presented in Chapter 3.

The system bus voltage magnitudes, transmission lines' loading and transmission active loss were monitored and recorded.

Bus Voltage Magnitude

Figure 4.4 shows the bus voltage magnitudes for the studied scenarios.

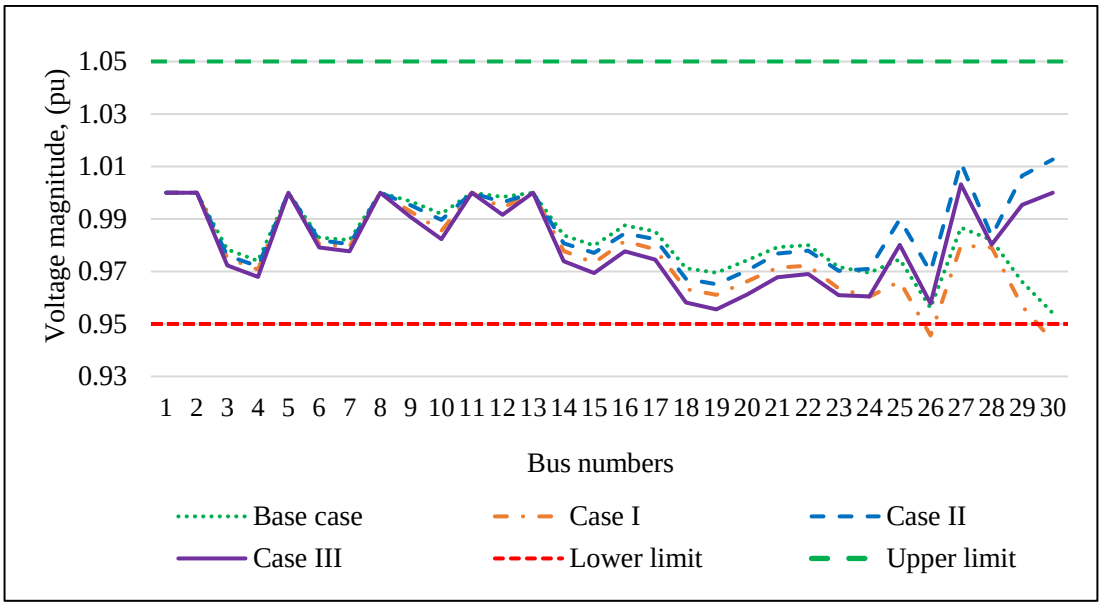

Figure 4.4: IEEE 30-Bus Voltage Magnitudes

Figure 4.4 shows the voltage magnitude were within the voltage limits (± 5 % of nominal voltage) for the Base case for all buses. When the load demand was increased by 10 % in Case I, voltage at buses 26 and 30 decreased to 0.9456 pu and 0.9434 pu respectively, which is below the 0.95 pu lower limit. The voltage violation is a result of an increase in the reactive power demand from increased load. To improve the voltage profile, 10 MVAr reactive power was injected at bus 30 in Case II. Case III had load demand increased by a further 10 % and there was no violation of the voltage magnitude limits.

Transmission Line Loading

The transmission line loading for the scenarios is given in Figure 4.5.

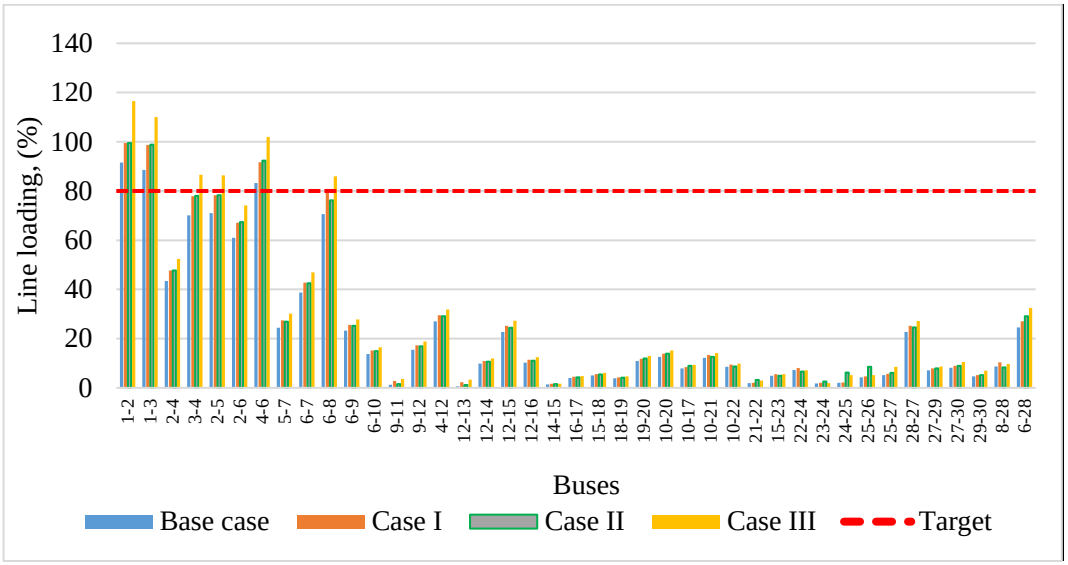

Figure 4.5: IEEE 30-Bus Transmission Lines' Loading

In Figure 4.5, all the transmission lines in Base case, Case I and Case II were loaded below the thermal capacities of the respective lines, with lines 1-2 and 1-3 for Case I and Case II being above 80 % and close to the 100 % loading limit. Case III showed violations of the thermal line loading limit at transmission lines 1-2, 1-3 and 4-6 causing congestion in the system. DTNEP was therefore executed to eliminate the congestion.

Active Power Losses

Figure 4.6 gives active power losses for the scenarios.

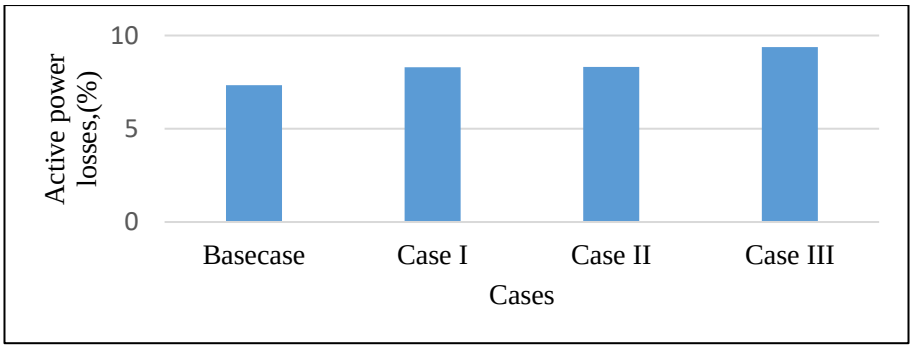

Figure 4.6: IEEE 30-Bus Active Power Losses

Figure 4.6 shows a continuous increase in active power losses with load growth. The losses increased from 7.34 % in the Base case to 9.38 % in Case III where the system was congested. The active power losses fell from 8.298 % in Case I to 8.315 % in Case II. This was attributed to the reactive power injected at bus 30 to restore voltage magnitude values within the (± 5 %) range. Providing reactive power support for congestion management also reduced the active power loss, improving the active power transferred.

4.3 Dynamic Transmission Network Expansion Planning

4.3.1 Garver's 6-Bus System

4.3.1.1 IBPSO Algorithm for Optimization of DTNEP Results

DTNEP task is performed to eliminate the system congestion created by the increasing system demand. IBPSO algorithm was used for optimization of the DTNEP results. The performance of the improved BPSO was analyzed and compared to the basic BPSO. The BPSO algorithm was run to select the optimal parameter values for DTNEP optimization initialized in Table 4.5.

Table 4.5: Value of Parameters for the IBPSO Algorithm

Parameter	Value	
	Garver's 6-bus network	IEEE 30-bus network
Population	20	100
Problem dimension	15	50
Number of iterations	500	1500
Minimum error	0.001	0.001
c_1	1.7	1.7
c_2	2.3	2.3
v_{max}	2	2
v_{min}	-2	-2

The value of parameters presented in Table 4.5 includes the population size, problem dimension, the learning factors for the algorithm (c_1), (c_2) and, the maximum and minimum velocity (v_{max}), (v_{min}), respectively, which solves for a particles maximum change in one iteration.

Figure 4.7 shows the convergence curve for IBPSO in comparison to BPSO.

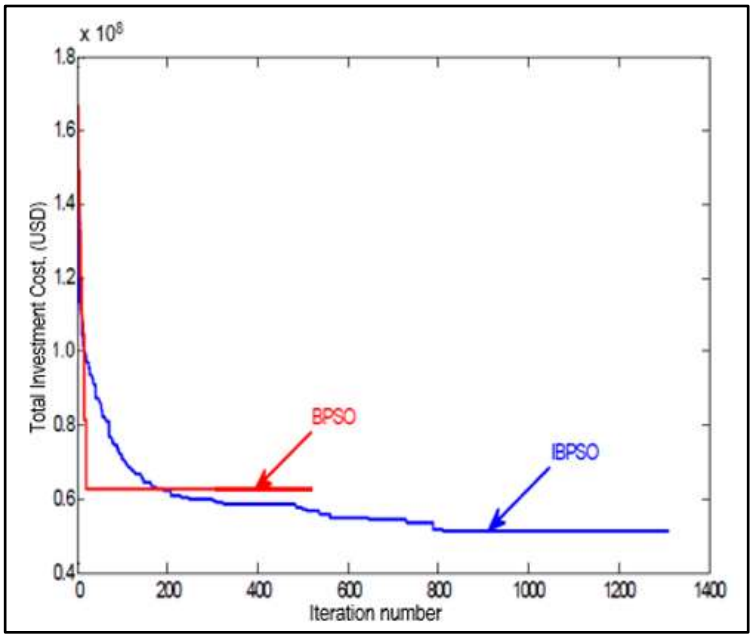

Figure 4.7: BPSO and IBPSO Algorithms Convergence Curves

In Figure 4.7, the convergence of BPSO was faster than for IBPSO algorithm. The IBPSO algorithm, however further searches the dimensional space area, by jumping particles out of local optima positions using Equations (3.17) – (3.19). IBPSO algorithm selected a set of transmission lines whose addition to the transmission network minimized the construction cost for the additional lines and lowered the active power losses in the transmission network.

A new load center was introduced in year 8 of the DTNEP. Figure 4.8 shows the variations in voltage magnitudes following the addition of the load center. Buses 1, 3 and 6 are generator buses and their voltage was maintained at 1.0 pu. The load center is equivalent to the summation of the 10 % load growth at every load bus.

4.3.1.2 TNEP without Considering Voltage Limits

Table 4.6 presents the additional transmission lines without voltage limits using IBPSO algorithm.

Table 4.6: Garver's 6-Bus Additional Transmission Lines without Voltage Limits

Additional lines	2-3, 3-5, 1-5, (2-6) ×2, (4-6) ×2.
Construction Cost (million USD)	190

From Table 4.6 without voltage limits, 7 additional lines were considered; one transmission line each in corridors n_{2-3}, n_{3-5} and n_{1-5}, and two each in corridors n_{2-6}, and n_{4-6} were required with at a construction cost of USD 190 million. Beginning year 8 had the pre-planned bus 6 linked to the network by the new lines n_{2-6}, and n_{4-6}.

The system bus voltages, transmission lines loading and active power losses were monitored and recorded for the 10-year expansion period.

Bus Voltage Magnitudes

Figure 4.8 shows the annual variations of bus voltage magnitudes over the 10-year planning period.

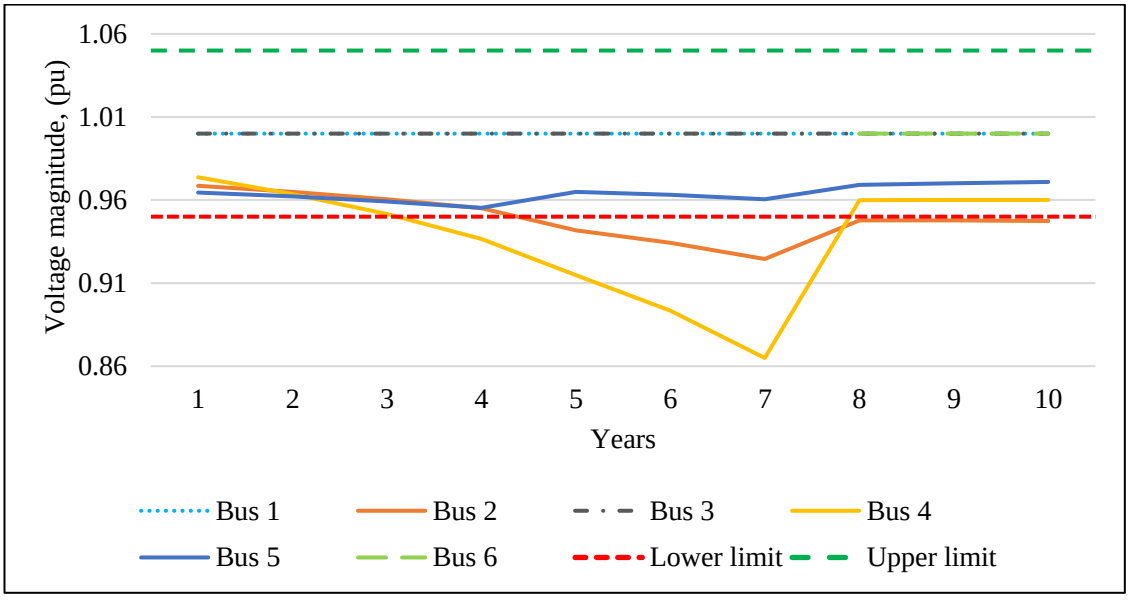

Figure 4.8: Garver's 6-Bus Annual Voltage Magnitudes without Voltage Limits

In Figure 4.8 without voltage limits, the voltages at buses 2 and 4 were lower than the 0.95 pu lower limit. Bus 2 violated the voltage lower limit in year 5 and Bus 4 in year 4 respectively. The lowest voltage magnitude registered was 0.8649 pu and 0.9245 pu at bus 4 and 2, respectively in the year 7. A new load center was introduced in year 8 of the DTNEP. The voltage magnitudes at buses 2 and 4 improved with the new load center. This was due to the system load distribution following addition of the new load center. Further, additional units from the generator buses 3 and 6 were brought online to cater for the generation requirement for load growth.

Transmission Line Loading

Figure 4.9 shows the annual transmission lines loading for the 10-year expansion period.

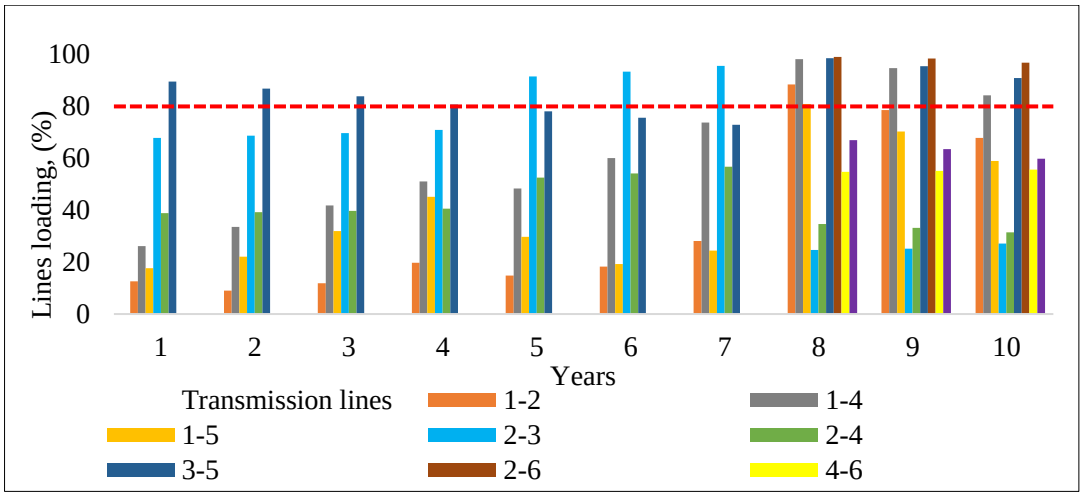

Figure 4.9: Garver's 6-Bus Annual Transmission Line Loading without Voltage Limits

Figure 4.9 without voltage limits, the power system was taken to be operational because all the transmission lines were loaded below their thermal capacities. The transmission lines 3-5 in years 1 through 3, 8 through 9, 2-3 in years 5 through 8, 1-4 and 2-6 each in the years 8 through 10 were loaded more than the 80 % line loading limit. In year 8, lines 2-3 and 3-5 were each loaded up to 99 % of their thermal loading capacity.

4.3.1.3 TNEP Considering Voltage Limits

Table 4.7 presents the additional transmission lines with voltage limits consideration using IBPSO algorithm.

Table 4.7: Garver's 6-Bus Additional Transmission Lines With Voltage Limits

Additional lines	(2-3) ×3, (3-5) ×2, (1-5) ×2, (2-6) ×2, (4-6) ×2, 1-4, 3-6.
Construction Cost(million USD)	286
Penalty (million USD)	1

With voltage magnitude limits in Table 4.7, 6 additional lines, two in corridors n_{2-3} and one each in corridors $n_{1-4}, n_{1-5}, n_{3-5}$ and n_{3-6}, were required, increasing the construction cost to USD 286 million, not including the USD 1 million penalty for voltage limit violation at bus 4. Additional lines n_{2-6}, n_{3-6} and n_{4-6} links the pre-planned bus to the network beginning the year 8.

Over the 10-year planning period, the system voltage profile, transmission lines loading and active power losses with voltage limits were monitored and recorded.

Bus Voltage Magnitudes

Figures 4.10 displays the annual variations of bus voltage magnitudes over the 10-year planning period.

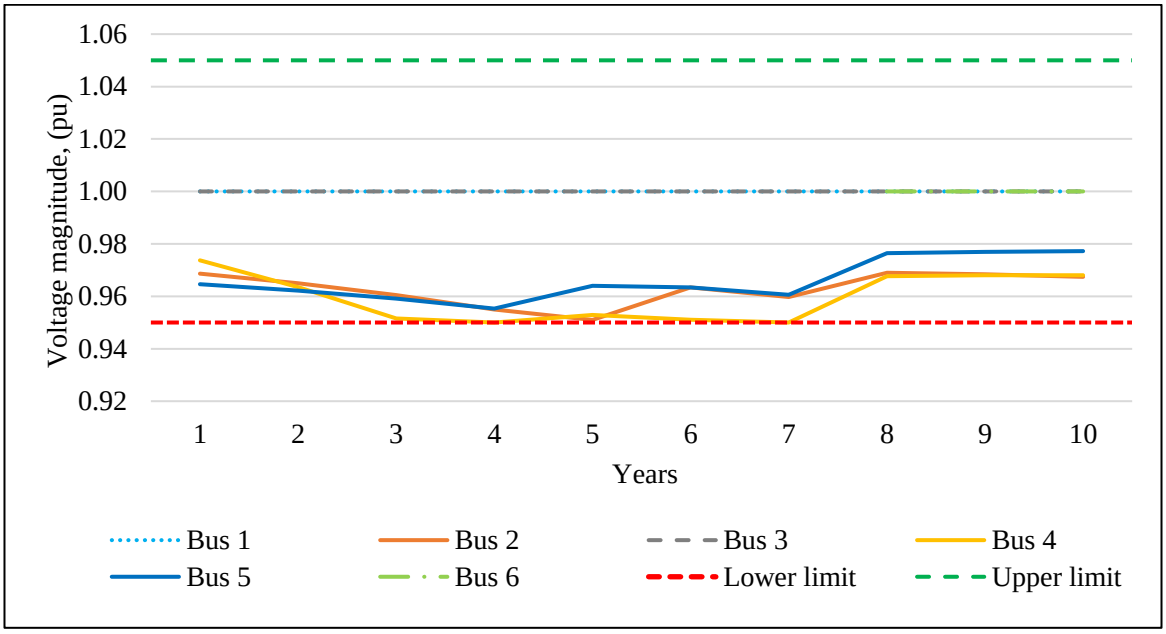

Figure 4.10: Garver's 6-Bus Annual Voltage Magnitudes Considering Voltage Limits

Figure 4.10 with voltage limits had no violation since all the bus voltage magnitudes were constrained to the 0.95-1.05 range. Voltage magnitude at bus 4 in year 7 was penalized according to Equation (3.9) for violating voltage limit.

Transmission Line Loading

Figures 4.11 shows the annual transmission lines loading over the 10-year planning period.

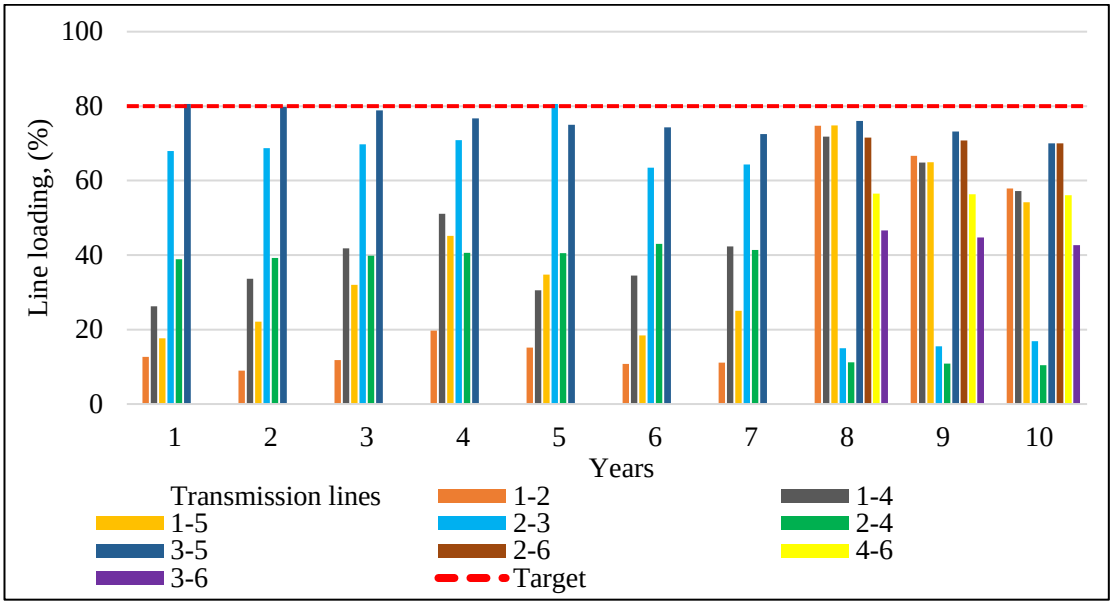

Figure 4.11: Garver's 6-Bus Annual Transmission Line Loading Considering Voltage Limits

Figure 4.11 with voltage limits showed that all the transmission lines were loaded below the 80 % limit. When the system voltage profile improved, the x reactive power requirement for transmission lines was lowered, raising the transmission system adequacy for power transfer.

Active Power Losses

Active power losses in the system were as given in Figure 4.12 without and with voltage magnitude limits for the 10-year expansion period.

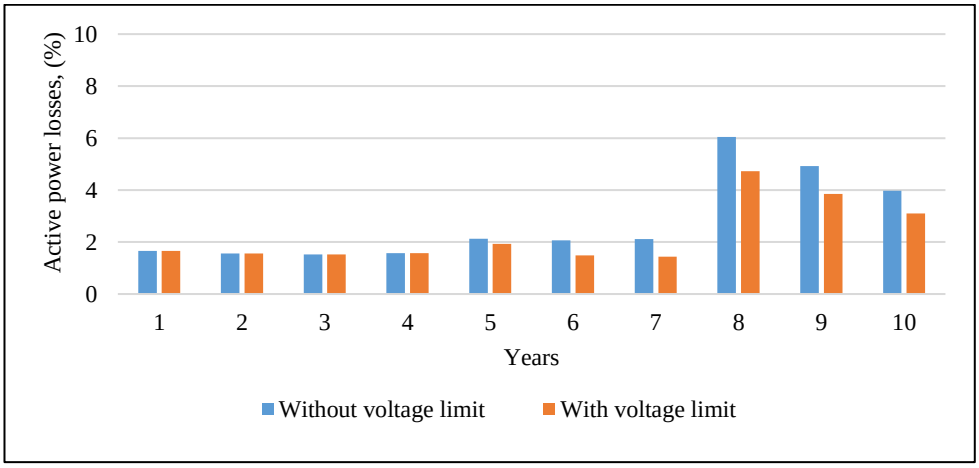

Figure 4.12: Graver's 6-Bus Annual Active Power Losses

In Figure 4.12, the active power losses neglecting voltage limits were higher in comparison with considering voltage limit. Without voltage limits, the transmission active power losses registered the highest of 6.05 % in year 8. The active power losses however, fell from 2.12 % to 1.93 % in year 5, with the drop evident through to final expansion in year 10. Improving the system bus voltages lowered the transmission line loading resulting in reduced active power loss as power loss is inversely proportional to the square of the voltage. Active power losses are a cost of system operation, any efforts to economically lower the power losses results in savings in the overall investment cost.

The active loss costs obtained using Equation (3.1) with and without voltage magnitude limits were as presented in Table 4.8.

Table 4.8: Cost of Losses for Garver's 6-Bus System

	Without voltage limits	**With voltage limits**
Cost of losses (million USD)	24.70	18.97

The costs of active power losses in Table 4.8 were reduced by 23.19 % when voltage limits were considered, thus saving on costs of transmission losses.

4.3.2 IEEE 30-bus System

DTNEP using IBPSO algorithm was also applied to IEEE 30-bus system for network system expansion. Through the expansion years, new load centers at bus 25 in expansion year 5 and at bus 9 in expansion year 7 were introduced. Generator units 8, 5, 13, 2 and 11 were also brought online to provide for generation due to load growth. The optimal topology was selected for two scenarios; - without and with voltage limits consideration.

4.3.2.1 TNEP without Considering Voltage Limits

IEEE 30-bus additional transmission lines without voltage limits were as shown in Table 4.9.

Table 4.9: IEEE 30-Bus Additional Transmission Lines without Voltage Limits

Additional lines	2-5, (1-2) ×2, 1-3, 4-6, 6-8, 3-4, 1-3, (6-10, 21-22, 22-24) ×2.
No. of additional lines	14
Total Construction Cost (million USD)	533

In Table 4.9, without voltage magnitude limits consideration 14 additional lines, one each in corridors $n_{2-5}, n_{1-3}, n_{4-6,}n_{6-8}, n_{3-4}$ and n_{1-3}, two each in corridors $n_{1-2}, n_{6-10}, n_{21-22}$ andn_{22-24} were required at a projected cost of USD 533 million.

The bus voltage magnitudes, the transmission lines' loading and active power losses were monitored and recorded for the 10-year expansion period.

Bus Voltage Magnitudes

The annual bus voltages for the 10-year expansion period are given in Figure 4.13.

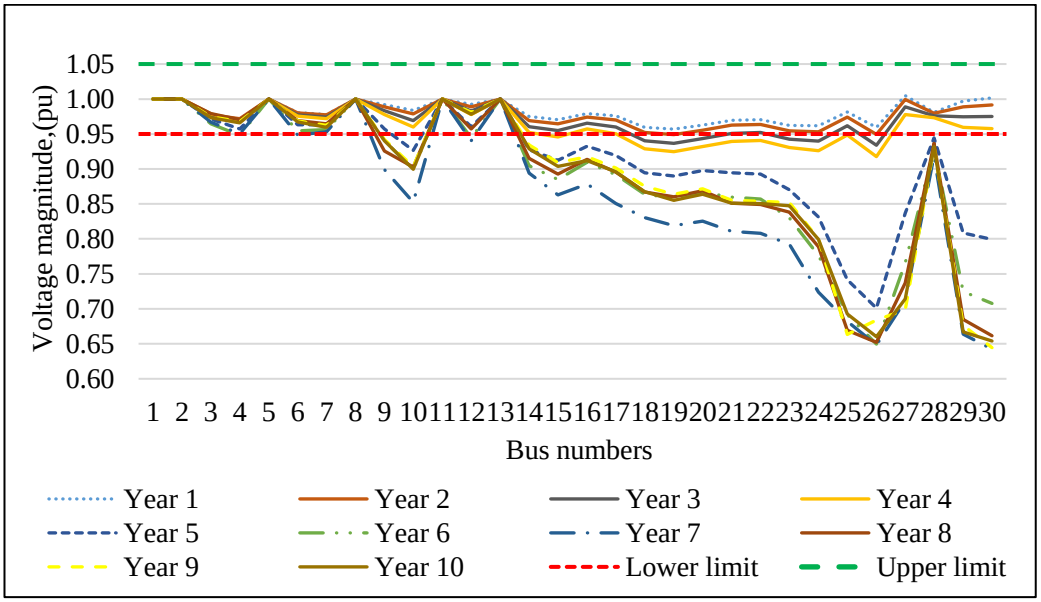

Figure 4.13: IEEE 30-Bus Annual Voltage Magnitudes without Voltage Limits

Figure 4.13 without voltage limits indicates that the bus voltage through the expansion years were lower than 0.95 pu. As the load continued to increase the voltage profile recorded a low of 0.654 pu at bus 30 during expansion year 4. The drops in bus voltage was due to increase in the current flowing through the transmission lines as the load demand was grown, which increased the transmission lines thermal resistance.

Transmission line loading

Figures 4.14 gives the system transmission line loading for the 10-year expansion period.

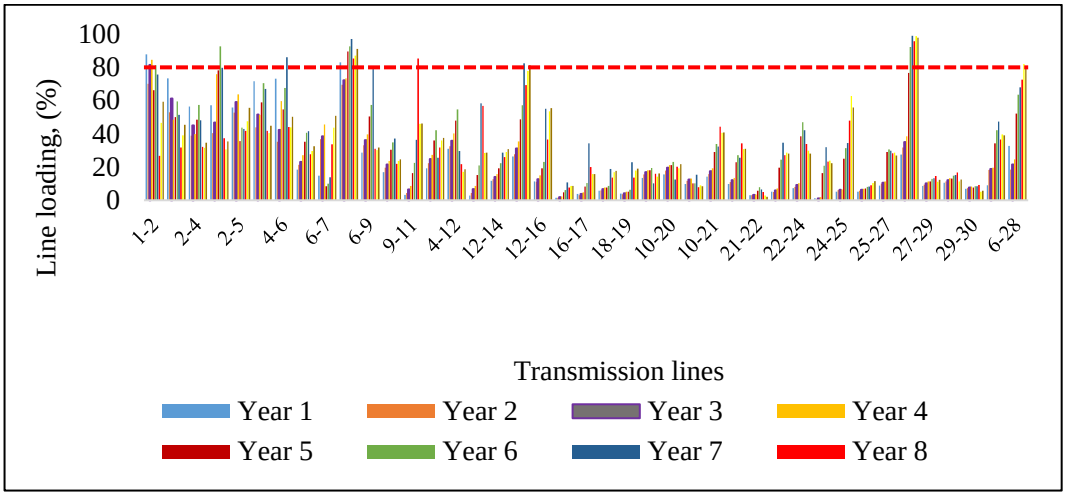

Figure 4.14: IEEE 30-Bus Annual Transmission Line Loading without Voltage Limits

Figure 4.14 without voltage limits showed all transmission lines operating within their thermal capacities after network system congestion was mitigated. Transmission lines 1-2, 3-4, 4-6, 6-8, 9-11, 12-15 and 28-27, however, were transmitting at above the 80 % line loading limit through the expansion period, threatening the system stability.

4.3.2.2 TNEP Considering Voltage Limits

IEEE 30-bus additional transmission lines with voltage limits consideration are given in Table 4.10.

Table 4.10: IEEE 30-Bus Additional Transmission Lines with Voltage Limits

Additional lines	**2-5, (1-2) ×2, 1-3, 6-8, 4-6, 6-8, 3-4, 1-3, 1-2, (6-10, 21-22, 22-24) ×2, 25-26, 28-27, 6-28, 16-17, 2-6, 9-11,4-12, 12-13, 27-30.**
No. of additional lines	24
Total Construction Cost (million USD)	777
Penalty (million USD)	60.76

When voltage limits were considered in Table 4.10, a further additional 10 lines, each in corridors n_{1-2}, n_{25-26}, n_{28-27}, n_{6-28}, n_{16-17}, n_{2-6}, n_{9-11}, n_{4-12}, n_{12-13} and n_{27-30} were selected raising the cost of construction to USD 777 million, excluding a penalty of USD 60.76 million for violations of bus voltage lower limit.

Bus Voltage Magnitudes

Figure 4.15 shows the bus voltage variations for the 10-year expansion period.

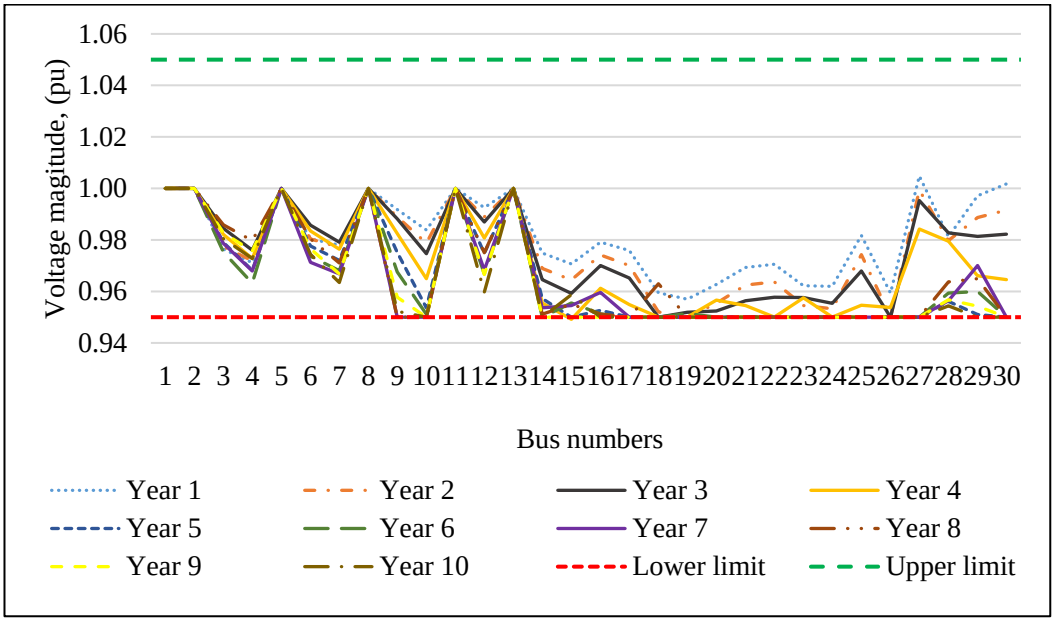

Figure 4.15: IEEE 30-Bus Annual Voltage Magnitudes Considering Voltage Limits

In Figure 4.15 when voltage limits were considered, the voltage magnitude values were within range. Bus 27 recorded the highest voltage magnitude value of 1.004 pu in year 1. Buses 9, 10, 14, 15, 17, 22, 24, 26, 27, 29 and 30 had the lowest voltage values of 0.95 pu.

Transmission Line Loading

Figures 4.16 gives the system transmission line loading for the 10-year expansion period.

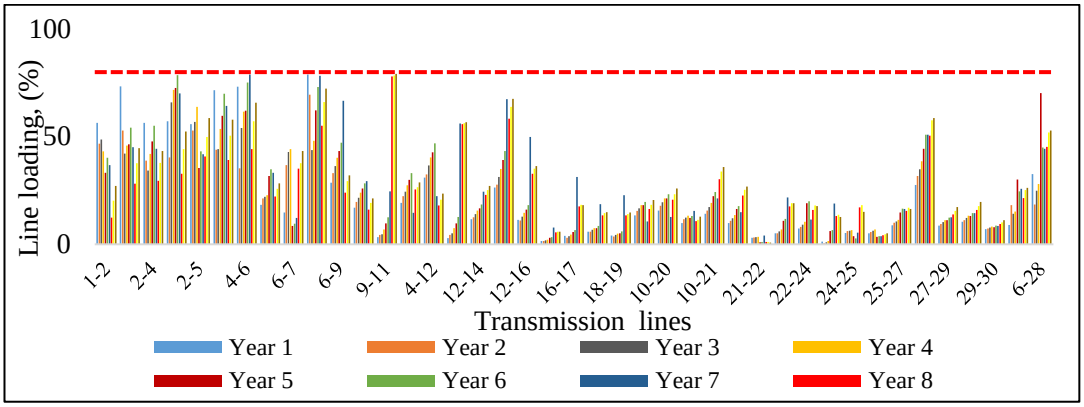

Figure 4.16: IEEE 30-Bus Annual Transmission Line's Loading Considering Voltage Limits

In Figure 4.16, when voltage magnitude limits were considered, all the transmission lines were loaded below 80 %. The reduced transmission line loading increased the transmission network system adequacy allowing more power to be transmitted.

Active power losses

The system active power losses without and with voltage limits for the 10-year expansion period are presented in Figure 4.17.

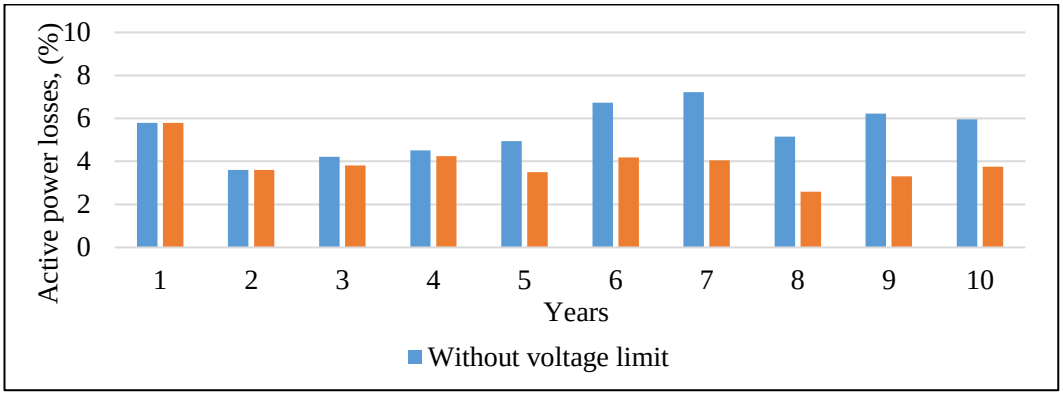

Figure 4.17: IEEE 30-Bus Annual Active Power Losses

Figure 4.17 shows that the active power losses without voltage limits were higher compared to voltage limits. The active losses increased to a high of 7.22 % in expansion year 7 without voltage limits and reduced to a low of 2.59 % with voltage limits consideration through the 10-year planning period. Reduced active power losses

resulted in lowering the costs of transmission losses given by Equation (3.1) as given in Table 4.11.

Table 4.11: Cost of Transmission Loss for IEEE 30-Bus

	Without voltage limits	**With voltage limits**
Cost of losses (million USD)	53.3	35.7

Table 4.11 shows costs of transmission losses which were reduced by 33.02 % when voltage limits were considered. Enforcing voltage magnitude limits reduced transmission losses and increased the adequacy of transmission lines for power transfer. Any reduction in costs of transmission losses causes an overall reduction in the total investment cost allowing for savings.

Table 4.12 gives the summary of the DTNEP results obtained using IBPSO.

Table 4.12: Summary of Results

	Garver's 6-bus		**IEEE 30-bus**	
	Without voltage limits	**With voltage limits**	**Without voltage limits**	**With voltage limits**
Additional transmission lines	2-3, 3-5, 1-5, (2-6) ×2, (4-6) ×2.	(2-3) ×3, (3-5) ×2, (1-5) ×2, (2-6) ×2, (4-6) ×2, 1-4, 3-6.	2-5, (1-2) ×2, 1-3, 4-6, 6-8, 3-4, 1-3, (6-10, 21-22, 22-24) ×2.	2-5, (1-2) ×2, 1-3, 6-8, 4-6, 6-8, 3-4, 1-3, 1-2, (6-10, 21-22, 22-24) ×2, 25-26, 28-27, 6-28, 16-17, 2-6, 9-11, 4-12, 12-13, 27-30.
Number of additional lines	7	13	14	24
Cost of construction (million USD)	190	286	533	777
Cost of losses (million USD)	24.70	18.97	53.3	35.7

Table 4.12 shows that considering voltage limits lowered the active power losses for Garver's 6-bus by 23.19 % and IEEE 30-bus by 33.02 %. The construction cost for additional transmission lines for both Garver's 6-bus and IEEE 30-bus test systems increased when voltage limits were included. This is as a result of a further 6 and 10 transmission lines that were needed to provide Garver's 6-bus and IEEE 30-bus voltage and the transmission line loading requirements respectively.

Voltage limits consideration in the developed methodology resulted to robust system voltage profile, reduced transmission line losses, and efficient power transfer due to reduced transmission line loading. The research contribution of this work include;

1. Enforcing voltage magnitude constraint on the DTNEP by applying a penalty for limits violation
2. Developing an improved BPSO (IBPSO) algorithm and applying it to the Garver's 6-bus and IEEE 30-bus test systems to optimize the DTNEP results.

4.4 Effectiveness and Validation of IBPSO Algorithm

Simulation of the DTNEP selected a set transmission lines for addition to the transmission network system at least cost. The additional lines selected when using IBPSO and BPSO algorithms were compared to additional lines when Linear population size reduction-Success History based Differential Evolution with Semi Adaptation hybrid-Covariance Matrix Adaptation (LSHADE-SPACMA) (Refaat et al., 2021), and Linear Programming (LP) (Garver, 1970) were used on Garver's 6-bus system. Table 4.13 gives the additional transmission lines for the algorithms.

Table 4.13: Garver's 6-Bus Additional Transmission Lines without Considering Voltage Limits

	LSHADE-SPACMA (Refaat et al., 2021)**, LP** (Garver, 1970)	**BPSO**	**IBPSO**
Additional lines	3-5, (2-6) ×4, (4-6) ×2.	3-5, (2-6) ×4, (4-6) ×2.	2-3, 3-5, 1-5, (2-6) ×2, (4-6) ×2.
No. of Additional lines	7	7	7
Construction Cost (million USD)	200	200	190

From Table 4.13, the transmission lines obtained using BPSO algorithm were; one in the n_{3-5} right-of-way, four in the n_{2-6} right-of-way, and two in the n_{4-6} right-of-way with a total investment cost from the formulation in Equation (3.1) projected to be USD 200 million. The additional lines topology is identical to using LSHADE-SPACMA (Refaat et al., 2021), and LP (Garver, 1970). Using IBPSO, one transmission line each in corridors n_{2-3}, n_{3-5} and n_{1-5}, and two each in corridors n_{2-6}, and n_{4-6} were selected. The total cost of construction using the formulation in Equation (3.1) was a projection of USD 190 million. The construction cost for the IBPSO algorithm was lower than for the BPSO algorithm by 5 % for the same number of additional lines. The use of IBPSO algorithm thus produced better results with minimal costs in comparison to BPSO algorithm. The number of transmission lines obtained with both BPSO and IBPSO algorithms was seven.

CHAPTER FIVE

CONCLUSION AND RECOMMENDATIONS

5.1 Conclusion

The developed methodology that uses IBPSO algorithm for DTNEP optimization included growing the load demand and adding generation capacity to match the demand for Garver's 6-bus and IEEE 30-bus systems resulting in congestion. To manage the congestion, reactive power was injected at buses below 0.95 pu while also increasing the load demand to a point of inadequacy in the system operation thus necessitating transmission network expansion. The cost incurred to construct the additional transmission lines and the cost of transmission active power losses were considered in the objective formulation. To eliminate violations, the bus voltage magnitude limits and transmission lines loading constraints were also included in the formulation. The research simulation was done for two scenarios; without and with voltage limits consideration. The conclusions from this research work were that growing the system load demand raised the transmission line active power losses. The utilization of reactive power compensation and developed DTNEP to mitigate and alleviate the network congestion respectively, resulted to a robust voltage profile, an uncongested network system and enhanced transmission lines' adequacy. The transmission lines for both Garver's 6-bus and IEEE 30-bus systems, were loaded below 80 % of their capacities in the developed methodology. The accuracy of IBPSO algorithm in selecting optimal additional transmission lines was better than BPSO algorithm. IBPSO allowed the particles to jump out of their local optima in the search space overcoming the shortcoming of BPSO algorithm being stuck in the local optima when optimizing DTNEP. The transmission active power losses were reduced by 23.19 % and 33.02 % for Garver's 6-bus and IEEE 30-bus test systems respectively. The cost of expansion was higher with voltage limit consideration compared to without voltage limit consideration for both test systems because of the additional lines needed to cater to the voltage requirement in the system.

5.2 Recommendations

This research was aimed at finding an optimal method for power system planning to be implemented in solving the TNEP problem. It was desirable that voltage limits consideration help reduce investment and active transmission loss costs. Further research may be done to include the long transmission lines while analyzing the bus voltage and transmission line loading. During reactive power compensation, besides static compensators, FACTs devices may be applied to assess performance on voltage regulation. The losses considered in this research were limited to the active power losses. Further research can be done to investigate effect of considering the different transmission losses in the objective formulation. The IBPSO algorithm can also be applied alongside other metaheuristic methods to better the convergence speed for TNEP studies. The methodology in this research can be implemented on a large power system. In GEP, further research may be done on the effect of renewable energy integration. In voltage control studies, Intermittent Renewable Resources and Neutral-Point Voltage can be used to justify investments in voltage control and to analyze the financial implications of optimized expansion.

REFERENCES

Abdelaziz, A. R. (2000). Genetic algorithm-based power transmission expansion planning. *7th IEEE International Conference on Electronic Circuits and Systems*, *78*, 642–645.

Abuishaiba, S., Youssef, M., & Tarrad, I. (2019). A Hybrid PSO–SA Algorithm for Maximizing the Data Rate for the Cognitive OFDM System. *International Journal of Scientific & Engineering Research*, *10*(2), 403–410.

Alhamrouni, I., Khairuddin, A., Ferdavani, A. K., & Salem, M. (2014). Transmission Expansion Planning using AC-based Differential Evolution algorithm. *IET Generation, Transmission, Distribution.*

Al-Saba, T., & El-Amin, I. (2002). The application of artificial intelligent tools to the transmission expansion problem. *Electrical Power System Resources*, *62*, 117–126.

Alvarez, R., Rahmann, C., Palma-Behnke, R., Estavez, P., & Valencia, F. (2018). Ant Colony Optimization Algorithm for Multiyear Transmission Network Expansion Planning. *2018 IEEE Congress of Evolutionary Computation (CEC)*, 1–6.

Andersen, B. R., & Nilsson, S. L. (2020). *CIGRE Study Committee B4: DC Systems and Power Electronics Flexible AC transmission systems FACTS*. Springer International Publishing.

Asadzadeh, V., Golkar, M. A., & Moghaddas- Tafresshi, S. M. (2011). Economics-Based Transmission Expansion Planning In Restructured Power Systems Using Decimal Codification Genetic Algorithm. *IEEE Jordan Conference on Applied Electrical Engineering and Computing Technologies (AEECT)*, 1–8.

Azeem, A., Ismail, I., Jameel, S. M., & Harindan, V. R. (2021). Electrical Load Forecasting Models for Different Generation Modalities: A Review. *IEEE Access*, *9*, 142223–142263.

Binato, S. G., de Oliveira, C. J., & Araujo, L. (2001). A greedy randomized adaptive search procedure for transmission expansion planning. *IEEE Transactions on AC Power Systems*, *16*, 247–253.

Binato, S., Periera, M. V. F., & Granville, S. (2001). A new Benders decomposition approach to solve power transmission network design Problems. *IEEE Transmission Power Systems*, *16*, 235–240.

Bizon, N., Shayeghi, H., & Mahdavi, N. T. (2013). *Analysis, Control and Optimal Operations in Hybrid Power Systems, Green Energy and Technology*. Springer:

Cassidy, F., & Schirra, G. W. (1997). Treatment of Inflation in Engineering Economic Analysis. *IEEE Transactions on Power Apparatus Systems*, *96*(3), 1027–1035.

Chanda, R. S., & Bhattacharjee, P. K. (1995). A reliability approach to transmission expansion planning using minimal cut theory. *Electric Power Systems Research*, *33*, 111–117.

Charles, J. K., Moses, P. M., & Mbuthia, J. M. (2020). An adaptive hybrid meta-heuristic approach for transmission constrained multi-objective GEP. *IEEE Power Energy Society/ IAS Power Africa*, 1–5.

Choi, J., & Lee, K. Y. (2022). Models and Methodologies. *Probabilistic Power System Expansion Planning with Renewable Energy Resources and Energy Storage Systems, IEEE*, 235–256.

Choi, J., & Mount, T. R. (2006). Transmission system expansion plans in the view point of deterministic, probabilistic and security reliability criteria. *The 39th Hawaii International Conference on System Science*, 1–10.

Conejo, A. J., Baringo, L., Kazempour, J., & Siddiqui, A. (2016). *Investment in Electricity Generation and Transmission, Decision Making under Uncertainty*. Springer International Publishing.

Das, J. (2015). *Power System Harmonics and Passive Filter Designs*. Wiley-IEEE Press.

Das, S., Verma, A., & Bijwe, P. R. (2020). Efficient multi-year security constrained ac transmission network expansion planning. *Electrical Power Systems Research*, *187*, 106–507.

Delson, J. K. (1992). Engineering Economics Literature on Inflation. *IEEE Transactions on Power Systems*, *7*(1), 73–80.

Deshpande, M. V. (2009). *Elements of Electrical Power Station Design.*

Freitas, P. F. S., Macedo, L. H., & Romero, R. (2019). A strategy for transmission network expansion planning considering multiple generation scenarios. *Electric Power Systems Research*, *172*, 22–31.

Fuerte Ledezma, L. F., & Gutiérrez Alcaraz, G. (2020). Hybrid Binary PSO for Transmission Expansion Planning Considering N-1 Security Criterion. *IEEE Latin America Transactions*, *18*(3), 545–553.

Garver, L. L. (1970). Transmission Network Estimation using Linear Programming. *IEEE Transaction on Power Applied Systems*, *7*, 1688–1697.

Gomes, P. V., & Saraiva, J. T. (2016a). Comparative analysis of constructive heuristics algorithms for transmission Expansion Planning. *University of Porto Journal of Engineering*, *2*, 55–64.

Gomes, P. V., & Saraiva, J. T. (2016b). Hybrid Discrete Evolutionary PSO for AC dynamic Transmission Expansion Planning. *IEEE International Energy Conference*, 1–6.

Grimble, M. J., & Johnson, M. A. (2015). *Advances in Industrial Control*. Springer.

Hemmatu, R., Hooshmad, R. A., & Khodabakhshian, A. (2013). Comprehensive review of generation and transmission expansion planning. *IET Generation, Transmission, Distribution*, *7*, 995–964.

Huanca, D. H., Gallego, L. A., & Lopez-Lezama, J. M. (2022). Transmission Network Expansion Planning Considering Optimal Allocation of Series Capacitive Compensation and Active Power Losses. *Applied Sciences*, *12*(1), 388.

IEEE Guide for Planning DC Links Terminating at AC locations Having Low Short-Circuit Capacities. (1997). *IEEE Standard 1204-1997*, 1–126.

Inyanga, F. E., Muisyo, I. N., & Kaberere, K. K. (2025). Optimization of dynamic transmission network expansion planning using binary particle swarm optimization algorithm. *Bulletin of Electrical Engineering and Informatics (BEEI)*, *14*(2), 861–870.

Jalilzadeh, S., Shayeghi, H., Mahdavi, M., & Haddadian, H. (2009). A GA based transmission network expansion planning considering voltage level, network losses and number of bundle lines. *American Journal of Applied Sciences*, *6*, 987–994.

Jenkins, N., Weedy, B. M., Ekanayake, J. B., Cory B. J., & Strbac, G. (2012). *Electric Power Systems* (Fifth edition). John Wiley & Son Ltd.

Jiankun, L., J. C., & Zhen, Q. (2017). Comparative analysis of FACTS devices based on the comprehensive evaluation index system. *MATEC Web of Conferences*, 15002.

Kaekhoungning, T., Premrudeepreechacharn, S., Wongsinlatam, W., Namvong, A., Remsungnen, T., Mueanrit, N., Sorn-in, K., Kravenkit, S., Siritaratiwat, A., Srichan, C., Khunkitti, S., & Surawanitkun, C. (2022).

Transmission Network Expansion Planning with High-Penetration Solar Energy Using Particle Swam Optimization in Lao PDR toward 2030. *Energies*, *15*(22), 8359.

Kavitha, D., & Swarup, K. S. (2010). Transmission Expansion Planning Using LP-Based Particle Swarm Optimization. *IEEE*.

Kennedy, J., & Eberhart, R. (1997). A discrete Binary Version of the Particle Swarm Algorithm. *Proceedings of the IEEE International Conference on Systems, Man and Cybernetics*, 4104–4108.

Kenya Transmission Construction Company Limited. (n.d.). *Transmission Master plan 2023-2042*.

Khandelwal, A., Bhargava, A., Sharma, A., & Sharma, H. (2019). Transmission network expansion planning using state-of-the-art nature inspired algorithms: a survey. *International Journal of. Swarm Intelligence*, *4*(1), 73–92.

Kishore, T. S., & Singal, S. K. (2014). Optimal Economic Planning of Power Transmission Lines: A review. *Renewable and Sustainable Energy Reviews, Elsevier*, *39*(C), 949–974.

Kundur, P. (1994). *Power System Stability and Control*. McGraw-Hill.

Kwang, Y. L., & Zita, A. V. (2020). *Applications of Modern Heuristic Optimization Methods in Power and Energy Systems.* Wiley- IEEE press.

Kwang', Y. Lee., & El-Sharkawi, A. M. (2008). *Modern Heuristics Optimization Techniques Theory and Applications to Power Systems*. Wiley & Sons.

Lai, L. L. (2001). *Power System Restructuring and Deregulation: Trading, Performance and Information Technology*. John Wiley and Sons.

Mahdavi, E., & Mahdavi, M. (2011). Evaluating the Effect of Load Growth on Annual Network Losses in TNEP Considering Bundle Lines and Voltage Levels using DCGA. *International Journal on Technical and Physical Problems of Engineering*, *3*(9).

Mahdavi, M., Macedo, L. H., & Romero, R. (2018). Transmission and Generation Expansion Planning Considering System Reliability and Line Maintenance. *Electrical Engineering (ICEE), Iranian Conference*, 1005–1010.

Mahdavi, M., Sabillon Antunez, C., Ajalli, M., & Romero, R. (2018). Transmission Expansion Planning: Literature Review and Classification. *IEEE Systems Journal*, *13*(3), 3129–3140.

Mathworks. (2018). *MATLAB programming software.* .

Meisam M., & Amir, B. (2018). BPSO Applied to TNEP Considering Adequacy Criterion. *American Journal of Neural Networks and Applications*, *4*(11), 1–7.

Migliavacca, G. (2016). *Advanced Technologies for Future Transmission Grids. Power systems for further volumes*. Springer.

Momoh, J., & Lamine, Mili. (2010). *Economic Market Design and Planning for Electric System*.

Monteiro, L. F. R., & Zambroni De Souza, A. C. (2021). Voltage Stability Planning for Modern Bulk Power System with Retiring Conventional Generation. *2021 International Conference on Electrical, Computer, Communications and Mechatronics Engineering (ICECCME)*.

Nezamabadi-pour, H., Rostami Shahrbabaki, M., & Maghfoori Farsangi, M. (2008). Binary Particle Swarm Optimization: Challenges and New Solutions. *The CSI Journal on Computer Science and Engineering*, *6*(1), 21–32.

Niharika, V. S., & Mukherjee, V. (2016). Transmission Expansion Planning: A review. *2016 International Conference on Energy Efficient Technologies for Sustainability*, 350–355.

Pablo, G., Villar, J., Diaz, C. A., & Campos E. A. (2014). Joint energy and reserve markets: Current implementations and modelling trends. *Electric Power Systems Research*, *109*, 101–111.

Rebennack, S., Pardalos, P. M., Pereira, M. V. F., & Iliadis, N. A. (2010). *Handbook of Power Systems, Energy Systems*. Springer.

Refaat, M. M., Aleem, S. H. E. A., Atia, Y., Ali, Z. M., & Sayeed, M. M. (2021). Multi-Stage Dynamic Transmission Network Expansion Planning Using LSHADE-SPACMA. *Applied Sciences*, *11*(5), 1–22.

Rider, M. J., Garcia, A. V., & Romero, R. (2007). Power System Transmission Network Expansion Planning using AC Model. *IET Generation, Transmission, Distribution*, *1*(5), 731–742.

Ritchie, H., Roser, M., & Rosado, P. (2023). *Energy*. Https://Ourworldindata.Org/Energy

Romero, R., Gallego, R. A., & Monticelli, A. (1996). Transmission system expansion planning by simulated annealing. *IEEE Transactions on Power Systems*, *11*, 364–369.

Romero, R., Monticelli, A., Garcia, A., & Haffner, S. (2002). Test Systems and Mathematical Models for Transmission Network Expansion Planning. *IEE Proceedings Generation Transmission & Distribution*, *149*(1).

Romero, R., Rocha, C., Mantovani, M., & Mantovani, J. R. S. (2003). Analysis of heuristic algorithms for the transportation model in static and multistage planning in network expansion systems. *IEE Proceedings on Generation Transmission and Distribution*, 521–526.

Saadat, H. (2002). *Power System Analysis*. McGraw-Hill.

Seifi, H., & Sepasian, M. S. (2011). *Power Systems for other volumes, Electric Power System Planning: Issues, Algorithms and Solutions*. Springer Science and Business Media.

Shayeghi, H., Jalilzadeh, S., Mahdavi, M., & Haddadian, H. (2009). Studying the effect of loss coefficient on Transmission Expansion Planning using Decimal Codification GA. *International Journal on Technical and Physical Problems of Engineering*, *1*(1).

Shayeghi H., & Mahdavi, M. (2013). *Application of PSO and GA for transmission Network Expansion Planning. In: Bizon, N., Shayeghi H., and Mahdavi, Tabatabaei, N. (eds) Analysis, Control and Optimal Operations in Hybrid power systems. Green Energy and Technology*. Springer.

Shayeghi, H., Mahdavi, M., Kazemi, A., & Shayanfar, H. A. (2010). Studying the effect of bundle lines on TNEP considering network losses using decimal codification genetic algorithm. *Energy Conversion and Management*, *51*, 2685–2691.

Shivaie, M., Weinsier, P. D., & Kiani-Moghaddam, M. (2019). *Modern Music-Inspired Optimization Algorithms for Electrical Power Systems Modeling, Analysis and Practice*. Springer.

Silva, E. L., Oritz, J. M. A., Oleveria, G. C., & Oleveria, B. S. (2001). Transmission network expansion planning under a Tabu search approach. *IEEE Transactions on Power Systems*, *16*, 62–68.

Silva, I. D. J., Rider, M. J., Romero, R., & Murari, C. A. (2005). Transmission network expansion planning considering uncertainness in demand. *IEEE Power Engineering Society General Meeting*, *2*, 1424–1429.

Sohtaoglu, N. H. (1998). The effect of economic parameters on power transmission planning. *9th Mediterranean Electrotech Conference*, 941–945.

Sum-Im, T., Taylor, G., & Irving, M. (2009). Differential Evolution algorithm for static and multistage transmission expansion planning. *IET Generation, Transmission and, Distribution*, *3*(4), 365–384.

Sun, G., Zhu, Z., Zhang, G., Xu, C., Wang, Y., Zhu, S., Chang, B., & Liang, R. (2022). Application of Mathematics Optimization in Data Visualization and Visual Analytics: A Survey. *IEEE Transactions on Big Data*.

Tietze, U., Shen, C. K., & Gamm, E. (2008). *Electronic circuits*.

Transmission Code 2007- Network and System Rules of the German Transmission System Operators (2007).

Ude, N. G., Yskandar, H., & Graham, R. C. (2019). A Comprehensive State-of-the-Art survey on the Transmission Network Expansion Planning. *IEEE Access*.

Wood, A. J., Wollenberg, B. F., & Sheble, G. B. (2014). *Power Generation, Operation, and Control* (3rd ed.). John Wiley & Sons.

Zaker, B., Hadavi, S., Arani, A. A., Ashrafi, F., & Gharehpetian, G. B. (2017). A new approach to enhance transient stability of power system and its impact on marginal prices. *Smart Grid Conference (SGC)*, 1–8.

Zhang, F., Hu, Z., & Song, Y. (2013). Mixed-integer linear model for transmission expansion planning with line losses and energy storage systems. *IET Generation, Transmission and Distribution*, *7*, 919–928.

Zhang, H., Heydt, G. T., Vittal, V., & Mittelmann, H. D. (2012). Transmission expansion planning using ac model: Formulations and possible relaxations. *IEEE Power and Energy Society Meeting*, 1–8.

Zhang, X. R. C., & Pal, B. C. (2006). *Flexible AC Transmission Systems: Modelling and Control*. Springer.

APPENDICES

Appendix I: Data for Garver's 6-Bus Test System

The load data for Garver's 6-bus test system is presented in Table A.1

Bus number	Active demand, P_d,(MW)	Reactive demand, Q_d (MVAR)
1	20	4
2	60	12
3	10	2
4	40	8
5	60	12

The generator data for Garver's 6-bus system is presented in Table A.2

Bus number	Generation capacity, (MW)	Active generation, P_g (MW)
1	150	90
3	360	120
6	600	545

The data for transmission line for Garver's 6-bus system is presented in Table A.3.

From bus	To bus	Resistance, (pu)	Reactance, (pu)	Line loading capacity, (MVA)
1	2	0.040	0.400	100
1	4	0.060	0.600	80
1	5	0.024	0.240	100
2	3	0.022	0.220	100
2	4	0.044	0.440	100
3	5	0.020	0.200	100

The data for the candidate line for Garver's 6-bus system is presented in Table A.4.

From bus	To bus	Resistance, (pu)	Reactance, (pu)	Line loading capacity, (MVA)	Length, (km)
1	2	0.040	0.400	100	100
1	3	0.038	0.380	100	95
1	4	0.060	0.600	80	150
1	5	0.024	0.240	100	60
1	6	0.068	0.680	100	170
2	3	0.022	0.220	100	55
2	4	0.044	0.440	100	110
2	5	0.026	0.260	100	65
2	6	0.030	0.300	100	75
3	4	0.062	0.620	100	155
3	5	0.020	0.200	100	50
3	6	0.048	0.480	100	120
4	5	0.063	0.630	100	157
4	6	0.034	0.340	100	85
5	6	0.064	0.640	100	160

The construction cost of transmission line is given in Table A.5.

Number of line circuits	Fixed cost of line construction/km (thousand USD)	Variable cost of line construction/km (thousand USD)
1	546.5	45.9
2	546.5	63.4

Appendix II; Data for IEEE 30-Bus Test System

The bus data for IEEE 30-bus test system is presented in Table B.1

Bus number	Bus type	Active demand, P_d (MW)	Active generation, P_g (MW)	Generation capacity (MW)	Reactive demand, Q_d (MVA)	Gs	Bs	Area	Voltage magnitude V_m (pu)
1	3	0.0	260.2	360.2	-16.1	0	0	1	1.050
2	2	21.7	40	140	50	0	0	1	1.043
3	1	2.4	0	0	1.2	0	0	1	1.021
4	1	7.6	0	0	1.6	0	0	1	1.012
5	2	94.2	0	100	19.0	0	0	1	1.010
6	1	0.0	0	0	0.0	0	0	1	1.010
7	1	22.8	0	0	10.9	0	0	1	1.002
8	2	30	0	100	30	0	0	1	1.010
9	1	0.0	0	0	0.0	0	0	1	1.041
10	1	5.8	0	0	2.0	0	19	1	1.045
11	2	0.0	0	100	0.0	0	0	1	1.045
12	1	11.2	0	0	7.5	0	0	1	1.047
13	2	0.0	0	100	0.0	0	0	1	1.041
14	1	6.2	0	0	1.6	0	0	1	1.042
15	1	8.2	0	0	2.5	0	0	1	1.038
16	1	3.5	0	0	1.8	0	0	1	1.045
17	1	9.0	0	0	5.8	0	0	1	1.040
18	1	3.2	0	0	0.9	0	0	1	1.028
19	1	9.5	0	0	3.4	0	0	0	1.026
20	1	2.2	0	0	0.7	0	0	1	1.030
21	1	17.5	0	0	11.2	0	0	1	1.033
22	1	0.0	0	0	0.0	0	0	1	1.033
23	1	3.2	0	0	1.6	0	0	1	1.027
24	1	8.7	0	0	6.7	0	4.3	1	1.021
25	1	0.0	0	0	0	0	0	1	1.000
26	1	3.5	0	0	2.3	0	0	1	1.000
27	1	0.0	0	0	0.0	0	0	1	1.000
28	1	0.0	0	0	0.0	0	0	1	1.000
29	1	2.4	0	0	0.9	0	0	1	1.000
30	1	10.6	0	0	1.9	0	0	1	1.000

Transmission line data for IEEE 30-bus system is given in Table B.2.

Line number	From bus	To bus	Resistance, (pu)	Reactance, (pu)	B_s	Line loading capacity, (MVA)	Length, (km)
1	1	2	0.0192	0.0878	0.0528	81	20
2	1	3	0.0482	0.1652	0.0408	81	58
3	2	4	0.0570	0.1737	0.0368	100	61
4	3	4	0.0132	0.0379	0.0084	120	13
5	2	5	0.0472	0.1983	0.0418	120	69
6	2	6	0.0581	0.1763	0.0374	100	61
7	4	6	0.0119	0.0414	0.09	100	14
8	5	7	0.0460	0.116	0.024	100	40
9	6	7	0.0267	0.082	0	100	29

Line number	From bus	To bus	Resistance, (pu)	Reactance, (pu)	B_s	Line loading capacity, (MVA)	Length, (km)
10	6	8	0.012	0.042	0	81	15
11	6	9	0	0.208	0	120	73
12	6	10	0	0.556	0	120	193
13	9	11	0	0.208	0	120	73
14	9	10	0	0.11	0	180	12
15	4	12	0	0.256	0	180	89
16	12	13	0	0.14	0	180	49
17	12	14	0.1231	0.2559	0	81	89
18	12	15	0.0662	0.1304	0	81	45
19	12	16	0.0945	0.1987	0	73	69
20	14	15	0.221	0.1997	0	100	70
21	16	17	0.0524	0.1923	0	90	67
22	15	18	0.1073	0.2185	0	120	76
23	18	19	0.0639	0.1292	0	70	45
24	19	20	0.034	0.068	0	70	24
25	10	20	0.0936	0.209	0	80	73
26	10	17	0.0324	0.0845	0	100	29
27	10	21	0.0348	0.0749	0	150	26
28	10	22	0.0727	0.1499	0	100	52
29	21	22	0.0116	0.0236	0	150	82
30	15	23	0.1	0.202	0	100	70
31	22	24	0.115	0.179	0	80	62
32	23	24	0.132	0.27	0	80	94
33	24	25	0.1183	0.3292	0	100	115
34	25	26	0.2544	0.38	0	100	132
35	25	27	0.1093	0.2087	0	120	73
36	28	27	0	0.396	0	90	15
37	27	29	0.2198	0.4153	0	90	145
38	27	30	0.3202	0.6027	0	90	210
39	29	30	0.2377	0.4533	0	80	158
40	8	28	0.0636	0.24	0.0428	80	70
41	6	28	0.0169	0.0599	0.073	80	21

The line resistance and reactance are provided for in each line segment of the test system. The approximate line length of each segment, are based on reactance per kilometer of each line and is taken as 0.002882692 Ω.

The data for IEEE 30-bus system candidate lines are presented in Table B.3.

From bus	To bus	Resistance, (pu)	Reactance, (pu)	Line loading capacity, (MVA)	Length, (km)	Cost (million USD)
1	3	0.0482	0.1652	100	58	31.29
2	4	0.057	0.1763	100	61	33.392
2	5	0.0472	0.1983	100	69	37.559
3	4	0.0132	0.0379	100	13	7.1785
4	6	0.0119	0.0414	100	14	7.8414
4	12	0	0.256	100	89	48.488
5	7	0.0460	0.116	100	40	21.971
6	8	0.012	0.042	100	15	7.9551
6	10	0	0.556	100	193	105.31
8	28	0.0636	0.24	100	70	45.458
9	11	0	0.208	100	73	39.397
10	21	0.0348	0.0749	100	26	14.187
12	13	0	0.14	100	49	26.517
12	16	0.0945	0.1987	100	69	37.635
14	15	0.2210	0.1997	100	70	37.824
15	23	0.1	0.202	100	70	38.26
16	17	0.0524	0.1923	100	67	36.423
18	19	0.0639	0.1292	100	45	24.471
22	24	0.115	0.179	100	62	33.904
25	27	0.1093	0.2087	100	73	39.529

Appendix III: Matlab Code

ACPF

```
data = loadcase(garvers1);
result = runpf (data);
```

BPSO script

```
 clc
 clear all
 tic


      %%initializing BPSO parameters < FEIOS%%
n = 50;                % population
dim = 15;              % problem dimension
x = load ('candidate.m');
vnew = rand(n, dim);    % randomly initialized velocity
w = 1;
posn = rand(n, dim);
sig = zeros(n, dim);
void = vnew;
fitness = zeros(1,n);
pbest = zeros(n ,dim);
fpbest = zeros(n );
fgbest = inf;
gbest = zeros(1,dim);
%%   initial population


vmax = 4;          %velocity maximum
vmin = -4;         %velocity minimum
r = rand (n, dim); %randomized matrix size
iter = 0;
maxiter = 500;     %maximum iteration
minerror = 0.001  % minimum error
%% incidence matrix
data =loadcase (garvers1);
dat = data.bus;
doc = data.branch;    %branch/ linedata
nhanh = 7;            %number of lines
nut = 5;              %number of buses
```

```
matrix = zeros(nhanh,nut);
    nutdau = doc(:,1);  % from bus
    nutcuot = doc(:,2); %to bus
% checking every branch/line
    for i =1: nhanh            matrix(i, nutdau(i))=1;
        matrix (i, nutcuot(i))=1;
    end
%fitness function
 result=runpf(data);          %AC power flow

%%%main loop %%%

while iter < maxiter ; error < minerror;

      iter = iter+1;
      mm1 =length(x (:, 1));  %candidate length

 for ii=1:mm1             %particle performance & fitness  calculation

    tc = (x(ii,9)*0.5465*10^6);
    fitness (ii) = (x(ii,9)*0.5465*10^6)

    fpbest = zeros(1,n);
    for i =1:n
       fpbest(i) = tc;
    end

 %updating pbest
      if fitness(ii)<fpbest(ii)
          pbest(ii,:)=x(ii,:);
          fpbest(ii)=fitness(ii);
      end

 %updating gbest
      if fpbest(ii) < fgbest
          gbest =pbest(ii,:);

      end
```

```
 c1=1.7;
 c2=2.3;
%velocity update
   void = vnew;
   for i = 1:n
        for j = 1:dim
           vnew   (i,j)=   w   *   vnew(i,j)+c1*r   (i,j)*(pbest(i,j)-
posn(i,j))...
                +c2*r (i,j)*(gbest(j)-posn(i,j));
           if abs (vnew (i, j)) ==abs (void (i, j))
              vnew (i, j) = rand (1, 1).*vnew (i, j);
           end
        end
   end

   % particle update
   for i = 1: n
       for k = 1: dim
           sig (i, k) = 1/ (1+exp (-vnew (i, k)));
            if r < sig (i, k)
                  posn (i, k) =1;
              else
              posn (i, k) =0;
           end
       end
   end
   end
end

%% store the best value
 F_ans = fpbest;                % best value in each run
 F_gbest= gbest;

 [bestFUN, bestRUN]= min (F_ans); % best position value
 Best_X = F_gbest (bestRUN);

plot (fitness)
xlabel ('Iteration number')
```

ylabel ('Total Investment Cost, (USD)')

IBPSO Script

```
clc
clear all
tic

      %%initialize BPSO parameters%%

n = 50;                    % population
dim = 15;                  % problem dimension
x = load ('candidate.m');
vnew = rand (n, dim);         % initializes velocity
w = 1;
posn = rand(n,dim);
sig = zeros (n, dim);
void = vnew;
fitness = zeros (1, n);
pbest =zeros (n, dim);
fpbest =zeros (n);
fgbest =inf;
gbest =zeros (1, dim);

%% values for initial population
Vmax =4;         % maximum velocity
vmin =-4;       % minimum velocity
r =rand (n, dim); %random number matrix
iter =0;
maxiter = 500;    % max iteration
minerror = 0.001   % minimum error

 % incidence matrix
data = loadcase(garvers1);
dat =data.bus;
doc =data.branch;   % branch/linedata
nhanh =7;           % lines
nut =5;             % buses
```

```
matrix=zeros(nhanh,nut);
    nutdau=doc(:,1);  % from bus
    nutcuot=doc(:,2); %to bus
    for i=1:nhanh    % checks every branch/line
        matrix(i,nutdau(i))=1;
        matrix(i,nutcuot(i))=1;
    end

%% calculating the fitness function for each candidate line

%%%main loop < FEIOS%%%
while iter<maxiter; error < minerror;

      iter=iter+1;

      mm1 =length(x(:,1));  %  candidate length

for ii =1:mm1                %particle performance and fitness
    result =runpf(data);
    tc=(x(ii, 9)*0.5465*10^6);
    fitness(ii) = (x(ii,9)*0.5465*10^6)
end
 fpbest = zeros(1,n);
 for I = 1:n
   fpbest(i)= tc ;
end

    %updating pbest
       if fitness(ii)< fpbest(ii)
          pbest(ii,:)= x(ii,:);
          fpbest(ii)= fitness(ii);
      end

    %updating gbest
      if fpbest(ii) < fgbest
              gbest = pbest(ii,:);

      end
```

```
   c1 =1.7;
   c2 =2.3;

     %velocity update
   void=vnew;
   for i = 1:n
        for j = 1:dim
           vnew(i,j)  =  w  *  vnew  (i,j)+c1*r  (i,j)*(pbest(i,j)-
posn(i,j))...
                +c2*r(i,j)*(gbest(j)-posn(i,j));
           if abs(vnew(i,j))== abs(void(i,j))
               vnew(i,j) = rand(1,1).*vnew(i,j);
           end
        end
   end

   % particle update
   for i=1:n
       for k=1:dim
           sig(i,k)= abs(2*(logsig(vnew  (i,k))-0.5)); %new transfer
function
            if r() < sig(i,k)
               posn(i,k)= xor(posn(i,k), 1);       %improved position
update
               else
               posn(i,k)= posn(i,k);
           end
       end
   end
end

%% store the best value
 F_ans = fpbest ;               % best value in each run
 F_gbest= gbest;

 [bestFUN, bestRUN]= min(F_ans); % best position value
 Best_X = F_gbest(bestRUN);
```

```
plot (fitness)
xlabel ('Iteration number')
ylabel ('Total Investment Cost,(USD)')
```

IBPSO with voltage limits script

```
clc
clear all
tic

      %%initialize BPSO parameters%%

n = 50;                    % population
dim = 15;                  % problem dimension
x = load('candidate.m');
vnew = rand(n,dim);         % initializes velocity
w = 1;
posn = rand(n,dim);
sig = zeros(n,dim);
void = vnew;
fitness = zeros(1,n);
pbest =zeros(n ,dim);
fpbest =zeros(n );
fgbest =inf;
gbest =zeros(1,dim);

%% values for initial population
Vmax =4;         % maximum velocity
vmin =-4;       % minimum velocity
r =rand(n,dim); %random number matrix
iter =0;
maxiter = 500;    % max iteration
minerror = 0.001; % min error
 % incidence matrix
data = loadcase(garvers1);
dat =data.bus;
doc =data.branch;  % branch/linedata
nhanh =7;          % lines
nut =5;            % buses
```

```
matrix=zeros(nhanh,nut);
    nutdau=doc(:,1);  % from bus
    nutcuot=doc(:,2); %to bus
    for i=1:nhanh    % checks every branch/line
        matrix(i,nutdau(i))=1;
        matrix(i,nutcuot(i))=1;
    end

%% calculating the fitness function for each candidate line

%%%main loop < FEIOS%%%
while iter<maxiter; error < minerror;
      iter=iter+1;

      mm1 =length(x(:,1));  %  candidate length

for ii =1:mm1                %particle performance and fitness
     result =runpf(data);

    if result.bus(:,8)<0.95
            lam=1000000;
        else
            lam=0;
    end
    % lineflow deviation
          if         sqrt(          result.branch(:,14)*2          +
result.branch(:,15)*2)>100

                p = 1000000;
             else
                p = 0;
          end

    penalty = sum(lam+p) ;
    tc=(x(ii, 9)*0.5465*10^6);
    fitness(ii) = (x(ii,9)*0.5465*10^6)+ penalty;
end
 fpbest = zeros(1,n);
```

```
 for I = 1:n
   fpbest(i)= tc ;
end
        %updating pbest
       if fitness(ii)< fpbest(ii)
          pbest(ii,:)= x(ii,:);
          fpbest(ii)= fitness(ii);
      end

    %%updating gbest
      if fpbest(ii) < fgbest
              gbest = pbest(ii,:);
      end
   c1 =1.7;
   c2 =2.3;
     %velocity update
   void=vnew;
   for i = 1:n
        for j = 1:dim
           vnew(i,j)  =  w  *  vnew  (i,j)+c1*r  (i,j)*(pbest(i,j)-
posn(i,j))...
                +c2*r(i,j)*(gbest(j)-posn(i,j));
           if abs(vnew(i,j))== abs(void(i,j))
               vnew(i,j) = rand(1,1).*vnew(i,j);
           end
        end
   end

   % particle update
   for i=1:n
       for k=1:dim
           sig(i,k)= abs(2*(logsig(vnew  (i,k))-0.5)); %new transfer
function
            if r() < sig(i,k)
               posn(i,k)= xor(posn(i,k), 1);       %improved position
update
               else
               posn(i,k)= posn(i,k);
           end
```

```
        end
    end
end

%% store the best value
 F_ans = fpbest ;                % best value in each run
 F_gbest= gbest;

 [bestFUN, bestRUN]= min(F_ans); % best position value
 Best_X = F_gbest(bestRUN);

plot (fitness)
xlabel ('Iteration number')
ylabel ('Total Investment Cost,(USD)')
```